



HAL
open science

Role of the Prion-like domain of Imp in neuronal RNP granule regulation

Jeshlee Cyril Vijayakumar

► **To cite this version:**

Jeshlee Cyril Vijayakumar. Role of the Prion-like domain of Imp in neuronal RNP granule regulation. Cellular Biology. Université Côte d'Azur, 2018. English. NNT : 2018AZUR4099 . tel-02273547

HAL Id: tel-02273547

<https://theses.hal.science/tel-02273547>

Submitted on 29 Aug 2019

HAL is a multi-disciplinary open access archive for the deposit and dissemination of scientific research documents, whether they are published or not. The documents may come from teaching and research institutions in France or abroad, or from public or private research centers.

L'archive ouverte pluridisciplinaire **HAL**, est destinée au dépôt et à la diffusion de documents scientifiques de niveau recherche, publiés ou non, émanant des établissements d'enseignement et de recherche français ou étrangers, des laboratoires publics ou privés.

THÈSE DE DOCTORAT

Rôle du domaine de type prion de Imp dans la régulation des granules RNP neuronaux

Jeshlee VIJAYAKUMAR

Institut de Biologie Valrose – Equipe Contrôle post transcriptionnel de la croissance et du guidage axonal

Présentée en vue de l'obtention du grade de docteur en discipline Interactions moléculaires et cellulaires d'Université Côte d'Azur

Dirigée par : Dr. Florence BESSE
Soutenue le : 13/11/2018

Devant le jury, composé de :
Martine SIMONELIG, PhD, IGH, France
Simon BULLOCK, PhD, MRC-LMB, UK
Simon ALBERTI, PhD, MPI-CBG, Germany
Arnaud HUBSTENBERGER, PhD, iBV, France
Florence BESSE, PhD, iBV, France

Rôle du domaine de type prion de Imp dans la régulation des granules RNP neuronaux

Jury :

Président du jury*

Martine SIMONELIG, PhD, IGH, France

Rapporteurs

Martine SIMONELIG, PhD, IGH, France

Simon BULLOCK, PhD, MRC-LMB, UK

Examineurs

Simon ALBERTI, PhD, MPI-CBG, Germany

Arnaud HUBSTENBERGER, PhD, iBV, France

Invités

Florence BESSE, PhD, iBV, France

Rôle du domaine de type prion de Imp dans la régulation des granules RNP neuronaux

Les ARNms des cellules eucaryotes sont liés à des protéines de liaison aux ARNs (RBPs) et empaquetés au sein d'assemblages macro-moléculaires appelés granules RNP. Dans les cellules neuronales, les granules RNP de transport sont impliqués dans le transport d'ARNms spécifiques jusqu'aux axones et dendrites, ainsi que dans leur traduction locale en réponse à des signaux externes. Bien que peu de choses soient connues sur l'assemblage et la régulation de ces granules *in vivo*, des résultats récents ont indiqué que la présence de domaines de type prion (PLDs) dans les RBPs facilite les interactions protéines-protéines et protéines-ARN, favorisant ainsi la condensation de complexes solubles en granules RNP.

La RBP conservée Imp est un composant central de granules RNP qui sont transportés dans les axones lors du remodelage neuronal chez la drosophile. De plus, la fonction de Imp est nécessaire au remodelage des axones lors de la maturation du système nerveux de drosophile. Une analyse de la séquence de la protéine Imp a révélé qu'en plus de quatre domaines de liaison aux ARNs, Imp contient un domaine C-terminal désordonné enrichi en Glutamines et Serines, deux propriétés caractéristiques des domaines PLDs. Lors de ma thèse, j'ai étudié la fonction de ce PLD dans le contexte de l'assemblage et du transport des granules RNP. J'ai observé en culture de cellules que les granules Imp s'assemblent en absence de PLD, bien que leur nombre et leur taille soient augmentés. Des protéines présentant une séquence PLD mélangée, au contraire, s'accumulent dans des granules au nombre et à la taille normaux, indiquant que l'état désordonné de ce domaine, et non sa séquence primaire, est essentiel à l'homéostasie des granules. De plus, des expériences de FRAP réalisées en culture de cellule et *in vivo* ont révélé que le domaine PLD de Imp favorise la dynamique des granules. *In vivo*, ce domaine est nécessaire et suffisant à l'accumulation axonale de Imp. Comme montré par une analyse en temps réel, l'absence de domaine PLD aboutit également à une diminution du nombre de granules axonaux motiles. Fonctionnellement, le domaine PLD de Imp est essentiel au remodelage neuronal car des protéines sans ce domaine ne sont pas capables de supprimer les défauts de repousse axonale observés après inactivation de *imp*. Enfin, la génération d'un variant de Imp dans lequel le domaine PLD a été déplacé en N-terminus a montré que les fonctions du PLD dans le transport des granules et dans leur assemblage sont découplées, et que la modulation des propriétés des granules Imp médiée par le domaine PLD n'est pas nécessaire au remodelage neuronal *in vivo*.

En conclusion, mes résultats ont montré que le domaine PLD de Imp n'est pas nécessaire à l'assemblage des granules RNP Imp, mais régule leur nombre et leur dynamique. De plus, mon travail a mis en évidence une fonction inattendue pour un domaine PLD dans le transport axonal et le remodelage des neurones lors de la maturation du système nerveux.

Mots clés : *Drosophile*, protéine de liaison à l'ARN, granule neuronale, RNP transport

Role of the Prion-like domain of Imp in neuronal RNP granule regulation

Eukaryotic mRNAs are bound by RNA Binding Proteins (RBP) and packaged into diverse range of macromolecular assemblies named RNP granules. In neurons, transport RNP granules are implicated in the transport of specific mRNAs to axons or dendrites, and in their local translation in response to external cues. Although little is known about the assembly and regulation of these granules *in vivo*, growing evidence indicates that the presence of Prion Like domains (PLD) within RBPs favours multivalent protein–protein and protein-RNA interactions, promoting the transition of soluble complexes into RNP granules. The conserved RBP Imp is as a core component of RNP granules that are actively transported to axons upon neuronal remodelling in *Drosophila*. Furthermore, Imp function was shown to be required for axonal remodelling during *Drosophila* nervous system maturation. Analyses of the domain architecture of the Imp protein revealed that, in addition to four RNA binding domains (RBD), Imp contains a C-terminal domain showing a striking enrichment in Glutamines and Serines, which is one of the characteristics of a PLD. During my PhD, I explored the function of the PLD in the context of granule assembly and transport. In cultured cells, I observed that Imp granules assembled in the absence of the PLD, however their number and size were increased. Proteins with scrambled PLD sequence accumulated in granules of normal size and number, implying that the degree of disorder of this domain, and not its sequence, is essential for granule homeostasis. Moreover, FRAP experiments, performed on cultured cells and *in vivo*, revealed that Imp PLD is important to maintain the turnover of these granules. *In vivo*, this domain is both necessary and sufficient for efficient transport of Imp granules to axons. These defects are associated with a reduction on the number of motile granules in axons. Furthermore, mutant forms lacking the PLD do not rescue the axon remodelling defects observed upon *imp* loss of function. Finally, a swapping experiment in which I moved Imp PLD from the C-terminus to the N-terminus of the protein revealed that the functions of Imp PLD in granule transport and homeostasis are uncoupled, and that PLD-dependent modulation of Imp granule properties is dispensable *in vivo*. Together, my results show that Imp PLD of is not required for the assembly of RNP granules, but rather regulates granule number and dynamics. Furthermore, my work uncovered an unexpected *in vivo* function for a PLD in axonal transport and remodelling during nervous system maturation.

Keywords : *Drosophila*, RNA binding proteins, neuronal granules, RNP transport

Table of Contents

Acknowledgements.....	ix
List of Figures.....	x
List of abbreviations.....	xii
1. Introduction.....	1
1.1. The prevalence of mRNA localization.....	2
1.2. Neurons are highly polarized cells.....	5
1.3. RNA Localization in dendrites and axons.....	9
1.4. Local translation in dendrites and axons.....	14
1.5. Advantage of RNA localization.....	18
1.6. Importance of Local Translation in neurons	
1.6.1 Local translation contributes to axon growth and maintenance.....	20
1.6.2 Local translation contributes to axon regeneration.....	22
1.6.3 Local translation contributing to plasticity.....	22
2. Mechanism of neuronal RNP Granule assembly and transport.....	23
2.1. Cis acting elements.....	24
2.2. Trans-Acting Factors.....	25
2.3. Assembly of RNP granules.....	25
2.4. Transport of Neuronal RNP granules.....	28
2.5. Prion-Like domains in RBP.....	31
2.5.1. Properties of PLD.....	33
2.5.2. Functions of PLD.....	36
3. Imp, a conserved RBP.....	37
3.1. Imp regulates the fate of associated transcripts.....	39
3.2. Imp, role in <i>Drosophila</i> Development.....	42
4. Aim of the thesis.....	46
5. Results.....	47
5.1. Summary of my thesis work I.....	47
5.2. Part I: Manuscript	
5.2.1. Abstract	
5.2.2. Introduction	
5.2.3. Results	

5.2.4.	Discussion	
5.2.5.	Material and methods	
5.2.6.	Figures	
5.2.7.	Supplemental figures	
5.3.	Summary of my thesis work II.....	50
5.3.1.	Imp PLD is may not modulated through serine phosphorylation.....	51
5.3.2.	Imp PLD restricts the transition into aggregate state.....	52
6.	Discussion.....	55
6.1.	The modulators of granule assembly.....	56
6.2.	Sequence features of the PLD.....	59
6.3.	Specific function of the PLD in the axonal transport of Imp granules to axon.....	60
6.4.	Conclusion.....	64
7.	References.....	65

Acknowledgement

I want to thank Florence for trusting me with this exciting project, her constant support, guidance and valuable advices throughout this project. I also owe her a huge debt of gratitude for also helping me settle in Nice, France and her assistance with all the French bureaucratic works.

I also want to thank all the past and present lab members whose support, helpful discussions and love made this a wonderful environment to work. A special mention to Caroline for helping me with living imaging. I also cherish all the non-scientific discussion with Nadia and Kavya, had over many coffees, which helped me destress and laugh.

A special mention to the fly community at the iBV for their tips and helps with fly lines. I also want to thank the PRISM, microscope facility for their help during the past four years.

I want to thank our collaborator, Dr. Alberti and his team for welcoming me in their lab and helping me get introduced to biochemistry and cell culture. Special mention to Daniel, Doris, Elisabeth and Titus for their help and interesting discussions with the project.

I want to extend my heartfelt gratitude to my parents for their unfaltering love and support and for going against the norms of their surrounding and allowing me to pursue PhD. A huge thank you to my husband, Daniel, for always being there for me, motivating me to press on and also for listening to all the practice talks and providing me with valuable suggestions.

List of Figures

- Figure 1: Schematic representation of the classical examples of asymmetric mRNA localization in different cell types.
- Figure 2: Schematic representation of the RNA localization pattern observed in Prokaryotes.
- Figure 3: Morphology of the neuron.
- Figure 4: Organization of the cytoskeleton along the neurite.
- Figure 5: Asymmetric localization of transcripts in neuronal sub-compartments.
- Figure 6: MS2-MCP based RNA tagging system.
- Figure 7: Detection of polyribosomes in the spine neck and axon segments.
- Figure 8: Single molecule imaging of transcripts and nascent peptides.
- Figure 9: Schematic representation of how cue-induced local translation influences the growth cone dynamics.
- Figure 10: Schematic representation of the types and assembly paradigm of RNP granules in a neuron.
- Figure 11: Schematic representation of the regulated process of assembly and transport of RNP granules neural cytoskeleton
- Figure 12: Role of PLDs in granule assembly and transition into pathological aggregates.
- Figure 13: Phylogeny and Structure of the Imp family of RNA-binding proteins.
- Figure 14: The brain of *Drosophila* and the sequential generation of the Mushroom Body neurons.
- Figure 15: Development of the MB gamma neurons
- Figure 16: Axonal Growth and Branching Defects in γ Neurons Mutant for *imp*
- Figure 17: In *Vitro* Phase transition assays with GFP Imp (A, A') or GFP Imp DPLD proteins (B, B').
- Figure 18: Model Illustrating the role of Imp PLD in granule homeostasis and Imp RNP

granule transport.

List of Figures from the Manuscript

- Figure 1: *Drosophila* Imp contains a C-terminal prion-like domain (PLD).
- Figure 2: Imp PLD is dispensable for RNP granule assembly.
- Figure 3: Imp PLD is both necessary and sufficient to restrict Imp granule size and number.
- Figure 4: Molecular determinants underlying Imp PLD function in the regulation of Imp granule assembly.
- Figure 5: Imp PLD promotes the exchange of Imp in and out granules.
- Figure 6: Imp PLD is essential for efficient localization of Imp to axons *in vivo*.
- Figure 7: Imp PLD promotes Imp granule motility.
- Figure 8: Imp PLD has independent functions in axonal remodeling and granule homeostasis.

Table

- Table 1: Summary of Imp variants and their respective phenotypes in S2R+ cells and brain.

List of Abbreviations

EM	-	Electron microscopy
ISH	-	Is Situ Hybridization
FISH	-	Fluorescence In Situ Hybridization
MT	-	Microtubule
RT-PCR	-	Reverse transcriptase polymerase chain reaction
TRAP	-	Translating ribosome affinity purification
MS2	-	Multiple stem loops
MCP	-	MS2 coat protein
PTM	-	Posttranslational modification
GFP	-	Green Fluorescent Protein
UTR	-	Untranslated Region
ORF	-	Open reading frame
scFV	-	Single variable fragment
MBP	-	Mylein Basic Protein
RGC	-	Retinal ganglion cell
CREB	-	cAMP responsive element binding
Impa-1	-	Myo-inositol monophosphate 1
PNS	-	Peripheral nervous system
LTP	-	Long term potentiation
LTD	-	Long term depression
RBP	-	RNA binding protein
RNP	-	RNA protein granules
LE	-	Localization element
RBD	-	RNA binding domain
KH	-	K-homology
RRM	-	RNA recognition motif
dsRBD	-	Double stranded RBD
ZnF	-	Zinc Finger motif
PAZ	-	Piwi argonaute/zwillie
PuF	-	Pumilio domain
IDR	-	Intrinsically disordered region

LLPS	-	Liquid liquid Phase separation
FRAP	-	Fluorescence recovery after photobleaching
PLD	-	Prion Like Domain
FUS	-	Fused in Sarcoma
MCID	-	Multiple copies of interaction domains
ZBP1	-	Zipcode binding protein 1
IGF2BP/Imp	-	Igf-II mRNA binding protein
CRD-BP	-	c-myc coding region instability determinant binding protein
iCLIP	-	Individual nucleotide resolution UV-cross linking and immunoprecipitation
PAR-iCLIP	-	Photoactivatable ribonucleoside iCLIP
MB	-	Mushroom Body
Chinmo	-	Chronologically inappropriate morphogenesis
SG	-	Stress Granules
hIMP1	-	Human Imp1
MCFO	-	Multicolour FlpOut

1 Introduction

Eukaryotic cells have evolved to maintain the stability of their internal environment through tight regulation of gene expression. Gene expression, composed of the two cardinal steps of transcription and translation, decodes genes to produce proteins which act as building blocks of all organisms. Regulation of transcription is the first step of gene expression. The coordinated effort of several factors such as transcription factors, chromatin regulators and the transcription machinery leads to regulated production of RNA transcripts, and has for long been established as a nuclear process (Shandilya and Roberts 2012) . However, the subcellular location of the translation machinery has remained a subject of debate for years. It was originally believed that proteins were translated in the nucleus based on studies that reported the isolation of polyribosomes from the nuclei, the presence of translational machinery in the nucleus, and detection of amino acids precursors in physically isolated nuclear preparations (Birnstiel and Flamm 1964; Goidl et al. 1975; Iborra et al. 2001; David et al. 2012)

However, the theory of nuclear translation was later abandoned based on electron microscopic (EM) images indicating the presence of molecular components necessary for translation outside of the cell's nucleus (Job and Eberwine 2001), and the absence of the complete set of translation machinery in the nucleus (Bohnsack et al. 2002; Dahlberg et al. 2003). Furthermore, studies indicated that the ribosomal units were functional only after maturation in the cytoplasm (Bohnsack et al. 2002; Dahlberg et al. 2003). Over the years, it further became apparent that translation machineries were not only localized at the periphery of the nucleus, close to nuclear export sites, but were also found in various cellular compartments. Indeed, biochemical and EM data reported the distribution and association of ribosomes like particles at the endoplasmic reticulum, and additionally along the mitotic apparatus and microtubules, as well as in axons or dendritic spines (Steward and Banker 1992; Job and Eberwine 2001; Lecuyer et al. 2009). These discoveries led to the speculation

that translation of mRNAs may occur locally in specialized subcellular compartments (Suprenant 1993). A breakthrough in this field came through the work of Jeff et al in 1983, which reported asymmetric subcellular localization of β -actin mRNA in ascidian eggs (Jeffery et al. 1983). Since then, several studies showed a myriad of examples of asymmetric localization of mRNAs in different model organisms, establishing that asymmetric mRNA localization was not restricted to a specific cell type (Figure 1). Moreover, these studies emphasized that mRNA localization was critical for cell development and cell functions, e.g. for embryogenesis (Weil 2014), neuronal synapse formation and plasticity (Wang et al. 2009; Holt and Schuman 2013), or cell migration (Shestakova et al. 2001).

In the first part of the introduction (1.1), I will briefly explain a few examples illustrating the conserved mechanism of RNA localization observed across various cell types and then continue to extensively present the techniques and information available about RNA localization and local translation, focusing on neurons (1.2-1.6). In the second part of the introduction (2.1-2.5), I will introduce the function, and the mechanism of assembly and transport of neuronal RNA-Protein granules. In the third part (3.1-3.3) I will introduce the role of the RNA Binding Protein Imp in RNA transport and regulation, and finally (4) end with the specific objectives of my thesis work.

1.1 The prevalence of mRNA localization

The best characterized roles of RNA localization were demonstrated in oocytes, yeast, migrating cells and polarized neurons. In *Drosophila* oocytes, the most investigated examples are the asymmetric localization of *gurken*, *oskar*, *bicoid* and *nanos* mRNAs. During oogenesis, these mRNAs localize to the anterior (*gurken*, *bicoid*) and posterior (*oskar*, *nanos*) poles of the oocyte, and initiate a series of events that are responsible for the elaborate body axis specification and patterning of the embryos (Fig. 1 A) (Ephrussi et al. 1991; Johnstone and Lasko 2001). Similar examples of localized RNAs have also been described in other model organisms such as *Xenopus* oocytes, where *Vg1* mRNA localization

to the vegetal pole results in the endodermal and mesodermal patterning (Fig. 1 B) (Yisraeli et al. 1990; Kloc et al. 2002b), and in Zebrafish oocytes, where *cyclinB*, *zDazl* and *vasa* mRNAs localize during oogenesis to the animal and vegetal poles and cortex respectively (Howley and Ho 2000). Asymmetric RNA accumulation is also important for differential fate specification, which is well demonstrated through the asymmetric localization of *Ash1* mRNA in the daughter cells of budding yeasts during late anaphase (Fig. 1 C). The local translation of the Ash1p protein represses transcription of the HO endonuclease specifically in the daughter cell, resulting in a mating type switch between the mother and daughter cell (Gonsalvez et al. 2005). Another described function of RNA localization is in establishing polarity and directed migration. Localization to the leading edge of migrating fibroblasts of mRNAs coding for cytoskeletal proteins such as β -actin or subunits of the Arp2/3 complex, has been shown to be important for polarity and motility (Fig. 1 D) (Lawrence and Singer 1986; Condeelis and Singer 2005; Liao et al. 2011).

Although the above studies documented RNA localization to specific cellular compartments, the number of such documented transcripts was relatively limited until the last decade. Significant advances in transcriptome-wide analysis have recently helped to unravel how prevalent the spatial distribution of many mRNAs is. Notably, the work of Lecuyer et al and followers, involving systematic high resolution In Situ Hybridization (ISH) in *Drosophila* tissues, showed that 71% of the transcripts exhibited differential subcellular localization (Lecuyer et al. 2007; Jambor et al. 2016; Wilk et al. 2016). Similarly, several groups performed genome-wide microarray analyses across different subcellular fractions of cell types such as *Xenopus* oocytes or fibroblasts, further identifying the enrichment of subsets of mRNAs involved in diverse functions such as cell motility, cytoskeletal organizations and regulating cell cycle (Blower et al. 2007; Mili et al. 2008). New image-based technologies combined with modified FISH technologies have also been beneficial in documenting the subcellular distribution of up to 1,000 transcripts in single cultured cells, highlighting the prevalence of asymmetric localization (Battich et al. 2013).

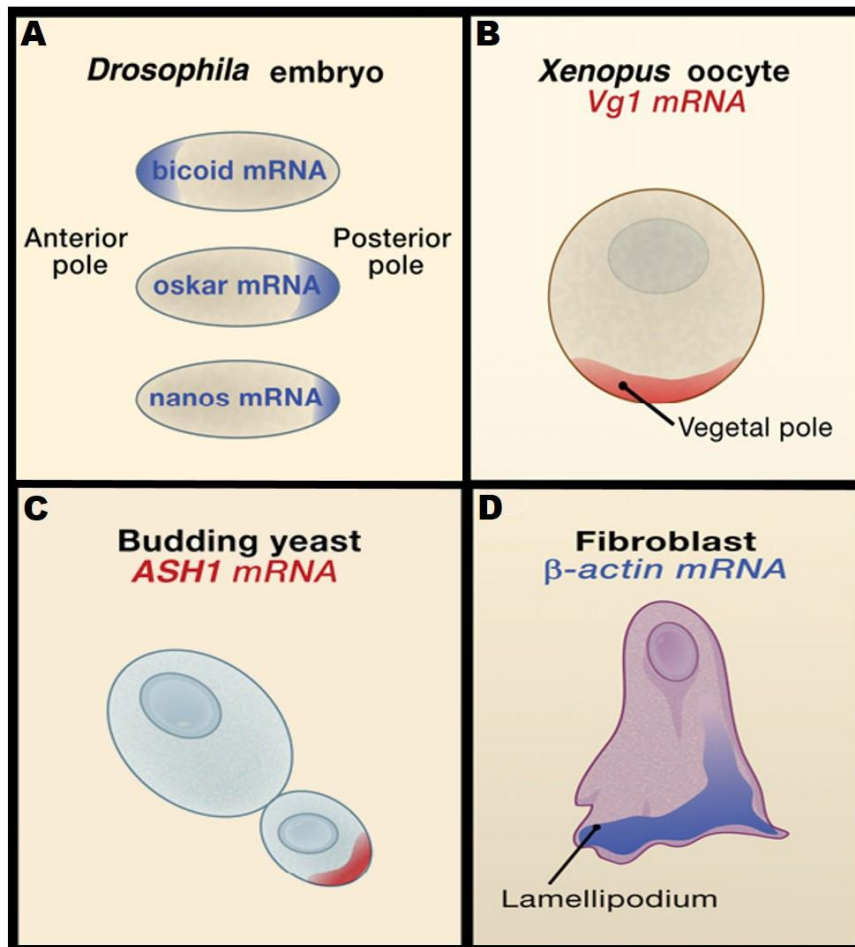


Figure 1: Schematic representation of the classical examples of asymmetric mRNA localization in different cell types.

A) Localization of *bicoid* mRNA to the anterior pole of the *Drosophila* embryo, and *oskar* and *nanos* mRNAs to the posterior pole B) *Vg1* mRNA localizes to the vegetal pole of the *Xenopus* oocyte. C) *Ash1* mRNA localizes to the bud tip of a budding yeast. D) β -actin mRNA localizes to the leading edge of migrating fibroblast cells.

Image adapted from (Martin and Ephrussi 2009).

The phenomenon of mRNA targeting was believed not to occur in prokaryotes owing to the understanding that RNA transcription was strictly coupled to protein synthesis. However, several pioneering studies using ISH and advanced live-cell imaging have shown over the past decade a non-random pattern of distribution of some RNAs in bacterial cells (Fig. 2) (Nevo-Dinur et al. 2011; Buskila et al. 2014). Induction of RNA transcription and live

imaging of tagged RNAs revealed the accumulation of RNAs at the poles, laterally along the cell wall (Valencia-Burton et al. 2009). Although the precise function of RNA localization in bacteria remains to be established, it demonstrates that this process is an integral part of gene expression that is conserved in prokaryotes and eukaryotes.

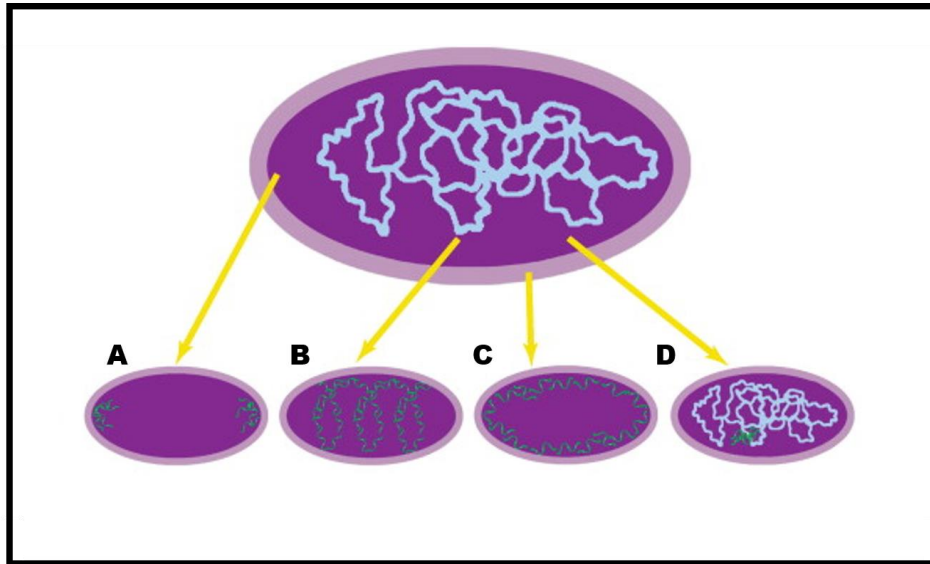


Figure 2: Schematic representation of the RNA localization pattern observed in prokaryotes.

Bacterial RNAs can localize to specific subdomains, typically showing one of the four following patterns of distribution: a) near poles, b) helix-like distribution in the cytoplasm, c) laterally along the cell wall, and d) close to the gene locus.

Thin green wavy lines represent RNA and the thick blue curly lines represent chromosomes (Nevo-Dinur et al. 2012).

1.2 Neurons are highly polarized cells

Neurons are highly complex cells with a polarized morphology; they contain distinct compartments: axon, cell body and dendrites (Fig. 3). Dendrites are long, branched extensions with specialized domains found on the dendritic surface and called the dendritic spines. Super resolution imaging revealed that spines can further be divided into multiple microcompartments (Chen and Sabatini 2012). Dendrites integrate synaptic inputs from

divergent cells, which are then relayed to the axon *via* the cell body (Gulledge et al. 2005). Axons are the longest cellular processes seen in animals and can form multiple branches, enabling contact with multiple targets and propagation of signal input to other cells (Prokop 2013). Functional circuits are formed during nervous system development, when growth cones, the motile sensory tip of axons, sense extracellular guidance cues and make their way through complex environments. Connectivity is then established via the formation of synapses, specialized junctions where the presynaptic axons contact the postsynaptic dendrites (Kalil and Dent 2014). Although neural circuits are established initially in response to developmental cues, local modulation of neuronal structure (termed remodeling) and modulation of synaptic strength are induced by neural activity, highlighting the plasticity of neuronal cells (Takeuchi et al. 2014).

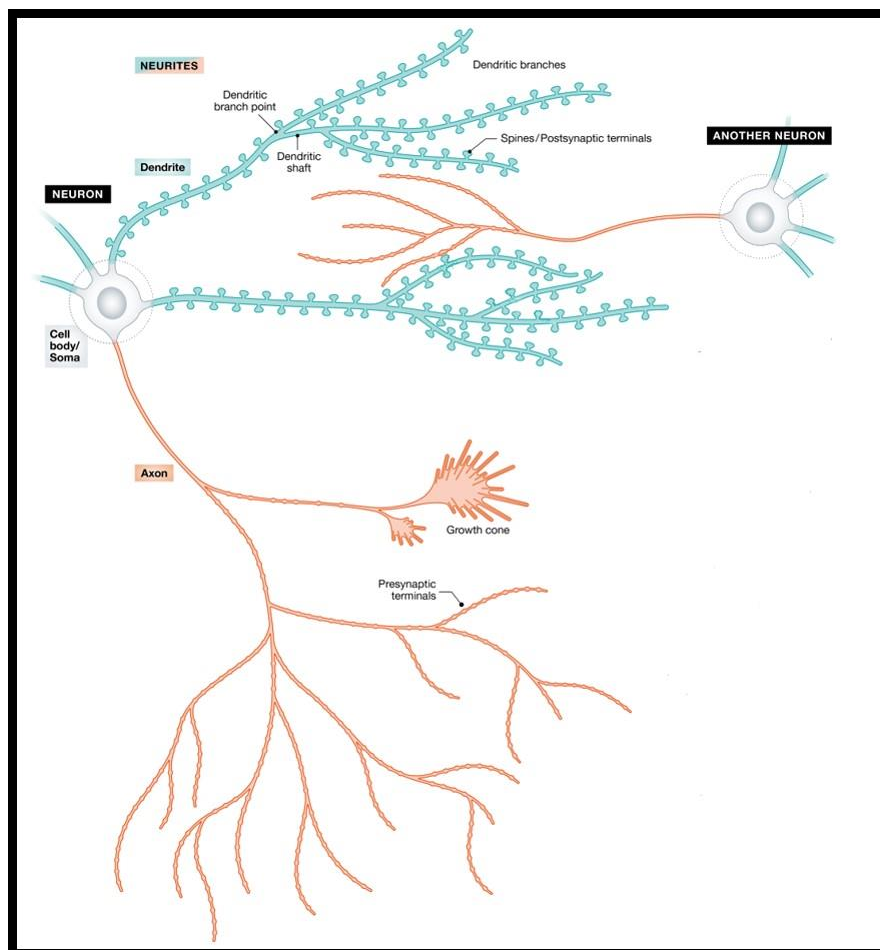


Figure 3: Morphology of the neuron.

Long Polarized extensions, axons (orange) and dendrites (blue), emerge from the cell body (gray) and travel through the complex environment to make synaptic contact with neighbouring neurons or other cells. The spiny protrusions of the dendrites, seen as mushroom shaped protrusions on the dendrites, are involved in forming the synaptic contacts with the presynaptic axons. Image adapted from (Rangaraju et al. 2017).

Both the initial growth and branching of a neurite, and its remodeling, depend on the coordinated regulation of neuronal cytoskeletal elements: actin, microtubule (MT) and neurofilaments. Focal accumulation of actin monomers and actin polymerization drive the formation of filopodia or lamellipodia from the cell body (Fig. 4 A, C) (Armijo-Weingart and Gallo 2017). While local F-actin polymerization generates the force necessary for neurite protrusion, neurite stabilization depends on the organization of the parallel arrays of tubulin heterodimers which constitute the MT network (Fig. 4 B, C). The formation of axon branches from the main axon follow a relatively similar event of actin accumulation, protrusion and MT stabilization-dependent growth (Pacheco and Gallo 2016). Several studies have indicated that F-actin bundles behave as predetermined tracks for the growth and stabilization of MTs. Furthermore, F-actin polymerization or retrograde flow of actin have been indicated to influence the assembly and disassembly of MTs (Coles and Bradke 2015; Cammarata et al. 2016). Thus, this concerted action of both actin and MTs is essential for the cellular events underlying neuron growth and motility.

The unique morphology of neurons, with their cellular protrusions extending mm or cm away from the cell body, poses serious challenges for the timely delivery of specific molecules to their appropriate subcellular destinations. To overcome these challenges, neurons have developed means to sustain such spatio-temporal demands (Gao 1998; Di Liegro et al. 2014). Among them, is the transport of mRNAs to dendrites and axons coupled to their local translation, a mechanism first hypothesized by Bodian et al. in the early 60s. In this study, ribosome ‘particles’ were not only observed in the soma, but also in the dendrites

of motor neurons via electron microscopy (Bodian 1965; Batista and Hengst 2016), leading the authors to speculate that local translation may exist and may be important for maintenance and function of neurons.

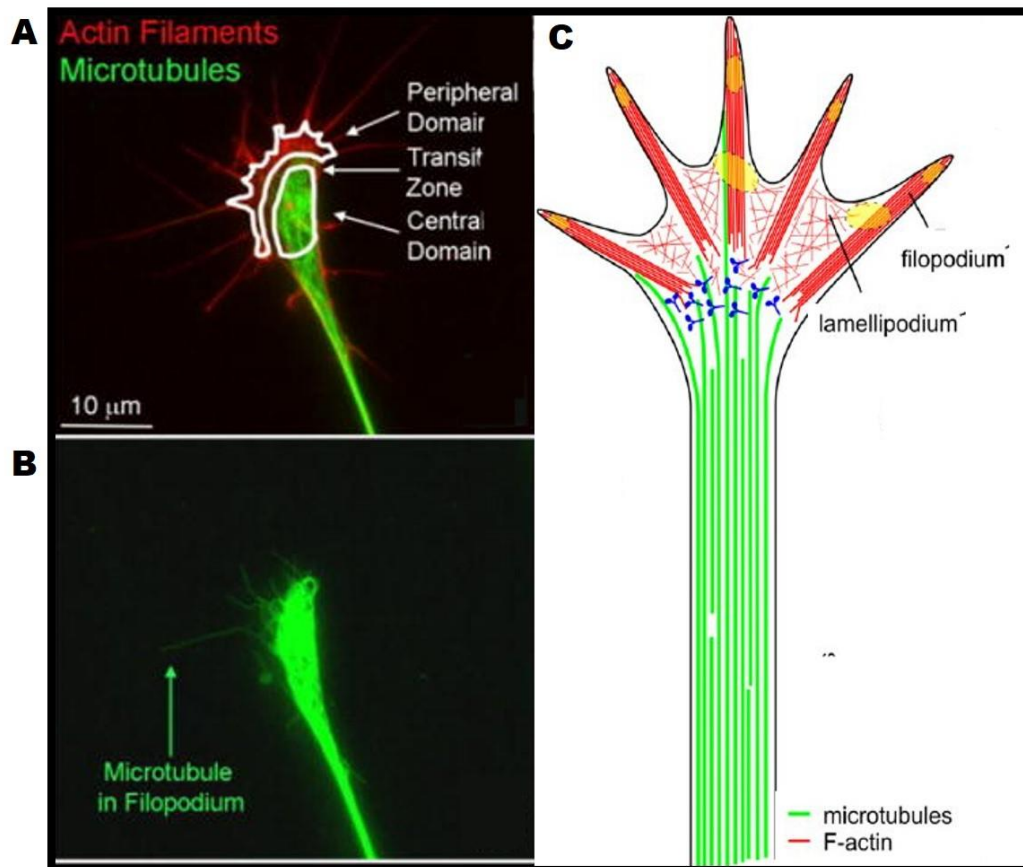


Figure 4: Organization of the cytoskeleton along the neurite.

Neurons have a very elaborate cytoskeletal structure which defines their morphology. A) Actin filaments (red in A, C) are seen enriched in the peripheral domain, of the growth cones of an axon. B) The microtubule (green in A, B, C) network is composed of tubulin heterodimers organized along the length of the neurite, and predominantly present in the central domain (Pacheco and Gallo 2016).

C) Schematic representation of the parallel array of MTs organized along the axon and the actin filaments on the growth cones. The growth cone mediates elongation and guidance through actin polymerisation and depolymerisation. The unipolar actin-rich filopodia extend from the lamellipodia which contain a dense mesh of actin polymer (Franz and Guck, 2010).

1.3 RNA Localization in dendrites and axons

Bodian's speculation was further substantiated by the identification of RNA along the neurites. Starting from the early 80s several studies, using various approaches, have provided evidence for the subcellular localization of mRNAs in neurons.

RNAs were initially detected using ISH technique. This method relies on chromogenic or fluorescently-labeled probes complementary to the transcript to be detected, and enables the detection of mRNAs expressed during various developmental stages and different environmental conditions. The first detected localized RNAs were revealed to code for proteins with multiple cellular functions (Burgin et al. 1990; Kleiman et al. 1990; Mohr 1999). For example, the detection of the mRNAs coding for proteins that regulate neuronal cytoskeleton such as, *MAP2* mRNA which promotes tubulin polymerization (Fig. 5 A), and *ARC* mRNA, an activity regulated cytoskeletal associated protein, particularly in dendrites strongly suggested that their local translation may promote dendrite morphogenesis by regulating cytoskeletal dynamics (Garner et al. 1988; Steward et al. 1998; Yao et al. 2006). A second group of mRNAs detected in the dendrites were transcripts encoding regulators of synaptic plasticity such as *CamKII α* or *neurogranin* mRNAs (Burgin et al. 1990; Berry and Brown 1996). The patterned accumulation of specific mRNAs along the dendrites also correlated with synapse maturation and neural activity. The work of Berry and Brown demonstrated the detection of *CamKII* mRNA at apical dendrites of the cerebral cortex and purkinje cells during the postnatal period coinciding with synaptogenesis. Then on, several works starkly illustrated the process of RNA sorting to dendrites supporting growth, morphogenesis and plasticity (Miller et al. 2002; Baj et al. 2011; Kim and Martin 2015). Similarly, mRNAs were also detected in the axons of invertebrates and vertebrates (Giuditta et al. 1980; Giuditta et al. 1986; Piper and Holt 2004). Particularly, the detection of mRNAs encoding cytoskeletal protein, like *β -actin* mRNA (Fig. 5 B), *Actin depolymerizing factor* and *tau*, highlighted their role in axon morphogenesis and neuronal polarity (Litman et al. 1993; Bassell et al. 1998; Wong et al. 2017). The detection of only a subset of RNAs in axon

and dendrites argued against random diffusion of mRNA into different compartments (Tang and Schuman 2002). Despite the widespread use, the ISH had significant limitations such as trouble of detecting transcripts that were expressed at low levels and the sensitivity of the probes in detecting RNA secondary structure.

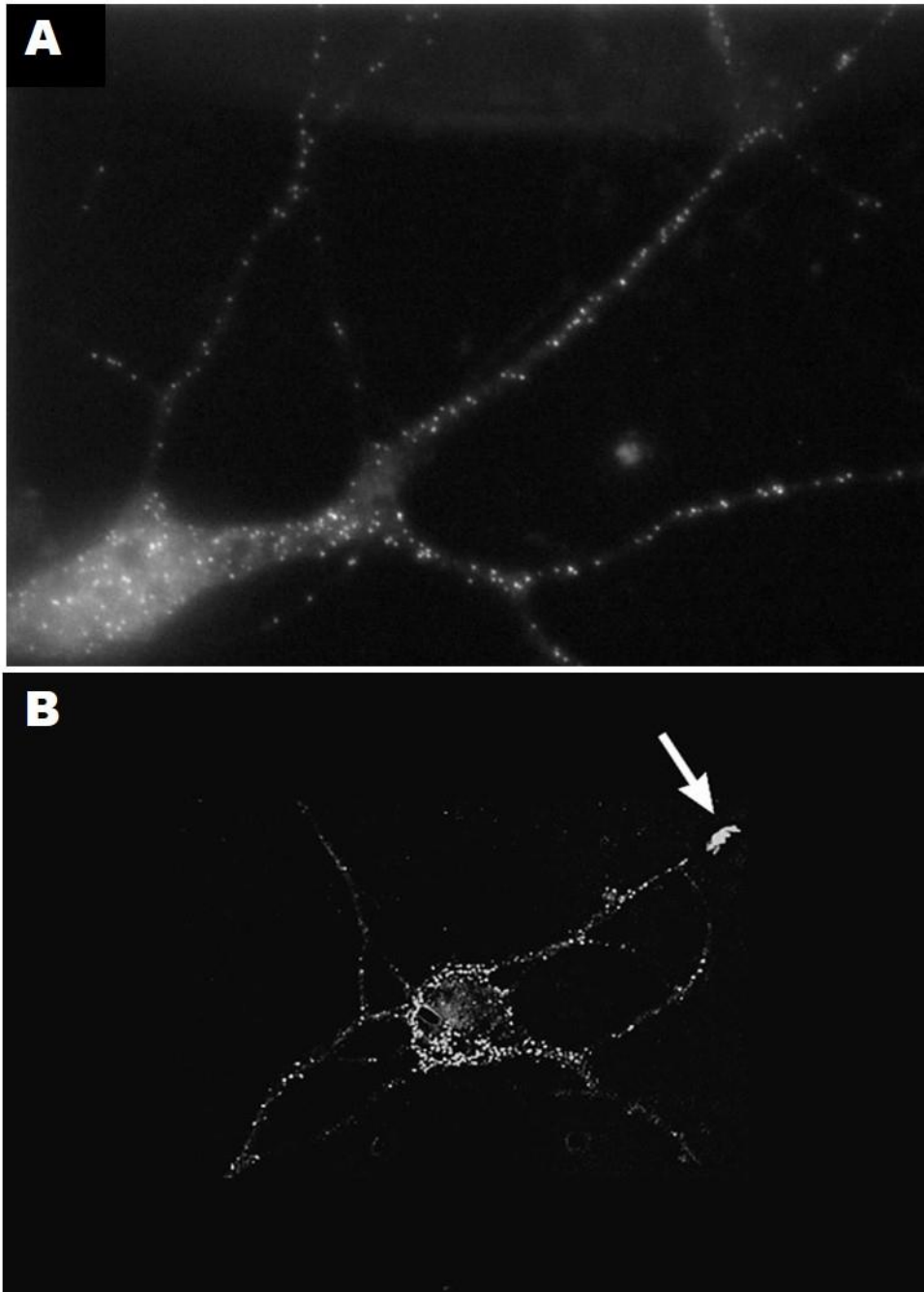


Figure 5: Asymmetric localization of transcripts in neuronal subcompartments

FISH technique indicates the specific localization of Map2 mRNAs (A), in the dendrites (Batish et al. 2012), and β -actin (B) mRNAs in the axons of cultured hippocampal neurons (Bassell et al. 1998). Arrow indicates the accumulation of mRNA in the growth cones of axons.

The reverse transcriptase polymerase chain reaction (RT-PCR) was an alternate technique that was used for candidate-based subcellular detection of transcripts (Surmeier et al. 1992; Miyashiro et al. 1994; Twiss and Fainzilber 2009). The RT-PCR techniques applied to fractionated neurites and soma revealed large number mRNAs expressed at low levels, including those encoding glutamate and dopamine receptors. Notably, this work explored the pattern and differential expressions of specific subunits of receptors which contributes to the physiological identity of the synapse (Miyashiro et al. 1994).

The studies outlined above unraveled the spatio-temporal accumulation of mRNAs in specific compartments. Yet, they have only been successful in identifying a few mRNAs in the neuronal processes. With the advent of microarray and high throughput RNA sequencing techniques, we now know that thousands of RNA molecules are localized to neuronal processes. Indeed, using microarrays to identify RNAs specifically extracted from isolated neuronal compartments provided a transcriptome-wide snapshot of the transcripts that were differentially enriched in axons, dendrites, or smaller structures such as growth cones. As revealed by these studies, the population of RNAs enriched in the neurites significantly changed during development and injury (Poon et al. 2006; Taylor et al. 2009; Zivraj et al. 2010; Gumy et al. 2011). Furthermore, the stage-specific sorting of transcripts such as *EphB4* mRNAs into dendrites and *tubb3* mRNAs into embryonic axons hinted towards a possible post-transcriptional mechanism that differentially regulates the sorting of transcripts from the soma to the neurites during development (Zivraj et al. 2010; Gumy et al. 2011). More recently developed high-throughput RNA sequencing methods, by enabling accurate measurement of transcript levels (Kukurba and Montgomery 2015), unveiled a large number

of previously undetected mRNAs that localize in specific neuronal sub-compartments (Cajigas et al. 2012; Minis et al. 2014; Zappulo et al. 2017). More specifically, deep-sequencing combined with advanced bioinformatics analyses enabled the detection of axonal mRNA motifs at the level of whole transcriptome, linking splice variants with specific axonal distributions (Taliaferro et al. 2014). With the interest of defining in a stage- and cell type-specific manner the pools of transcripts that are translationally active, diverse and more advanced methods of deep sequencing have recently been developed, including ribosome profiling (ribo-seq), the Axon TRAP (translating ribosome affinity purification) and SynapTRAP, methods to isolate specific ribosome-bound mRNAs from the axons and synaptoneurosomal fractions respectively (Shigeoka et al. 2016; Ouwenga et al. 2017). These studies revealed a complex population of axon-specific mRNA isoforms that are dynamically targeted during development and in mature axons. The presence of such a wide array of transcripts further implied a role for local protein synthesis in response to growth and maintenance.

To gain insights into the temporal dynamics of RNA localization, RNA labeling methods and imaging techniques with increasing temporal resolution were developed. The first attempt at live imaging was done using a cell permeable Syto 14 dye, which labels nucleic acids. Although this technique enabled live imaging of RNA axonal transport, it failed to distinguish different transcripts (Knowles et al. 1996). The more advanced MS2-MCP system facilitated single molecule imaging of specific exogenous and later endogenous RNAs. The MS2-MCP system relies on the ability of the phage RNA binding protein MS2 coat protein (MCP) to bind the RNA secondary structures formed by the MS2 stem loops (Bertrand et al. 1998; Buxbaum et al. 2014). Target RNAs are tagged with multiple stem loops (MS2) and co-expressed with MCP protein containing a nuclear localization signal and fused to a fluorescent protein (Fig. 6). Thus, the tagged transcripts are fluorescently labeled upon MCP-MS2 interaction. Notably, the high specificity and affinity of MCP for MS2 tags, together with the multimerization of MS2 sequences on target mRNAs, lead to high signal to

noise ratios enabling imaging with high spatio-temporal resolution. This technique revealed that although a vast majority of localizing RNAs was non-motile, a fraction of granules exhibited active unidirectional and bidirectional transport (Rook et al. 2000; Park et al. 2010; Misra et al. 2016) and enabled the dissection of the machinery required for active transport (Dichtenberg et al. 2008). Furthermore, single molecule live imaging revealed that localization of mRNAs at specific compartments occur in a translation independent manner (Dynes and Steward 2012).

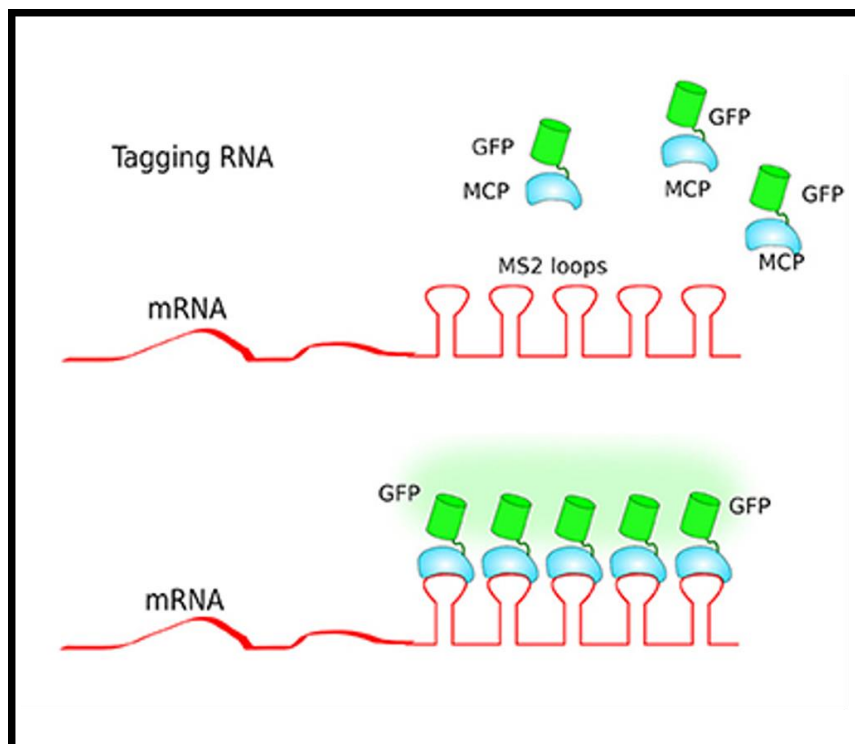


Figure 6: MS2-MCP based RNA tagging system.

mRNAs of interest are tagged with repeated MS2 stem loop structures recognised by chimeric MCP-GFP fusion proteins, thus enabling RNA tagging and visualization of reporter or endogenous RNAs in live cells (Czapinski et al. 2017).

Thus, methods ranging from ISH, single resolution imaging of RNA to advanced high throughput sequencing have now provided researchers with a more comprehensive list of the

complex population of transcripts that are specifically enriched in neuronal protrusions. They have been instrumental in expanding our knowledge of the repertoire of localized RNA controlling diverse cellular processes in neurons (*e.g.*, axon growth and maintenance, memory and plasticity).

1.4 Local translation in dendrites and axons

A hallmark discovery that led to the theory of local protein synthesis was the detection of polyribosomes in the neurites. EM analyses led to the identification of polyribosomes precisely positioned at the base of dendritic spines (Fig. 7 A, B) (Steward and Levy 1982; Steward and Ribak 1986). Polyribosomes were particularly abundant in the synaptic region during synaptogenesis and declined with synapse maturation (Steward and Falk 1986; Deitch and Banker 1993). During synaptic stimulation however, polyribosomes have been documented to translocate to spine heads (Ostroff et al. 2002). Although the presence of translation machinery components in axons had for long remained controversial (Piper and Holt 2004), ribosomes had been detected in the axons of both growing (Bassell et al. 1998) and mature neurons (Steward and Ribak 1986; Koenig et al. 2000).

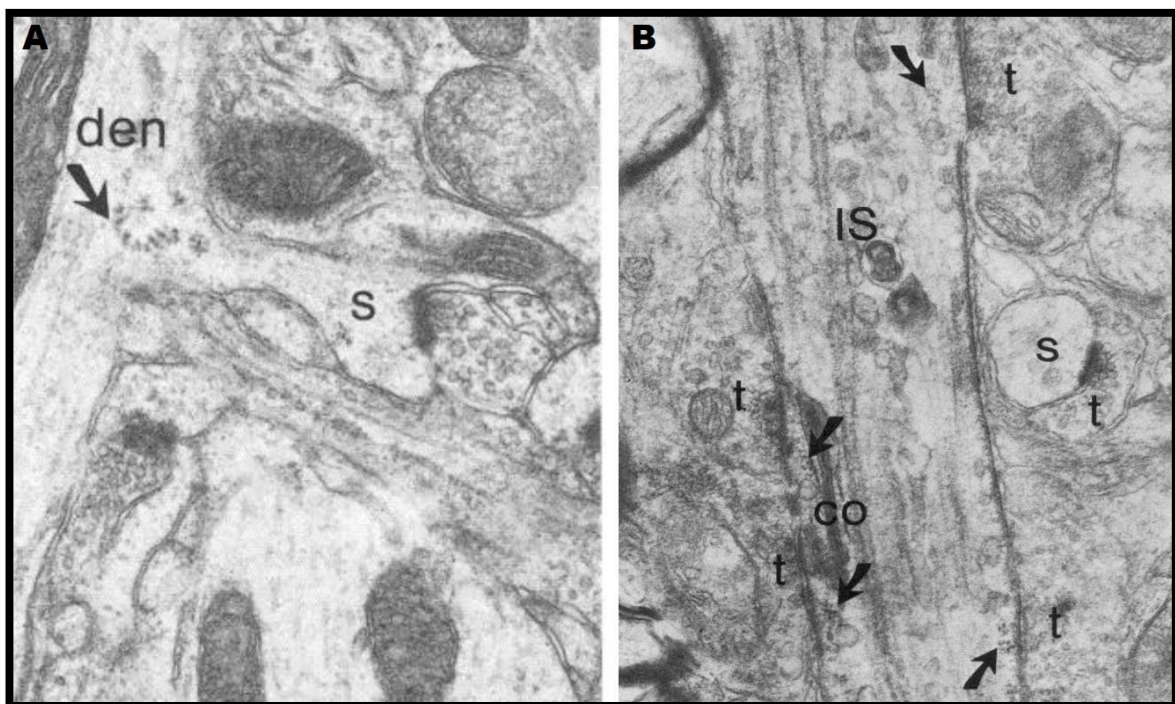


Figure 7: Detection of polyribosomes in the spine neck and axon segments.

Electron microscopy images of dentate gyrus cells illustrating the distribution of the polyribosomal rosettes (arrow in A) observed on the dendritic spines (S), and the distribution of polyribosomes (arrows in B) located in the axon initial segment, directly under the synaptic terminals of pyramidal neurons (Steward and Levy 1982; Steward and Ribak 1986).

Confirming the capacity of neurites to support local synthesis of both cytosolic and transmembrane proteins, electron microscopy and immunocytochemical studies have also indicated the presence of golgi-like structures and various components of the translational machinery in both axons and dendrites (Rook et al. 2000; Steward and Schuman 2001; Zheng et al. 2001; Willis et al. 2005; Merianda et al. 2009; Moon et al. 2009). This, together with the presence of localized mRNAs led to the hypothesis that localized structures and machineries could mediate local translation and posttranslational modification (PTM) of proteins (Steward et al. 1988; Steward and Schuman 2001). Importantly, this suggested that local translation could account for an immediate response to external cues, conferring greater flexibility to growth and plasticity.

Although several studies reported specific enrichment of mRNAs (e.g. *β -actin*, *Arc* and *CamKIIa*) and their corresponding protein products in response to growth factors and activity in activated synapses (Steward et al. 1998; Ouyang et al. 1999; Scheetz et al. 2000), it remained unclear that local translation occurred specifically at the synapses, due to the lack of sufficient information to refute rapid transport of protein from the cell body or from the neighboring Schwann cells (Alvarez et al. 2000; Koenig et al. 2000; Court et al. 2008).

Pioneering studies provided evidence for local *de novo* protein synthesis using microlesion approaches to isolate neurites from soma combined with addition of translational inhibitors, demonstrating its role in facilitating long-lasting synaptic enhancement in response to growth factors (Kang and Schuman 1996), or in promoting chemotropic response of axons to attractive and repelling cues (Campbell and Holt 2001).

These studies thus provided compelling evidence for local translation of protein in neurites that support growth and plasticity. Other studies developed cell culture techniques in which neurons are plated in compartmentalized chambers containing a porous membrane that allows the penetration of neurites exclusively into the distal compartments. This technique not only enables separation of cell bodies from neurites, but also eliminates glial cells and other possible contaminants. When combined with metabolic pulse labelling approaches in which radiolabeled amino acids are incorporated by newly synthesized proteins, these studies indicated the competence of the somaless neurite to locally produce *de novo* proteins (Torre and Steward 1992; Feig and Lipton 1993; Eng et al. 1999; Zheng et al. 2001).

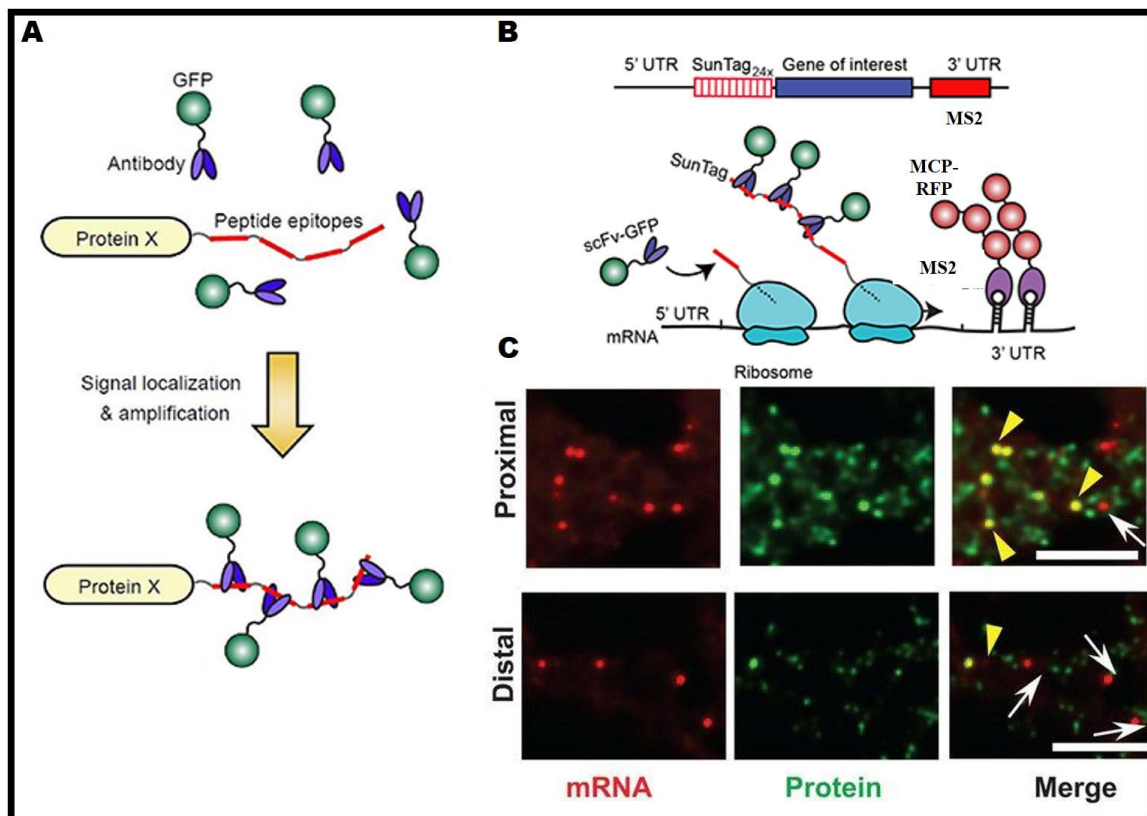


Figure 8: Single molecule imaging of transcripts and nascent peptides.

A) Scheme of the SunTag single molecule imaging system. Nascent peptides are labelled by the binding of co-expressed GFP-fused antibodies clustered on the translating protein (Tanenbaum et al. 2014). B) Simultaneous usage of the SunTag and MS2-MCP systems enables detection of both transcripts (MS2-MCP-RFP) and nascent peptides (scFv –GFP) (Yan et al. 2016). C) Primary

hippocampal dendrites co-expressing a MS2-MCP mRNA and scFv-GFP. Both repressed mRNAs (red, white arrows) and translated mRNAs (yellow, yellow arrows) are detected, with changes in the relative frequency of repressed mRNAs along the proximo-distal axis of the dendrite. Fixed imaging using single molecule FISH (red – mRNA) and Immunofluorescence (green – protein) (Wu et al. 2016).

Fluorescent reporters proved beneficial for understanding spatio-temporal translation patterns in neurons. Local translation at hotspots near ribosomes and synaptic sites was convincingly reported using a destabilized and membrane-tagged form of the green fluorescent protein (GFP) flanked by the 5' and 3' Untranslated Regions (UTR) of CAMKII mRNA in dendrites (Aakalu et al. 2001). Photoconvertible and photobleachable reporters have also been important in understanding protein translation at subcellular domains (Leung et al. 2006; Strohl et al. 2017). For example, the Kaede photoconvertible protein undergoes an irreversible green to red photo-conversion upon Ultraviolet illumination and enables the visualization of newly synthesized protein which appears green (Leung et al. 2006). More recently, a single molecule approach to detect individual translation sites was made possible through the Suntag system (Fig. 8 A). This method combines the previously explained MS2-MCP technique (for live imaging of mRNA) with the Suntag technology, to visualize nascent peptides (Fig. 8 B) (Tanenbaum et al. 2014). The Suntag technology consists in tagging the open reading frame (ORF) of interest with multiple copies of a cognate peptide recognized by a co-expressed single chain variable fragment (scFV) fused to a fluorescent protein (Morisaki et al. 2016; Wang et al. 2016; Wu et al. 2016; Yan et al. 2016). This technique was also instrumental in providing quantitative readouts of translational events i.e., initiation, elongation and pauses.

Proteomic approaches have also been used for systems-wide detection of the proteins present in the different sub-compartments of a neurite (Shigeoka et al. 2016; Zappulo et al. 2017; Cagnetta et al. 2018). Zappulo et al. used neuronal fractionation, and performed mass spectrometry, ribo-seq and RNA-seq on neurite and soma fractions. This work demonstrated

that the proteome detected in the neurites mostly corresponds to the population of neurite-localised and actively translated transcripts. Recently, the work of Cagnetta et al characterized the dynamic change of basal and specific attractive and repulsive cue-dependent remodelling of nascent translatoemes (Cagnetta et al. 2018). This approach, performed on somaless axons, also revealed the existence of cue-specific patterns of translated proteins. Thus, proteomic approaches proved beneficial in unravelling the subcellularly synthesised proteomic landscape.

Taken together, the above highlighted studies have now provided conclusive evidence for the coupled process of RNA localization and subsequent local translation as a mechanism for decentralization of gene expression.

1.5 Advantage of RNA localization

The coupled process of spatio-temporal sorting of transcripts and local translation has several advantages over transport of proteins. First, the intracellular cytosolic environment is heavily crowded and estimated to contain 5-40% of various biological macromolecules (Uversky 2017). In this respect, transport of a single copy of mRNA is energetically more favorable, reduces the cost of the transport of several proteins and additionally prevents mis-localization of the transcripts (Medioni et al. 2012). Second, efficient and rapid partitioning of mRNAs and translation enables the cells to promptly adapt to developmental cues and environmental changes. Moreover, since few copies of mRNA is sufficient to synthesis sufficient protein through several rounds of translation, the response is more robust. For example, rapid and increased accumulation of β -actin mRNA and protein at the growth cones have been observed within 2 mins after treatment with chemo-attractants (Zhang et al. 2001). Similarly, another study reported protein synthesis-dependent accumulation of Cofilin at the growth cone within 5 minutes in response to a chemo-repellant (Piper et al. 2006). Third, targeted localization and translation is beneficial for increasing protein concentration locally, at specific subcellular location. For example, a

study performed on migrating fibroblasts estimated that local β -actin translation supplies only 7% of the actin consumed for actin polymerization at the leading edge. This small percentage of translated products may still prove beneficial for actin polymerization and growth, if it generates significantly higher protein concentration at specific local sites (Condeelis and Singer 2005). Indeed, several lines of work have shown translation-dependent local increases in actin concentration and their role in regulating growth and branching (Zhang et al. 2001; Leung et al. 2006; Yao et al. 2006; Wong et al. 2017). Fourth, localized translation of protein restricts the availability of proteins at sites where they could be toxic or interfere with cell function. For example, the myelin basic protein (MBP) is a sticky protein that can interact non-specifically with any cell membrane and needs to be restricted to the processes of oligodendrocytes. This is achieved by targeting of *MBP* mRNA to this region coupled to localised protein synthesis (Smith et al. 2001). Last, newly-synthesized proteins produced locally have a PTM profile distinct from that of “aged” proteins transported from the cell body. Immunocytochemical studies indicated the presence of golgi complexes in the dendrites and indicated that certain newly transcribed proteins acquire glycosylation (Steward and Schuman 2001). Although this experiment did not reveal the protein or groups of proteins undergoing PTM nor its functional relevance, the data strongly suggested that protein glycosylation may occur in dendrites and axons. One study showed the enrichment and local translation of cAMP responsive element binding protein (CREB) at the distal ends of axons in response to nerve growth factor. This study further showed that the locally synthesized CREB protein are the source of the phosphorylated CREB that are retrogradely transported to the nucleus and are important for the activation of transcription of CRE-dependent transcription factors and for axon survival (Cox et al. 2008).

1.6 Importance of Local Translation in neurons

1.6.1 Local translation contributes to axon growth and maintenance

During growth and pathfinding, growth factors and guidance cues, present at specific stages and locations, precisely regulate the migration of axons and dendrites through a complex environment to reach their final target. Different guidance cues have been shown to activate specific signaling pathways that trigger rapid mRNA translocation and translation of cytoskeletal regulators such as β -actin, Cofilin, or RhoA (Campbell and Holt 2001; Leung et al. 2006; Holt and Schuman 2013; Piper et al. 2015; Wu et al. 2016). Consequently, the newly synthesized proteins modulate the dynamic organization of the actin/ MT cytoskeleton, thus supporting growth, branching and retraction (Fig. 9) (Cioni et al. 2018).

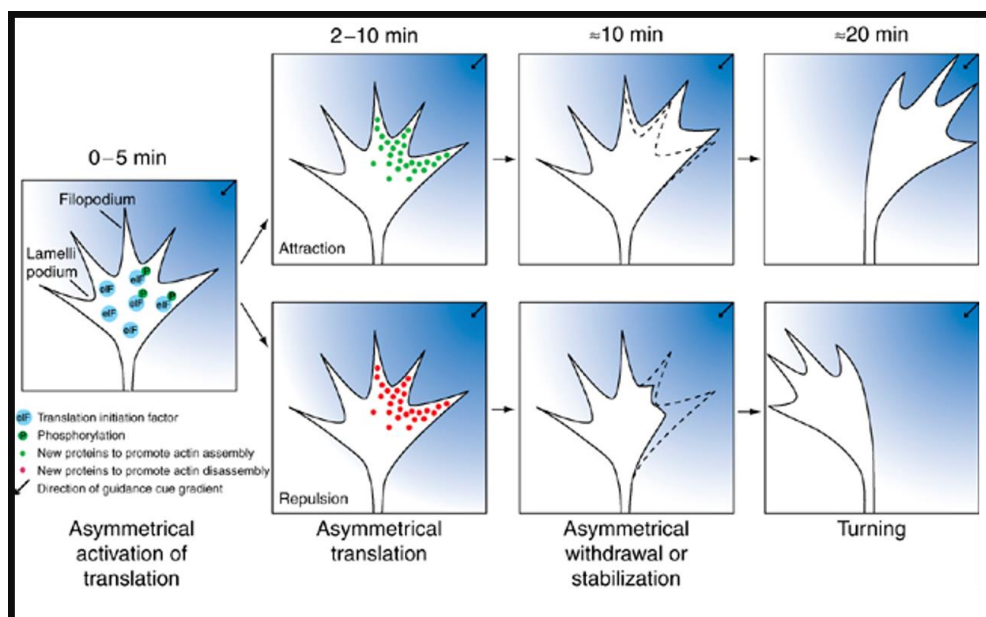


Figure 9: Schematic representation of how cue-induced local translation influences the growth cone dynamics.

Guidance cues induce chemotropic response by binding to specific receptors that activate specific downstream signalling pathways. This results in an immediate and robust local translation of mRNAs that influences the cytoskeletal network (β -actin mRNA in particular). Attractive guidance cues induce translation of genes involved in growth cone stabilization and extension, while repulsive cues induce translation of genes involved in retraction and turning away from the guidance cue (Lin and Holt 2007).

For example, *in vitro* neuron culture studies demonstrated a marked increase in β -actin mRNA localization and translation at the growing tips of axons, in response to Netrin-1, BDNF or Shh chemoattractants (Leung et al. 2006; Yao et al. 2006; Welshhans and Bassell 2011; Lepelletier et al. 2017). This accumulation resulted in axon outgrowth and turning. Similarly, the chemorepellent Semaphorin 3a (sema-3a) has been shown to induce local protein synthesis and growth cone collapse. For example, Sema-3a elicits a rapid localization and translation of the actin regulator Rho. In cultured DRG axons mechanically isolated from the soma, inhibiting Rho protein synthesis, or more specifically abolishing the activity of RhoA, abolished growth cone collapse (Wu et al. 2005). Moreover, an increasing number of studies from developing cultured neurons and *in vivo* systems have revealed that a wide repertoire of mRNAs are targeted to specific subcellular compartment in response to extracellular cues and their translation is fundamental for growth (Hengst et al. 2009; Leung et al. 2013; Cagnetta et al. 2018). During development and also upon reaching the target, axons form branches that facilitate target innervation. *In vivo* live imaging of the *Xenopus* retinal ganglion cell (RGC) axons elegantly demonstrated the docking of RNA at specific 'hot spots' and the accumulation of *de novo* synthesis of β -actin at these spots. This precise localization of the RNA correlated with new branch emergence and inhibition of local translation resulted in reduced axonal arborizations (Wong et al. 2017).

In addition to growth and branching, local synthesis of proteins and retrograde transport of the signals from axon to nucleus have been shown to promote neuron survival. Several *in vitro* studies have demonstrated the activation of anti-apoptotic and pro-survival transcriptional factors such as CREB and its activators myo-inositol monophosphatase 1 (Impa-1), are essential for the survival of the axon (Cioni et al. 2018). Furthermore, cue-induced transport and local translation of lamin B in *in vivo* RGC axons has shown to be crucial for axon integrity (Yoon et al. 2012).

1.6.2 Local translation contributes to axon regeneration

A striking feature of axons is the decline of mRNAs and polyribosomes as they progressively mature and cease to grow. This observation prompted scientists to test the capacity of a neuron to regenerate following injury. Both *in vivo* and *in vitro* studies have now established that peripheral nervous system (PNS) neurons can regenerate following axotomy or crush by eliciting a cascade of axonal response. Interestingly, the ability to regenerate is at least partially due to mRNA recruitment and local protein synthesis at the site of injury (Verma et al. 2005; Costa and Willis 2018). Indeed, local translation of axonally-localized mRNAs has been described to participate to the retrograde signal that facilitates global response by activating genes and specific signaling pathways.

For example, *Importin-β* and *vimentin* mRNAs are locally translated in the axon following injury. Axonally synthesized Importin-β then assembles into a heterodimeric complex with Importin-α and dynein complex (Hanz et al. 2003) and is translocated to the nucleus. As revealed by *in vivo* RNA deep sequencing data of wildtype and conditional knockout of *importin-β* 3'UTR mice, this translocation is essential for induction of the regeneration-associated transcriptome (Perry et al. 2012; Batista and Hengst 2016). Notably, similar studies have further shown the participation of local translation and subsequent retrograde signaling to the activation of a transcriptional response essential for post-traumatic neuronal regeneration (Ben-Yaakov et al. 2012; Baleriola and Hengst 2015; Rozenbaum et al. 2018).

1.6.3 Local translation contributing to plasticity

Plasticity describes the change in strength of synaptic connections in response to neuronal activity and learning. An increase in synaptic strength after synaptic stimulation is called long-term potentiation (LTP) while a decrease in synaptic strength following synaptic stimulation is called long-term depression (LTD). The cellular modifications that underlie LTP or LTD require *de novo* proteins synthesis. Kang and Schumann provided the direct

evidence for local protein synthesis leading to synapse enhancement (Kang and Schuman 1996). Experiment on rat hippocampal slices separated from the cell body resulted in synaptic enhancement in response to neurotrophins. Absence of such plasticity in the presence of protein synthesis inhibitors revealed that synaptic plasticity requires local protein translation.

Interplay between synaptic plasticity and local protein synthesis has been well studied using the invertebrate model, *Aplysia*. An elegant cell culture system was developed where the bifurcated sensory neuron makes contact with two motor neurons. Repeated application of the neurotransmitter serotonin to one of the motor neuron resulted in enhanced branch specific protein synthesis, which was abolished in the presence of protein synthesis inhibitors. This work also demonstrated that local protein synthesis was important for plasticity (Martin et al. 1997). Furthermore, several studies showed that branch specific transient transport and translation of mRNA encoding synapse related molecules such as eEF1A, sensorin A, are important for the maintenance of synapse (Schacher et al. 1999; Hu et al. 2003; Si et al. 2003; Lyles et al. 2006).

Taken together, the above studies established that neuronal activity modulates protein translation at the synapse, which in turn is important for plasticity of the synapse.

2 Mechanism of neuronal RNP Granule assembly and transport

The localization of RNA at specific subcellular sites occurs through various mechanisms such as diffusion and entrapment, local translation, local degradation and active transport (Dahm et al. 2007). It is now becoming evident that mRNAs in neurons are not localized as individual molecules but predominantly in the form of granules containing few RNA molecules and multiple regulatory components (De Graeve and Besse 2018). Following transcription, nascent transcripts are recognized by RNA Binding Proteins (RBPs) that dictate the final destination of the transcript (Muller-McNicoll and Neugebauer 2013). The recognition of the transcripts is mediated through interaction *via* sequence/ structural

motifs in RNA and specific modular domains found within RBPs. Upon nuclear export, the mRNA-protein particles modulate the assembly of mRNAs into larger membrane-less organelles, and enable distinct steps of post-transcriptional mRNA processing (Fig. 10 A). These granules have been observed to exhibit a wide range of sizes (100nm- 1000nm), and are characterized by the absence of a defining membrane (Anderson and Kedersha 2009). These organelles referred to as RNA protein granules (RNP) orchestrate the life cycle of an mRNA, beginning from RNA maturation including splicing and polyadenylation followed by downstream regulatory events, nuclear export and cytoplasmic localization of mRNAs and degradation (Kress et al. 2004; Glisovic et al. 2008; Tutucci and Stutz 2011). The transport RNP granules are then transported along the cytoskeleton in a translationally repressed manner to their destination for local translation. This multi-step RNA localization process will be explained in detail below.

2.1 Cis acting elements

Localization elements (LE), more commonly known as *cis*-elements, are motifs found within localized mRNAs that address mRNA to their specific destination. Strategies to identify *cis*-elements responsible for transport were initially based on reporter constructs fused to truncated parts of a localizing mRNA (Doyle and Kiebler 2011). These studies demonstrated that the information encoded by LEs can be either primary sequences or secondary structures, or a combination of both (Kloc et al. 2002a; Xing and Bassell 2013). The primary sequences could be tandem repeats of few nucleotides to >1 kb long sequence (Jambhekar and Derisi 2007). These *cis*-acting elements are predominantly found in the 3' UTR of the mRNA (for example, the 54nt sequence present in the 3'UTR of *β-actin* mRNA, sufficient to localize to axon and dendrites), while in some mRNAs they are present in the 5' UTR (for example, the 62nt long sequence in the 5'UTR of BC1 mRNA involved in dendrite targeting) (Mayford et al. 1996; Muslimov et al. 1997; Zhang et al. 2001; Vuppalanchi et al. 2010). Cis elements could also be sequences that form complex secondary structures (Meer

et al. 2012). For example, the G-quadruplex structures present in the 3' UTR of *PSD-95* and *CamKIIa* mRNAs have been shown to be important for localization (Pratt and Mowry 2013).

Interestingly, to date, no consensus sequences have been observed for mRNAs that are directed to the same subcellular compartment. The *cis*-elements are recognized by *trans*-acting factors (RNA binding proteins and associated proteins), which recruit motor proteins and link mRNAs to the transport machinery.

2.2 Trans-Acting Factors

Biochemical approaches, sequencing and computational analysis of DNA sequences brought to the spotlight a specific group of proteins called RBPs, based on their ability to bind RNA (Calabretta and Richard 2015). RBPs are modular in nature and can bind to a large number of mRNA targets *via* one or many RNA Binding Domains (RBD). Some well characterized canonical RBDs include the RNA recognition motif (RRM), the K-homology domain (KH), the double stranded RBD (dsRBD), the Zinc Finger motif (ZnF), the Piwi/Argonaute/ Zwillie domain (PAZ), the Sm domain, the DEAD/DEAH box and pumilio domain (PuF) (Glisovic et al. 2008; Kishore et al. 2010). Recent development in the field of RBP-RNA interactome capture and mass spectrometry lead to identification of an even larger group of RBPs (1,500). Quite intriguingly, this revealed that, in addition to the canonical folded domains, RBPs contain non-canonical domains exhibiting structural heterogeneity (Calabretta and Richard 2015; Hentze et al. 2018). The non-canonical domains are involved in RNA-protein interactions, and are broadly categorized as Intrinsically disordered regions (IDR) described in more details in section 2.5.

2.3 Assembly of RNP granules

Spatial organization of mRNAs by RBPs occur through the dynamic assembly of higher order structures referred to as RNP granules. Analysis of the neuronal RNP constituents from embryonic and young brain tissues revealed that these assemblages are enriched in mRNAs, RBPs, ribosomes, translational machinery, translational repressors and

motor proteins (Kanai et al. 2004; Elvira et al. 2006; Besse and Ephrussi 2008; El Fatimy et al. 2016; De Graeve and Besse 2018). A more systematic analysis of the proteomes of two distinct dendritically localized RNP granules, characterized by the presence of the RBPs Barentz and Staufen, revealed that the granule composition is heterogenous, and that these two granules share only a third of their components (Fritzsche et al. 2013). Similarly, FISH experiments have revealed that transcripts that are localized to the dendrites compartment are not sorted to the same granules (Mikl et al. 2011; Batish et al. 2012). Furthermore, the composition and properties of the RNP granules have been shown to change in space and in response to development and neuronal activity (De Graeve and Besse 2018). Thus, it is now emerging that RBPs associate with mRNAs to modulate the assembly of the mRNAs into diverse range of membrane-less organelles, recruit additional regulatory factors and enable distinct steps of post-transcriptional mRNA processing (Kress et al. 2004; Glisovic et al. 2008; Tutucci and Stutz 2011). Neuronal cells have been shown to contain different types of RNPs of varying constituents, size and shapes. These RNPs are classified based on their subcellular localization, composition and function, and commonly comprise stress granules, P bodies and transport granules (Fig. 10 A) (Courchaine et al. 2016).

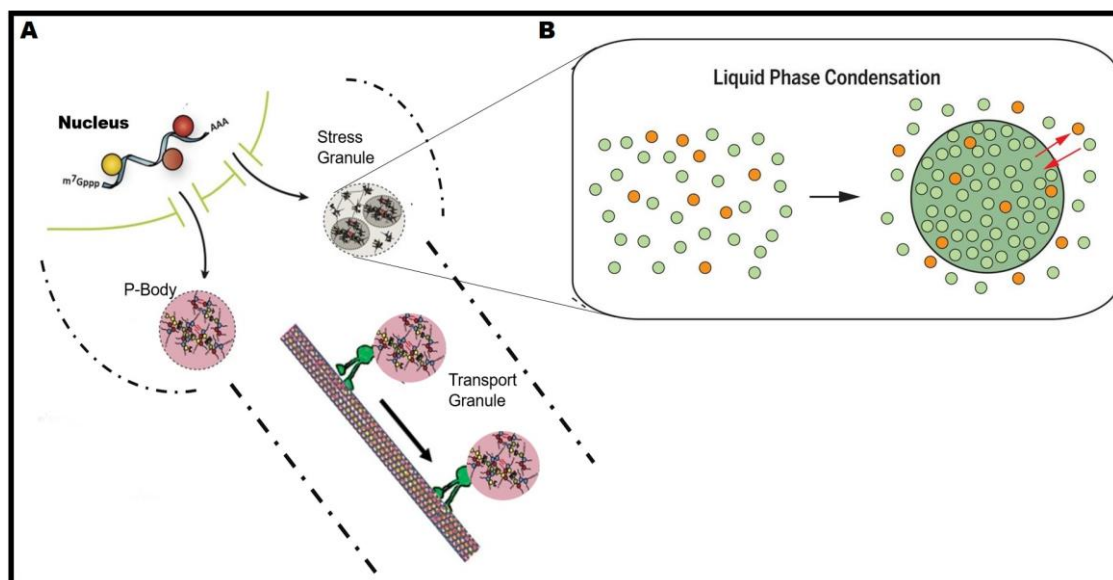


Figure 10: Schematic representation of the types and assembly paradigm of RNP granules in a neuron.

A) Following transcription, mRNAs are bound by RNA Binding Proteins and assemble into a diverse range of RNP granules. The functions of RNP granules include protecting the transcripts during various stress conditions (Stress granules), transporting the transcripts to specific subcellular compartments for local translation (Transport granules), and targeting the transcripts for degradation or translation silencing (P-Body) (Image adapted from (Protter and Parker 2016)). B) RNP granules can be formed by liquid-liquid phase separation, where an initially homogenous liquid solution demixes into two distinct phases, with one phase robustly increasing the local concentration of proteins and RNA (Protter and Parker 2016; Shin and Brangwynne 2017).

The assembly of RNP granules has recently been proposed to occur through a process known as liquid-liquid phase separation (LLPS) (Fig. 10 B) (Hyman et al. 2014). Cell free approaches have been crucial in understanding the process of LLPS and in dissecting the hierarchical process underlying their assembly. The *in vitro* phase separation experiment involves the demixing of poorly concentrated homogenous solution into a depleted phase and a crowded phase, thereby increasing the local concentration for specific proteins and nucleic acids (Weber and Brangwynne 2012; Courchaine et al. 2016). The dense phase then allows for the selective recruitment of further components. The assembly and disassembly properties of the droplets are regulated by several factors such as salt, temperature, pH, RNA and PTMs. The liquid like feature of RNP granules was hypothesized based on their ability to assume spherical shape governed by surface tension, fusion and dripping due to shear stress (Gomes and Shorter 2018). Moreover, RNP granules are in a dynamic state, rapidly exchanging molecule with the cytoplasm and having a fast-internal recovery as judged by Fluorescence Recovery After Photobleaching Technique (FRAP). As described below, compartmentalization into dynamic assemblies likely favours the controlled localization of specific molecules to specific subcellular domains along the cytoskeleton of the neuronal cell.

2.4 Transport of neuronal RNP granules

The transport of neuronal RNP granules to subcellular compartments is a highly regulated process (Fig. 11). Development of live imaging techniques enabled visualization of the dynamic trajectories of mRNAs along the axons and dendrites. Imaging of exogenous and endogenously-labelled RNA revealed that about 10% of labeled RNP granules were motile, exhibiting active directed movements that are dependent on an intact MT network (Knowles et al. 1996; Rook et al. 2000; Kanai et al. 2004; Dynein and Steward 2007; Park et al. 2014). Motile RNP granules exhibit different types of motion, transitioning between long pauses and short mobile phases with a global net bias in their trajectory (De Graeve and Besse 2018). Motion was shown to depend on intact microtubules, and the velocity of RNP transport suggests that transport is dependent on the activity of opposing molecular motors such as kinesin and dynein (Kiebler and Bassell 2006; De Graeve and Besse 2018). Indeed, purification of proteins associating with the conventional kinesin KIF5 identified several RBPs such as FMRP, Pur- α , Staufen as well as dendritically localized mRNAs such as *CamKII* and *Arc* RNA (Kanai et al 2004). As a proof of concept, knockdown of either kinesin or dynein impaired transport of localized mRNAs such as *MBP*, *Arc*, or *CamKII α* , in cultured neurons, thus affecting their cellular function (Carson et al. 2001; Aronov et al. 2002; Kanai et al. 2004; Dichtenberg et al. 2008; Ma et al. 2011).

More detailed investigation of the interplay between kinesin and several different RBPs revealed a specific mechanism of mRNA transport. This process involves interaction of RNP granule components and motor proteins. The motor proteins behave as adaptor molecules linking the RNP granules to the neuronal cytoskeleton network and are involved in both short-range and long-range transport. Several studies have shown RNP granule components physically interact with both MT-dependent and actin-based motor proteins (Huang et al. 2003; Davidovic et al. 2007; Dichtenberg et al. 2008; Bianco et al. 2010; Yoon et al. 2016; Urbanska et al. 2017). For example, FMRP associates with Kinesin in an RNA-dependent manner, an interaction that is dramatically increased upon stimulation of

cultured neurons (DICTENBERG et al. 2008). Likewise, intact actin filaments and interaction with plus end directed myosin Va have also been shown to be important for the short-range transport of RNP granules to somatodendritic compartments and to dendritic spines (YOSHIMURA et al. 2006; BALASANYAN and ARNOLD 2014; DE GRAEVE and BESSE 2018). However, it is still unclear what molecular mechanisms govern the recruitment of specific motor proteins to the granules. Nonetheless, these studies were instrumental in demonstrating that a discrete population of RNAs and RBPs are found associated to motor proteins, and that motor proteins facilitate the distribution of RNP granules. While MT-based transport is required long distance transport of cargoes, actin-based transport may be involved in local delivery and docking of the RNP granules (KNOWLES et al. 1996; YOON et al. 2016).

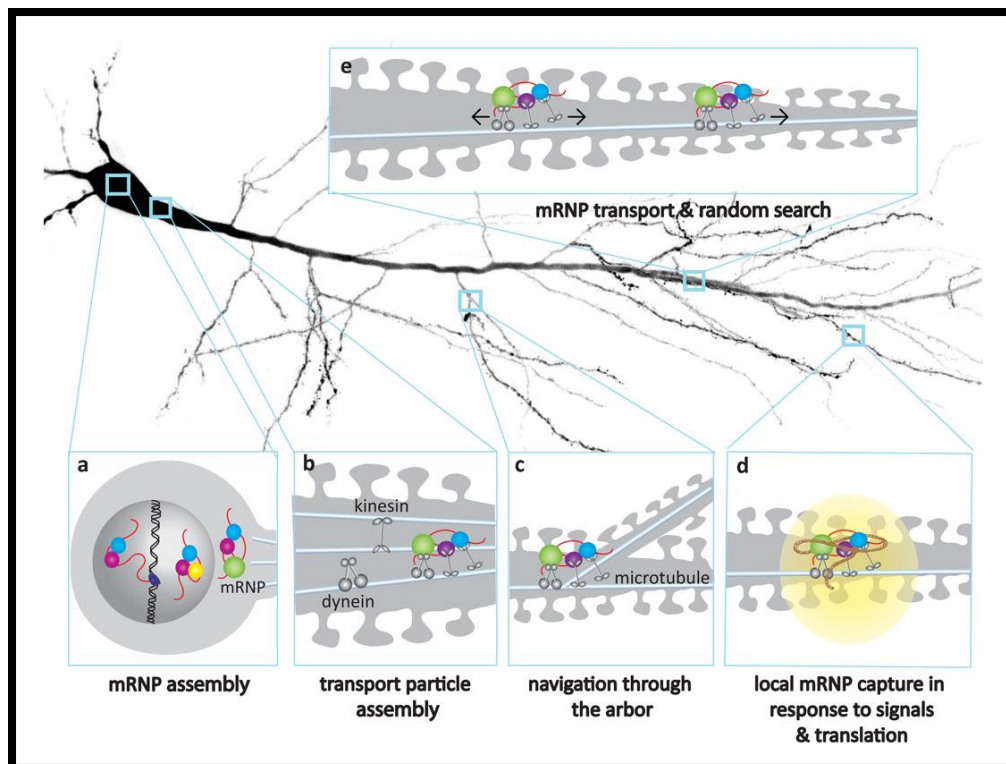


Figure 11: Schematic representation of the regulated process of assembly and transport of RNP granules neural cytoskeleton.

(A) mRNA-RBP interaction leads to the assembly of RNP granules. B) In neurons, RNP granules undergo active bidirectional transport along the neuronal cytoskeleton via opposing motor proteins, such as kinesin or dynein. These motors are recruited to the RNP granules and C) assist in sorting the granules to specific subcellular compartments along the axons and dendrites. D) RNP granules can

dock at specific regions in response to extracellular cues or neural activity. Local translation of the transported transcript supports growth, maturation and plasticity (Buxbaum et al. 2014).

The transport of the RNP granules had been suggested to occur in a translationally repressed manner based on experimental data that revealed the presence of specific translational repressors in transport granules (Kanai et al. 2004; Barbee et al. 2006; Elvira et al. 2006; Sossin and DesGroseillers 2006; Fritzsche et al. 2013; El Fatimy et al. 2016). Furthermore, purification of neuronal RNP granules revealed that they sedimented in fractions distinct from polysomal fractions, further suggesting that the granules were translationally silent (Krichevsky and Kosik 2001). Through the utilization of different experimental approaches, such as *in vitro* translation systems and ribopuromylation, it was revealed that indeed RNP granules remain in a translationally repressed state (Darnell et al. 2011; Graber et al. 2013; Pimentel and Boccaccio 2014). This mode of translational repression allows for the controlled expression of mRNA at specific subcellular location and prevents the degradation of the transcript during transport (Kiebler and Bassell 2006; Besse and Ephrussi 2008).

Following the transport of translationally repressed transcripts, RNP granules are docked at specific sub-compartments, where the transcripts are released for local translation of associated mRNAs. Immunofluorescence and live imaging of cultured neurons have revealed a precise positioning of RNP granules at axon and dendritic branch points and in dendritic spines (Dynes and Steward 2012; Urbanska et al. 2017; Wong et al. 2017). Such precise docking of RNP granules have been correlated with local protein synthesis and new branch emergence (Wong et al. 2017).

Thus, these studies show a complex multistep regulatory process occurring right from assembly of the granules until the transport and local translation. Furthermore, studies over the years have highlighted the prominent role played by RBPs in the post-transcriptional regulation of mRNA in space and time.

2.5 Prion-like domains in RBPs

IDRs or Intrinsically disordered proteins are abundant in nature, found approximately in 40% of the eukaryotic proteome and are involved in various cellular functions (Babu 2016). The presence of IDRs within RBPs appear to be conserved from yeast to human. Such domains have for long been poorly studied, but gained wide attention during the past few years owing to their distinct structural features and lack of stereospecific interactions and functional property. IDRs exhibit conformational flexibility, adopting a range of 3D structures, but can fold upon binding to interacting partners (Tompa 2005; Uversky 2015). The structural polymorphism of IDRs provides the flexibility to transiently interact with multiple partners (Fonin et al. 2018). IDRs have been shown to play an essential role in various cellular process such as assembly and guidance of RNP granules, cell signaling and control pathways (Toretsky and Wright 2014; Frege and Uversky 2015). Furthermore, IDRs have been shown to be targets of various PTMs, such as phosphorylation, methylation, acetylation, which can modulate their interaction with target partners (Wright and Dyson 2015; Bah and Forman-Kay 2016). To date, a precise unifying definition of IDRs is still lacking, and various algorithms using specific sets of rules to detect IDRs within a protein have been developed and used (Li et al. 2015). A general rule however is that IDRs are domains composed of at least 30 residue that i) have a biased amino acid composition, and ii) lack order promoting amino acids. Different classes of IDRs have been defined based on the nature of their enriched residues: while charged acidic or basic residues are characteristic of RGG repeat-containing domain such as the one found in DDX4, uncharged polar residues with interspersed aromatic residues are characteristic of Prion-like domains (PLDs) such as the one found in TDP43 (Alberti and Hyman 2016; Uversky 2017).

Initially, Prion-like domains acquired their name based on their sequence similarity to the mammalian and yeast prion proteins with self-replicating properties. The mammalian prion protein can adopt different conformations with distinct cellular functions. The normal cellular form (PrP^c) can transform into the prion form (PrP^{sc}) assembling into β -amyloid

fibrils, thus endowing cells with infectious properties (Shorter and Lindquist 2005). The fungal prion protein Sup 35, an essential component of the translation termination machinery, has been well studied because of its self-templating property. The N-terminal domain of this protein is rich in glutamine and asparagine and has been shown to be essential for nucleation, subsequent polymerization and stabilization of a functionally inactive amyloid state (Ross et al. 2005b). Following the discovery of Sup 35, three other self-templating prion proteins were detected in *S. cerevisiae*: Ure2p, Rnq1p and Swi1p. Comparison of the fungal prion proteins and mammalian proteins showed no sequence similarity but showed a striking enrichment for glycine and uncharged polar amino acids, such as glutamine and asparagine (Malinovska et al. 2013b). This sequence conservation prompted scientists to develop a genome-wide search for “prion-like” domains in other species (Alberti et al. 2009; King et al. 2012). The first algorithm was based on the detection of amino acid sequences that are longer than 60, with an enrichment in asparagines and glutamines (Alberti et al. 2009). Of the 200 proteins identified using this algorithm, 24 proteins were shown to contain a PLD and confer prion characteristics. Subsequently, several algorithms with advanced compositional search that are more adapted to a wide range of species have been developed to screen for proteins with a PLD. These analyses revealed that PLDs are quite common in eukaryotic proteins and are overrepresented in RBP (30%) and DNA Binding Protein (33%) (March et al. 2016; Harrison and Shorter 2017). Recently, a precipitation experiment performed on mouse tissues and mouse cell line with an aggregation inducing drug (biotinylated isoxazole) resulted in the precipitation of RBPs that were constituents of neuronal transport granules, stress granules and P bodies and have been implicated in several neurodegenerative disorders. Quite interestingly, the precipitated pool of RBPs also had a striking enrichment for PLD (Kato et al. 2012). The predominance of the PLD in RBP and the self-templating property of PLD thus suggested a possible role for this domain in the macro-molecular assembly of RNP granules.

Following these initial observations, several labs have set out to understand the physicochemical properties underlying granule assembly, and the contribution of RBP-associated PLDs in this process. As described below, a multitude of these studies were based on *in vitro* cell free approaches in which RNP assemblies were reconstituted *in vitro* using purified RBPs containing PLD.

2.5.1 Properties of PLD

The role played by PLDs in granule assembly only recently began to be unraveled, pioneered by the work on Fused in Sarcoma (FUS) PLD. FUS is an RBP that contains a N-terminal PLD and a RRM domain. It is involved in DNA repair and gained attention because clusters of neurodegenerative disease-causing mutations were identified in its PLD (Ravanidis et al. 2018). *In vitro* assays revealed that the isolated PLD of FUS was sufficient to facilitate the demixing of molecules from solution and their assembly into liquid-like droplets reminiscent of RNP granules found in living cells (Lin et al. 2015). Subsequent studies with different PLD-containing proteins revealed that PLDs from various RBPs were sufficient to promote demixing and high-order structure assembly (Kwon et al. 2013; Lin et al. 2015; Molliex et al. 2015). Thus, multivalent interactions achieved through PLDs have been shown to be important for liquid like properties of the phase separated droplets. Furthermore, these studies also demonstrated that the requirements for droplet organization, formed either from the full-length protein or the isolated PLDs, were dependent on protein concentration, salt, temperature, crowding and PTMs, such as phosphorylation, sumoylation etc (Fig. 12) (Kato et al. 2012; Patel et al. 2015; Monahan et al. 2017; Boeynaems et al. 2018; Carpenter et al. 2018). However, the assembly of these droplets occurred in conditions which were not near to the physiologic salt and protein concentrations. Remarkably, addition of RNA to the mixture promoted LLPS at a more physiologically relevant salt and protein concentration (Lin et al. 2015; Smith et al. 2016). Furthermore, addition of an RNA altered the material properties i.e., increased the fluidity of the liquid droplets. (Zhang et al. 2015). Here, RNA could either function as a negatively

charged molecule involved in electrostatic interactions or are involved in multivalent interaction with the RBDs and the PLD (Boeynaems et al. 2018).

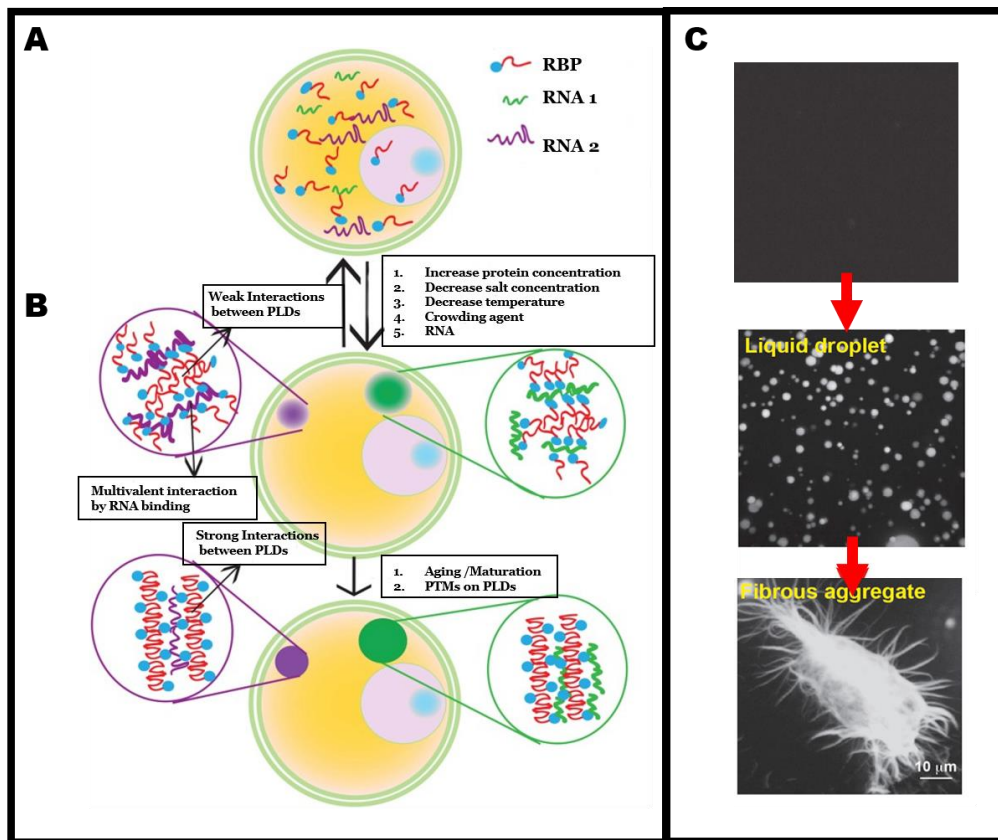


Figure 12: Role of PLDs in granule assembly and transition into pathological aggregates.

A) Schematic representation of RNP granule formation and maturation. RNP granules can assemble *via* LLPS, which is sensitive to changes in protein concentration, salt, temperature, RNA concentration or macromolecular crowding. RNP granules contain proteins that are enriched for PLDs. B) The liquid-like behaviour of these granules depends on weak interactions involving PLDs as well as RNA and RBDs. These liquid-like assemblies can mature into solid-like structures with stronger interaction between molecules, possibly involving fibrillization (Guo and Shorter 2015). C) Cell- free approach demonstrating the LLPS-driven formation of liquid droplets followed by a transition into a solid fibrous aggregate. The RNP granule component, FUS, separates from the solution into liquid droplets and matures into solid aggregates after 5h incubation (Patel et al. 2015).

Accumulating evidence from the recent past has thus far shown that multiple interactions between RNP components underlie the assembly of phase-separated RNP

assemblies. In this context, PLD could either function as the scaffold for granule assembly through multivalent non-specific interactions, or provide a means enhance their assembly and dynamics (Fig. 12) (Lin et al. 2015; Li et al. 2018; Protter et al. 2018). Quite intriguingly, a recent study on Pab1 protein expanded the proposed role of PLDs and showed that Pab1 PLD was dispensable for granule assembly, and that demixing was abolished in the presence of RNA (Riback et al. 2017). This study suggested that the phase separation was rather mediated through weak electrostatic interaction involving protein-protein interaction. Furthermore, two recent studies, using yeast PLD containing protein, highlighted a rather new function for the PLD as solubilizers of proteins and prevent the transition of the protein into aberrant aggregates (Franzmann and Alberti 2018; Franzmann et al. 2018; Kroschwald et al. 2018). Thus, the role of PLD could be seen as either organizers of the RNP granules or solubilizers and regulate the material property of the granules.

Phase separation can also be triggered through multiple copies of interacting domains (MCID) that are involved in multivalent heterotypic interactions with proteins and nucleic acids (Li et al. 2012; Zeng et al. 2016; Wheeler and Hyman 2018). The Rosen lab elegantly demonstrated the involvement of multiple copies of folded protein-protein interaction domains in the *in vitro* phase separation of two signalling proteins (Li et al. 2012). This phase separation was dependent on both the protein concentration and valency of the interacting partner. Furthermore, this study and others were able to show that addition of RNA to MCID proteins further promotes droplet formation (Li et al. 2012; Zhang et al. 2015). Thus, these studies demonstrated that multivalent heterotypic interactions between RNA molecules and RBD can regulate phase transition in addition to IDRs.

Together, these studies have shown that governing principle for the assembly of RNP granules could be through multivalent interactions, arising either through IDRs or multiple folded domains, or the concerted action of both.

2.5.2 Function of PLDs

An interesting question to address is if the PLD-mediated higher order assembly is essential for a cell. Studies are now beginning to show that the oligomeric assembly has both beneficial and deleterious effect to a cell depending on the environmental condition and cell type.

PLDs have been implicated with a pivotal role for adaptive learning and memory (Keleman et al. 2007; Fiumara et al. 2010; Heinrich and Lindquist 2011; Kruttner et al. 2012; Bakthavachalu et al. 2018). In *Drosophila*, the CPEB orthologue Orb2 contains an RNA-binding domain, a zinc finger domain, and an amino-terminal PLD. Orb2 proteins are involved in the expression of synapse-specific proteins and required for long-term memory (Mastushita-Sakai et al. 2010; Kruttner et al. 2012). The *Drosophila* Orb2A isoform exists in 2 different states, monomeric and oligomeric state similar to prion like properties (Kruttner et al. 2012; Majumdar et al. 2012). Interestingly, the PLD of Orb2 has been shown to be important for the assembly into oligomeric state, and this activity-induced conformational switch is essential to relieve translational repression and trigger long term memory (Khan et al. 2015).

In addition to this physiological function, lines of evidence compiled over the last years have indicated a compelling link between RBDs enriched in PLD and neurodegenerative diseases. A hallmark of neurodegenerative disease is the accumulation of protein aggregates occurring either due to protein misfolding, or due to altered homeostasis (King et al. 2012). Strikingly, pathological protein inclusions observed in patients affected with neurodegenerative diseases revealed a disturbing number of RBPs that are particularly enriched with PLDs (Gitler and Shorter 2011; Harrison and Shorter 2017). Recent work proposed that the dynamic RNP granule assembly is a metastable state, and that a change in the morphology and/or dynamic properties of RNP granules underlies the transition into persistent pathological amyloid aggregates (Lin et al. 2015; Molliex et al. 2015; Patel et al.

2015; Aguzzi and Altmeyer 2016; March et al. 2016). Mutations within the IDR, or proteome imbalance due to aging, would thus result in the alteration of the physiological function of the protein, leading to a shift in the maintenance and clearance of RNP granules, change in the interactions with components of the RNP granules and/or misfolding of the RBP due to repetitive assembly and disassembly (Fig. 12 C) (Aguzzi and Altmeyer 2016). Furthermore, this altered homeostasis of RNP granules would also disrupt RNA recognition and gene expression (Conlon and Manley 2017).

As mentioned earlier, mutations predominantly found in the PLD of FUS leads to both familial and sporadic amyotrophic lateral sclerosis. FUS positive inclusions have been detected in the cytoplasm of degenerating neurons (Ravanidis et al. 2018). Indeed, *in vitro* studies have now shown that disease linked mutations and ageing lead to the transitioning of the liquid droplets into stable aggregated fibrous state (Fig. 12 C') (Murakami et al. 2015; Patel et al. 2015).

Although a paradigm for the assembly of the RNP granules and maturation into pathological aggregates have been described *in vitro*, a direct *in vivo* link between PLDs and pathological aggregate assembly is still lacking.

3 Imp, a conserved RBP

β-actin mRNA was one of the first-studied transcripts for its subcellular distribution pattern in migrating chicken fibroblasts (Lawrence and Singer 1986) and neurons (Bassell et al. 1998). In both cell types, localization is driven by a 54-nucleotide *cis*-element located in the 3'UTR of *β-actin* mRNA. An UV-crosslink of the *β-actin cis*-element from chick embryo fibroblasts followed by a purification of associated *trans*-acting factors led to the identification of the 68kDa Zipcode Binding Protein 1 (ZBP1) (Ross et al. 1997). Subsequently, independent studies identified ZBP1 orthologues in a wide range of organisms including human, containing 3 variants, Igf-II mRNA Binding Proteins (IGF2BP 1-3 or Imp 1-3), murine c-myc coding region instability determinant binding protein (CRD-BP),

Xenopus Vg1 RNA-binding protein (Vg1RBP) and *Drosophila* Imp (Fig. 13 A). These proteins have been shown to bind a number of mRNA targets including *IGF-II*, β -actin, *Vg1*, or *c-myc* (Deshler et al. 1998; Doyle et al. 1998; Nielsen et al. 1999; Zhang et al. 1999; Nielsen et al. 2000), and are involved in posttranscriptional events such as RNA localization, RNA stabilization and translational inhibition (Kislauskis et al. 1994; Doyle et al. 1998; Huttelmaier et al. 2005).

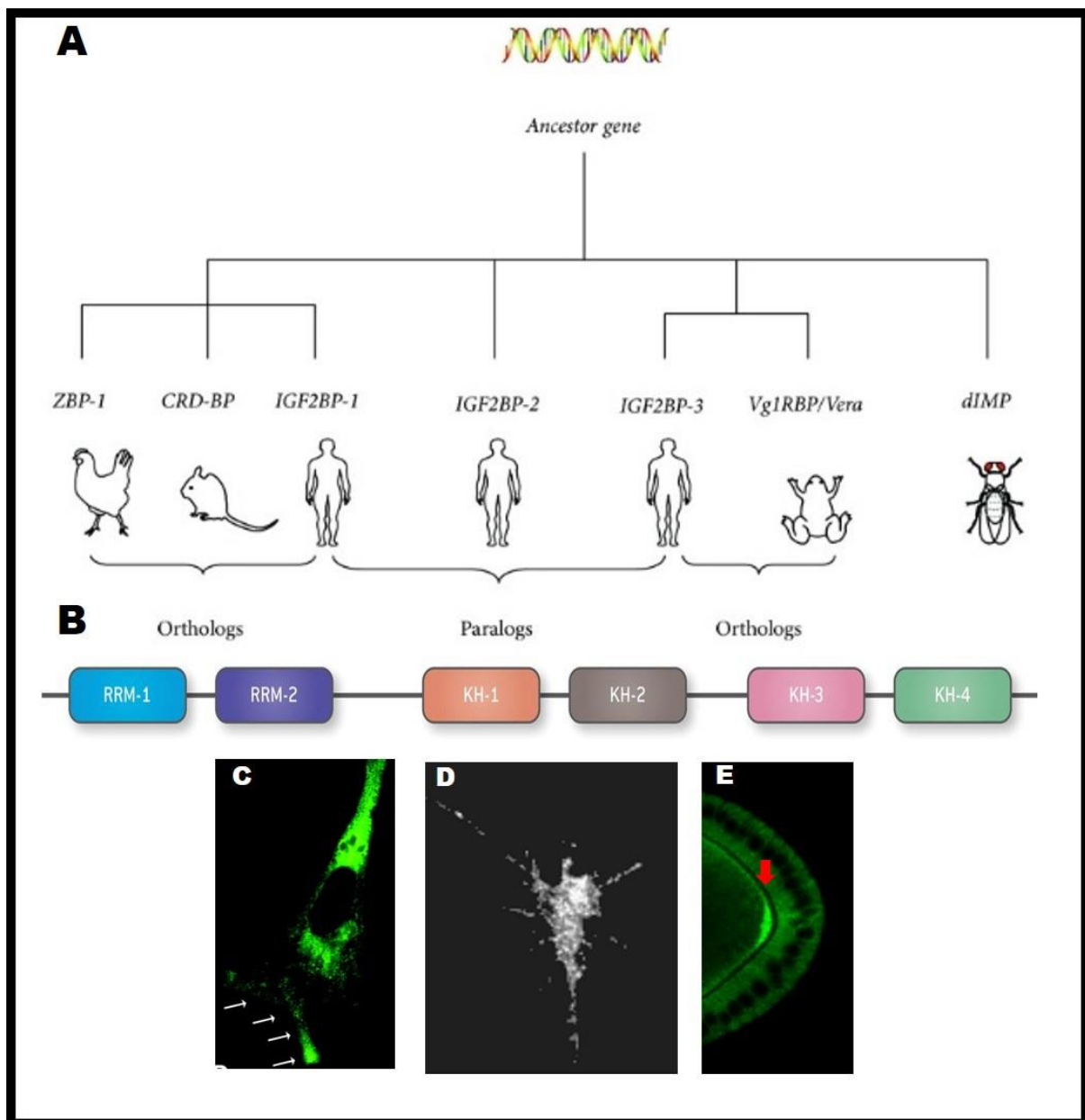


Figure 13: Phylogeny and Structure of the Imp family of RNA-binding proteins.

A) Phylogenetic tree showing the phylogeny of Imp family members (Cao et al. 2018). B) Schematic representation of the domain architecture of Imp protein. Most Imp proteins contain two N-terminal RNA Recognition Motif domains (RRM 1 and 2 represented in blue and purple) followed by four C-Terminal K-Homology domains (KH 1,2,3,4 are represented in orange, brown, pink and green respectively) (Degrauwe et al. 2016a). Examples of the distribution of Imp in the cytoplasm and as granular structures (white arrow) along the leading edge of a migrating cell (C), along the growth cones of vertebrate neurites (D) and concentration of Imp as a crescent (red arrow) at the posterior pole of the stage 9 *Drosophila* oocyte (E) (Farina et al. 2003; Leung et al. 2006; Munro et al. 2006).

3.1 Imp regulates the fate of associated transcripts

Imp proteins show similarity at the structural level, containing 6 canonical RBDs with variabilities mostly observed in the linker regions. Imp contains two RRM at the N-terminal followed by 4 KH domains (Nielsen et al. 2000) (Fig. 13 B). *In vitro studies* have shown that KH domains (1-4) are critical for the interaction of the protein with transcripts, with KH 3-4 having a higher affinity for interaction (Farina et al. 2003; Chao et al. 2010), and the RRM domains involved in the stabilization of the complexes (Cao et al. 2018). Structural analysis of the KH34 domain of the Imp1 protein revealed that the domain adopts an anti-parallel pseudodimer conformation exposing the RBD. This precise orientation of the domains optimizes the interaction with two non-sequential motifs within a single transcript, thus increasing the affinity and specificity of the interaction (Chao et al. 2010).

Interaction of Imp to its target transcripts via the KH domains results in the assembly of RNP granules that are distributed throughout the cytoplasm and cellular protrusions (Zhang et al. 2001; Farina et al. 2003) (Fig. 13 C,D,E). Although some of Imp targets had been identified in different species, transcriptome-wide studies using Rip-seq, individual-nucleotide resolution UV-cross-linking and immunoprecipitation (iCLIP) and photoactivatable ribonucleoside-iCLIP (Par-iCLIP) on cells have now provided a comprehensive understanding of the transcripts that interact with Imp (Jonson et al. 2007; Hafner et al. 2010; Hansen et al. 2015; Conway et al. 2016; Degrauwe et al. 2016b). These studies have shown that Imp interacts with a large number of protein-coding transcripts,

predominantly by binding to their 3'UTRs. These transcripts are involved in cell organization, cell survival, cell signaling neuronal development, cytoskeletal rearrangement and reproduction. Pull down of Imp-1 and analysis of the proteomic data through mass spectrometry has further revealed that the Imp RNP complexes contain a unique identity, distinct from stress granules or P-bodies (Jonson et al. 2007). Specifically, Imp was shown to interact with several RBPs and ribosomal proteins in an RNA-dependent fashion (Weidensdorfer et al. 2009). This study further revealed that although Imp interacts with several RBPs, the association with few is critical for the stabilization of associated transcripts (Weidensdorfer et al. 2009). Furthermore, the Imp complexes were shown to contain proteins released from mRNAs upon translation (e.g. exon junction complex and CBP80), indicating that Imp binds repressed mRNAs (Jonson et al. 2007). In accordance with this, independent studies showed that Imp may associate with nascent transcripts in the nucleus (Gu et al. 2002; Oleynikov and Singer 2003; Pan et al. 2007), and regulate the export and localization of translationally repressed transcripts to specific subcellular domains (Huttelmaier et al. 2005).

Live imaging of Imp granules in different living systems revealed that transport of these granules is active, motor-driven (Zhang et al. 2001; Tiruchinapalli et al. 2003), and mediated either through actin microfilaments (Farina et al. 2003; Oleynikov and Singer 2003) or MT-networks (Elisha et al. 1995; Nielsen et al. 2000; Medioni et al. 2014) depending on the cell type. However, studies have now begun to show that Imp granule localization and anchoring could be regulated by the concerted action of both actin and MT network (Nalavadi et al. 2012; Urbanska et al. 2017). For example, a recent study showed that Imp interacts with the actin-based myosin Va motor in an RNA-dependent manner. Inhibition of myosin Va leads to an increased number of Imp RNP granules, and a robust accumulation of granules in the axons of cultured neurons, suggesting that myosin Va normally functions to limit the interaction of Imp granules to the MT based motor proteins (Nalavadi et al. 2012). This suggests that Imp RNP granules may be docked to specific

cytoplasmic sites in cell bodies, and following extracellular stimuli, Imp RNP granules associates with kinesin (Urbanska et al. 2017) and are transported.

Imp family of proteins are regarded as oncofetal proteins due to their biphasic protein expression during development and later in transformed cells. Gene deletion experiments have been instrumental in understanding the physiological role of Imp during development. Knockout of Imp resulted in mice that were 40% smaller and exhibited mortality (Hansen et al. 2004). However, increased expression of Imps correlates with poor prognosis and enhanced metastasis in various cancers including colorectal cancers, tumours of the hepato-biliary system, and breast carcinoma. *In vivo* studies have shown that forced expression of Imp1 in mammary epithelial cells induce mammary tumours in up to 95% of cases (Tessier et al. 2004). Mechanistically, Imps were shown to play a significant role in promoting cell survival and self-renewal, through protection of mRNAs from degradation and subsequent upregulation of several oncogenic transcripts (Jonson et al. 2014; Degrauwe et al. 2016b). Indeed, several studies indicated that Imp interacts with several transcripts and proteins and are involved in various important aspects of cell function (Degrauwe et al. 2016b). Examples of the crucial role of Imp proteins in regulating the life cycle of mRNAs will be briefly described below.

- (i) During development, Imp proteins are involved in the localization of regulatory mRNAs supporting growth or fate specification. For example, Vg1RBP interacts with *Vg1* mRNA and localizes it to the vegetal poles of *Xenopus* oocyte (Deshler et al. 1997; Yaniv et al. 2003); it is also necessary for the migration of neural crest cells in *Xenopus* embryo (Yaniv et al. 2003). Furthermore, ZBP1 dependent localization of β -actin mRNA along the shaft or to the growth cones of vertebrate neurites is essential for guidance and branching of axon and dendritic processes (Tiruchinapalli et al. 2003; Perycz et al. 2011; Welshhans and Bassell 2011; Kalous et al. 2014; Gaynes et al. 2015; Lepelletier et al. 2017).

- (ii) Imp is involved in the protection and stabilization of transcripts from miRNA degradation by binding to miRNA recognition sites (Toledano et al. 2012; Goswami et al. 2015; Degrauwe et al. 2016a; Degrauwe et al. 2016b). For example, a study revealed Imp expression during development determines the fetal neural stem cell fate. Imp promotes the self-renewal of neural stem cell by protecting the stability of mRNAs like *Ccnd2* and *Hgma* that are targets of the let7-miRNA (Nishino et al. 2013).

3.2 Imp, role in *Drosophila* Development

Drosophila imp is an essential gene, as *imp* null mutants are zygotic lethal, dying during the late pharate stage. Similar to its vertebrate orthologues, *Drosophila* Imp is involved in the post-transcriptional regulation of different mRNAs during development. During oogenesis, Imp forms cytoplasmic granules that are transported in a dynein-dependent manner to oocytes (Fig. 13 E). Furthermore, it binds to the asymmetrically localized *oskar* and *gurken* mRNAs, and its overexpression perturbs dorsoventral patterning, suggesting a developmental role during embryogenesis (Geng and Macdonald 2006; Munro et al. 2006; Boylan et al. 2008).

The expression of Imp and post-transcriptional regulation of its target transcripts have been shown to be important during the spatio-temporal development and maturation of the nervous system, particularly in the Mushroom Body (MB) (Boylan et al. 2008; Medioni et al. 2014). MBs are a pair of prominent neuropil structures found in the central brain, and are the centre of learning and memory in *Drosophila* (Fig 14. A) (Heisenberg 2003). Each MB is derived from four neuroblasts which divide repeatedly from embryogenesis until late pupal stage and produce around 2,500 Kenyon cells (Fig 14. B) (Ito and Hotta 1992). Three distinct classes of MB neurons, born sequentially, extend their axons ventrally along the peduncle and, upon reaching the tip of the peduncle, bifurcate to form the so-called dorsal and medial lobes (Fig 14. C). The γ neuron are generated during

embryogenesis, followed by the $\alpha'\beta'$ neurons during late larval development and finally the $\alpha\beta$ neuron during metamorphosis (pupal stage). While the larval γ neurons extend axonal branches into both lobes, during metamorphosis they undergo stereotypic pruning and later extend adult specific axonal branches specifically along the medial lobe (Lee et al. 1999; Yu and Schuldiner 2014).

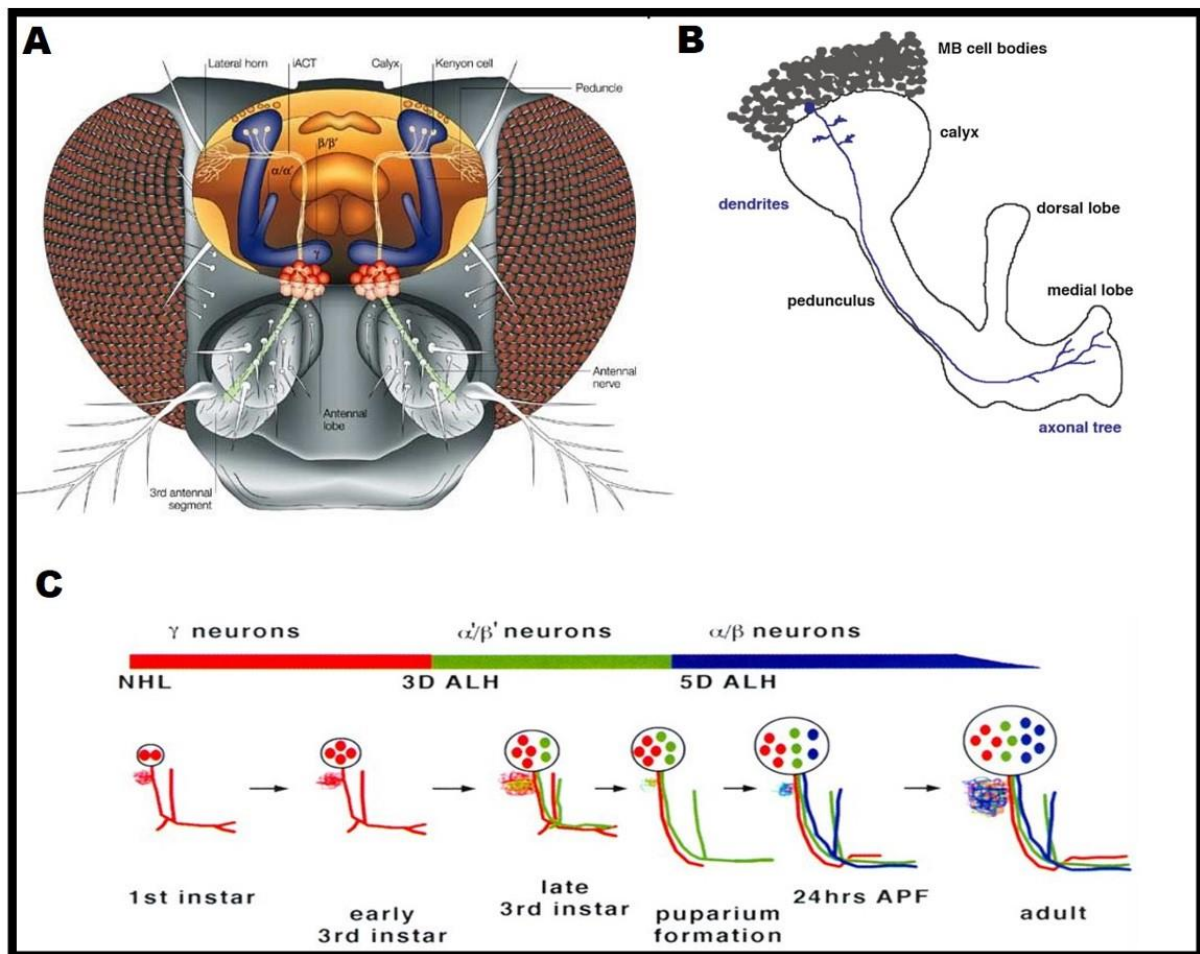


Figure 14: The brain of *Drosophila* and the sequential generation of the Mushroom Body neurons.

A) Schematic representation of an adult *Drosophila* head. Mushroom bodies are represented as dark blue L shaped structures located in the central brain (Heisenberg 2003). B) Schematic representation of an adult MB. Each MB is generated from 4 neuroblasts and consists of around 2,500 neurons. MBs are organized in a stereotypic pattern: their cell bodies lie in the dorsal region, with the dendrites projecting just beneath them, and the axons projecting more ventrally into the dorsal and medial lobes. The projection pattern of a single MB γ neuron is shown in blue (Medioni et al. 2014). C) The

MB neurons are classified into three types based on their axonal projection patterns and their time course of development. γ neurons (red) are born before the mid-3rd instar stage, α'/β' neurons (green) are born between the mid-3rd instar stage and PF, and α/β neurons (blue) are born after metamorphosis (Lee et al. 1999). NHL and ALH stand respectively for newly hatched larvae and after larval hatching.

Transcriptional profiling of the MB neuroblasts at specific time points during the larval and pupal stages revealed the temporally-controlled expression of *imp*, and its role in dictating MB neuronal fates (Liu et al. 2015). Indeed, Imp is expressed abundantly during larval stage, and its expression declines 36h after metamorphosis onset (APF). Depletion of Imp resulted in the premature generation of pupal-specific $\alpha\beta$ neurons and small size MB lobe. More specifically, Imp has been proposed to post-transcriptionally regulates the chronologically inappropriate morphogenesis (Chinmo) transcription factor, whose expression determines the temporal MB neuronal fate. In addition to specifying the fate of larval γ neuron in dividing neuroblast, Imp function is also essential in post-mitotic differentiated γ neurons, for the regrowth and branching of adult-specific γ axons that develop after pruning of the larval axons (Medioni et al. 2014). Imp assembles into RNP granules containing the actin regulator encoding *profilin* mRNA in the cell body of MB γ neurons. Imp RNP granules are restricted to the cell body during the initial growth of the γ neurons (Fig 15. B). During metamorphosis, Imp RNP granules are actively transported along the MT in a developmentally regulated manner (Fig 15. B) (Medioni et al. 2014). Furthermore, *imp* function is essential for the growth and branching of the adult specific axons (Fig. 16). How this developmentally-controlled translocation of Imp to axons is regulated has remained unclear.

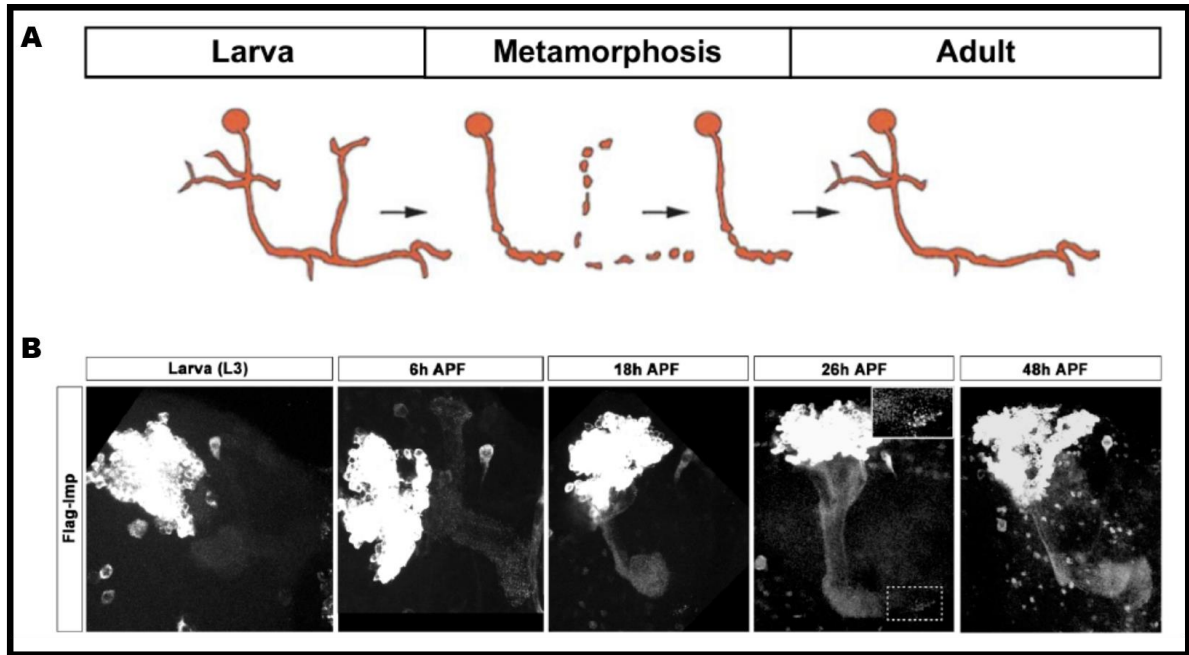


Figure 15: Development of the MB gamma neurons

A) Schematic representation of γ neuron developmental pruning and regrowth. Adapted from (Luo and O'Leary 2005). γ neurons change their neuronal projection pattern during development. During the larval stage, γ axons first extend main axonal branches in both the medial and dorsal lobes. During metamorphosis, these branches undergo programmed degeneration and later extend their adult specific branch along the medial lobe. B) MBs of 201Y-Gal4, UAS-Flag-Imp/+flies dissected at different stages of development, and double-stained with anti-Flag (upper panel). The inset shown for the 26hAPF stage corresponds to higher magnification. Imp proteins are present in the MB cell bodies during the larval stage. During metamorphosis, the Imp RNP granules are transported along the axon in a developmentally regulated manner (Medioni et al. 2014).

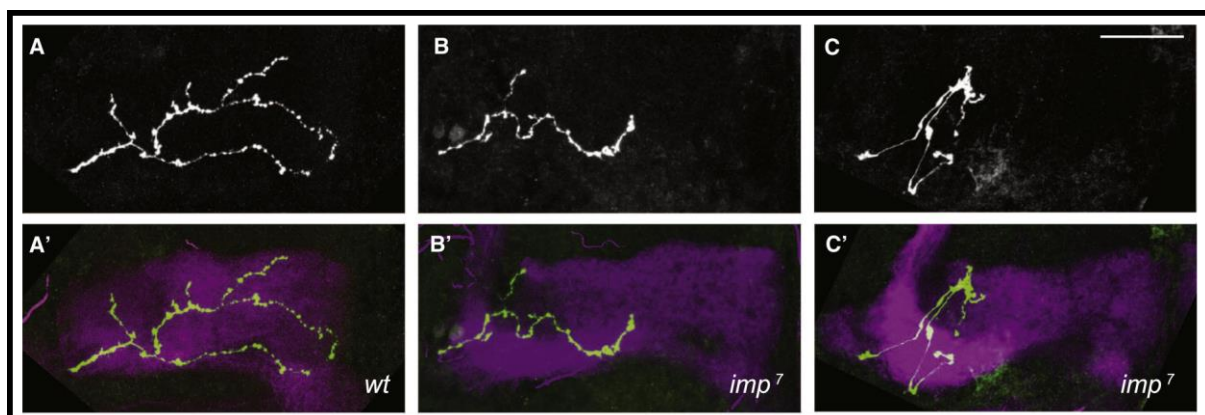


Figure 16: Axonal Growth and Branching Defects in γ Neurons Mutant for *imp*

(A–C') Axonal projections of single wild-type (A) and *imp*⁷ (B and C) adult γ neurons labeled by GFP (A–C; green in A'–C') using the MARCM technique. The shape of the MB medial lobe is highlighted by FasII staining (magenta in A'–C'). Scale bar, 20 μ m. Single axons homozygous for the *imp*⁷ null mutant allele show axon re-growth and branching defects (B, B', C, C') (Medioni et al. 2014).

4 Aim of the thesis

Previous work from our group has uncovered the role of *Drosophila* Imp as a core component of the neuronal RNP granules that are involved in polarized growth and branching of Mushroom Body (MB) γ axon. While analysing the domain structure of the Imp protein, it was noticed that in addition to four RNA binding domains, Imp contains a disordered C-terminal domain showing a striking enrichment in Glutamines and Serines. Based on its lack of structure and biased amino acid composition, this domain has the characteristics of a PLD, suggesting it could either play a role in granule assembly or modulate the material properties of RNP granules. The main objectives of my PhD work were to investigate the *in vivo* function of this domain, and to elucidate its molecular role in the assembly and functional regulation of neuronal Imp granules.

To understand the role of Imp PLD in the assembly of RNP granules, I first assessed the ability of Imp proteins lacking the PLD to assemble into RNP granules in both cultured cells and cell bodies of MB γ neurons. Then, I further characterized the material properties of RNP granules conferred by the PLD, and the molecular requirements underlying PLD function in granule assembly. Imp PLD requirement was compared to that of Imp KH RNA binding domains. To further investigate the molecular mechanism underlying granule assembly, I attempted to perform *in vitro* reconstitution assays from purified Imp wild-type and mutant proteins.

To explore the physiological functions of Imp PLD, I took advantage of the previously known role of Imp in γ axon growth and branching and studied the function of Imp PLD *in vivo* in the context of maturing brains. Using endogenous and exogenous GFP tagged wildtype and mutant Imp proteins, I investigated the transport and localization of Imp granules, as well as the ability of Imp variants to support γ axon growth and branching. Overall, this work sheds light on the role of the PLD of Imp in granule assembly and transport.

5 Results

5.1 Summary of my thesis work I

During my 4 year PhD work, I sought to decipher the function of the C-terminal PLD of *Drosophila* Imp. To study the mechanisms underlying the assembly and regulation of Imp granules and the contribution of the PLD to the function of the protein, I used two complementary cellular systems: i) a population of central nervous system (CNS) neurons that undergo extensive remodeling during metamorphosis (MB γ neurons), a process requiring *imp* function, and ii) a cell line exhibiting a large cytoplasm in which Imp granules can be actively transported (S2R+ cells).

The first part of my results unraveled two essential functions for Imp PLD: one in the regulation of granule homeostasis, and one in the axonal transport of Imp granules. Furthermore, I demonstrated that these two roles are uncoupled

Imp PLD function in granule homeostasis

Previous results from the lab showed that *Drosophila* Imp assembles into cytoplasmic RNP granules in both S2R+ cells (unpublished) and CNS neurons (Medioni et al. 2014). I first questioned the importance of interaction of Imp with RNA for granule component coalescence. I observed that a mutant form of Imp that lacks the ability to bind RNA lost its capacity to assemble into granules and predominantly localized in the nucleus. To elucidate the role of the PLD, a truncated variant of Imp lacking the PLD (Imp Δ PLD) was constructed. Expression of the truncated version of Imp revealed that Imp Δ PLD could assemble into RNP granules in S2R+ cells and *in vivo*. Furthermore, smFISH experiment revealed that *in vivo* granules contain *profilin* mRNA, a described target of Imp. However, quantification of the RNP granules that assembled in S2R+ cells indicated a significant increase in the number and size of Imp granules in the absence of the PLD. These experiments hinted that, in contrast to predominant current models, the PLD has a propensity to prevent the hyper aggregation of the RNP granules. To confirm this result, I

fused the PLD of *Drosophila* to the human orthologue of Imp that naturally lacks a PLD. This gain of function study further substantiated the role of PLD in restricting Imp RNP granule size and number. To test if the sequence of the Imp PLD is essential for granule homeostasis, I designed two scrambled versions (V2 and V4) by randomly rearranging the position of amino acids within the PLD, ensuring that the newly generated sequences maintain a similar score in algorithms used to predict disorder. The two scrambled versions of PLD (Imp ScrPLD) assembled into granules in cultured cells and in MB γ neurons and were similar both in number and size to the Imp wild-type granules. Together, these data revealed that PLD is essential for regulating granule homeostasis, and that PLD primary sequence is not necessary for this regulation.

To characterize the function of Imp PLD in imparting dynamics to the granules, I performed FRAP experiments in mammalian cells (Hela cells), *Drosophila* cells and in the cell body of MB γ neurons. Results from all three different cell types consistently demonstrated that the PLD promotes the turnover of Imp molecules in and out complexes.

Axonal Transport and neuronal remodeling

Previous results demonstrated that Imp RNP granules are actively transported to axons upon developmental remodelling, and that *imp* supports γ axon re-growth and branching at that stage. Taking advantage of a CRISPR line expressing truncated Imp Δ PLD proteins from the endogenous locus, I showed that Imp Δ PLD proteins failed to localize to axons from metamorphosis onwards. *In vivo* live imaging experiments revealed that there was a decrease in the number of both anterograde and retrograde granules in axons, and an increase in the velocity of retrograde granules. These defects in axonal transport are linked to defects in axon growth and branching. Indeed, single neuron labelling experiment showed 10% of adult γ axons failed to grow and branch properly in the CRISPR Δ PLD line. Furthermore, expression of Imp Δ PLD proteins could not rescue the *imp* axon remodelling defects in MARCM experiments. Thus, the PLD of Imp is not only important for granule

homeostasis of Imp granules, but is also essential physiologically, for Imp-dependent growth and branching of axonal branches.

Uncoupled role in granule homeostasis and axon transport

Surprisingly, my data further showed that these two roles of the PLD of Imp are independent. In order to understand the importance of the position of the PLD, I generated a variant of Imp with the PLD at the N-terminus. This variant, when expressed in S2R+ cells accumulated as large granules, and FRAP experiment showed significantly less recovery that for Imp wild-type proteins. Strikingly, however, the proteins were efficiently transported to γ axons and supported growth and branching.

Thus, these results suggest that the PLD of Imp has two independent functions: one in the restriction of granule size (which requires a C-ter PLD), and the other in the polarized growth of axons.

A manuscript describing these results was submitted to Nature communication and is inserted at the end of this section. This manuscript is now under revision.

5.2 Part I: Manuscript

The prion-like domain of *Drosophila* Imp has two independent functions in axonal transport and RNP granule homeostasis

Jeshlee Vijayakumar¹, Charlène Perrois¹, Marjorie Heim¹, Luc Bousset², Simon Alberti³ and
Florence Besse^{1,*}

1: University Côte d'Azur, CNRS, Inserm, Institute of Biology Valrose, Nice, France

2: Paris-Saclay Institute of Neuroscience, Paris, France

3: Max Planck Institute of Molecular Cell Biology and Genetics, Dresden, Germany.

*: Corresponding author: besse@unice.fr

Tel: (33) 492076434

Key words: neuronal granules; RNP complex; mRNA transport; RNA-binding protein; developmental neuronal remodeling; *Drosophila*

5.2.1 Abstract (150 words max)

Prion-like domains (PLDs), defined by their low sequence complexity and lack of structure, are present in hundreds of human proteins. Although gain-of-function mutations in the PLDs of neuronal RNA binding proteins were linked to neurodegenerative disease progression, the physiological role of PLDs and their range of molecular functions are still largely unknown. Here, we show that the PLD of *Drosophila* Imp, a conserved component of neuronal RNP granules, is essential for the developmentally-controlled localization of Imp RNP granules to axons and regulates *in vivo* axonal remodeling. Furthermore, we demonstrate that Imp PLD restricts, rather than promotes granule assembly, revealing a novel modulatory function for PLDs in RNP granule homeostasis. Strikingly, swapping the position of Imp PLD compromises RNP granule dynamic assembly but not transport, suggesting that these two functions are uncoupled. Together, our study uncovers a key physiological function for PLDs in the spatio-temporal control of neuronal RNP assemblies.

5.2.2 Introduction

Following transcription, splicing and nuclear processing, eukaryotic mRNAs are exported to the cell cytoplasm as ribonucleoprotein complexes (RNPs) containing RNA molecules and associated regulatory proteins. Individual RNPs can further assemble into higher order structures detected by light microscopy and referred to as RNP granules (Muller-McNicoll and Neugebauer 2013). Cytoplasmic RNP granules of different sizes, composition and properties have been defined over the last past decades, including large macromolecular complexes such as P-bodies, stress granules, germ cell granules or neuronal granules (Anderson and Kedersha 2009). These assemblies are enriched in helicases, regulators of mRNA translation and stability, and/or molecular motors. They represent a very efficient and flexible means to compartmentalize and regulate gene expression (Anderson and Kedersha 2009; Buchan 2014; Mitchell and Parker 2014). Neuronal granules, in particular, have been implicated in the long-distance transport of mRNAs to axons or dendrites, and in their local translation in response to external cues (Kiebler and Bassell 2006; Besse and Ephrussi 2008; Holt and Schuman 2013; De Graeve and Besse 2018). By enabling precise and dynamic spatio-temporal expression of mRNAs involved in cytoskeletal remodeling, synaptic activity or cell signaling, neuronal granules promote functional and structural plasticity in both developing and mature neurons. Their function underlies many fundamental neuronal processes regulated by extrinsic signals, such as synaptic plasticity, axon or dendrite growth and branching, as well as axon survival or regeneration (Doyle and Kiebler 2011; Jung et al. 2012; Holt and Schuman 2013; Glock et al. 2017). To date, however, the cellular and molecular principles underlying the assembly, transport and regulation of neuronal RNP granules are still poorly understood.

Numerous recent studies have suggested that the assembly of macromolecular RNP granules is mediated by the process of liquid-liquid phase separation, *i.e.* the demixing of a homogenous solution into a soluble phase in which RNA and associated proteins are dispersed, and a condensed phase in which these components are concentrated in droplets

with semi-liquid behavior (Weber and Brangwynne 2012; Courchaine et al. 2016; Alberti 2017). Once assembled, these RNP droplets undergo constant changes at the molecular level, as illustrated by the relatively fast exchange (from seconds to minutes) of RNP components (Kedersha et al. 2005; Aizer et al. 2008; Zhang et al. 2011; Hubstenberger et al. 2013; Patel et al. 2015). This property enables RNP granules to rapidly change their size, number and/or composition, and can be modulated in response to physiological cues or environmental stresses (Hubstenberger et al. 2013; Buxbaum et al. 2014; Schisa 2014; Nott et al. 2015; Riback et al. 2017; Khayachi et al. 2018). As revealed by recent *in vitro* studies, the establishment of multivalent protein-protein and protein-RNA interactions is a key factor driving the coalescence and maintenance of dynamic RNP assemblies (Li et al. 2012; Burke et al. 2015; Lin et al. 2015; Molliex et al. 2015; Zhang et al. 2015). In this context, the role of intrinsically disordered prion-like domains (PLDs), found at high frequency in RNP granule components (Kato et al 2012; Kind et al 2012; Malinovska et al 2013), has raised strong interest. PLDs are composed of repeated stretches of uncharged polar and aromatic amino acids, rendering them very interactive and able to drive the formation of transient interaction networks underlying condensation reactions. Consistent with this idea, PLDs studied so far promote self-assembly in reconstituted systems, and seed phase separation into RNP droplets (Kato et al. 2012; Lin et al. 2015; Molliex et al. 2015; Patel et al. 2015). Interestingly, alterations in PLD functionality have been linked to the progression of several neurodegenerative diseases including amyotrophic lateral sclerosis (ALS) or frontotemporal dementia (FTD) (King et al. 2012; March et al. 2016). Disease-causing mutations identified in the PLDs of different RNA binding proteins, indeed, were shown to alter granule properties and promote the formation of abnormal solid aggregates, a hallmark of ALS and FTD (Kim et al. 2013; Murakami et al. 2015; Patel et al. 2015). Surprisingly, although a clear link has now been established between alteration of PLD function and disease, the physiological function of PLDs in the assembly and regulation of neuronal RNP granules largely remains to be demonstrated.

Here, we have explored the role of a PLD found in *Drosophila* Imp, a known component of neuronal RNP granules belonging to the conserved family of VICKZ RNA binding proteins. In both vertebrate and invertebrate neurons, Imp family members are packaged together with target mRNAs into microscopically visible granules that are transported to the axons and/or dendrites of neuronal cells (Tiruchinapalli et al. 2003; Leung et al. 2006; Nalavadi et al. 2012; Medioni et al. 2014). As best described for Vg1RBP and ZBP1, two vertebrate orthologs of Imp, Imp proteins not only promote the microtubule-dependent transport of their targets such as β -actin mRNA, but also control their translational regulation (Yao et al. 2006; Sasaki et al. 2010; Welshhans and Bassell 2011; Patel et al. 2012; Buxbaum et al. 2014; Yoon et al. 2016). Functionally, Vg1RBP/ZBP1-dependent localization and translational control of β -actin promote axon navigation (Leung et al. 2006; Yao et al. 2006; Lepelletier et al. 2017), as well as dendritic growth and branching (Perycz et al. 2011) in developing neurons. In *Drosophila* brains, Imp assembles into neuronal RNP granules that contain the actin regulator-encoding *profilin* mRNA. These granules undergo precise spatio-temporal regulation during nervous system maturation, and are dynamically recruited to axons upon developmental remodeling (Medioni et al. 2014). Moreover, Imp function is required for completion of axonal branch remodeling, in particular for the regrowth and branching of adult axons that occur after pruning of immature branches.

In this study, we find that *Drosophila* Imp contains a PLD that is not required for RNP granule assembly in cells and *in vivo*. Imp PLD, rather, regulates granule properties by limiting the clustering of Imp molecules, and by promoting their exchange in and out of granules. Such functions do not depend on PLD primary sequence. *In vivo*, Imp PLD promotes the motility of axonal Imp granules, and is both necessary and sufficient for efficient localization of Imp to axons. Furthermore, it regulates the *imp*-dependent axonal remodeling that occurs during brain maturation. Surprisingly, swapping the position of Imp PLD revealed that its function in the modulation of Imp granule assembly and dynamics can

be uncoupled from that in axonal transport. Together, our findings reveal a novel *in vivo* function for a PLD in the formation of transport-competent neuronal granules. By uncovering an unexpected function of a PLD in RNP granule homeostasis, they also shed new light into the molecular principles and requirements underlying RNP granule assembly and regulation in living cells.

5.2.3 Results

***Drosophila* Imp contains a C-terminal prion-like domain**

Analysis of the primary sequence of *Drosophila* Imp revealed that the C-terminal most region of the protein is highly enriched in uncharged polar amino acids, in particular in glutamines that are clustered in stretches of 3-5 residues (31 glutamines over a 95 amino acid length; Figure 1A). This C-terminal domain has an amino acid composition typical of that described for low-complexity prion-like domains (PLD) (Alberti et al. 2009), and was identified as such in a genome-wide *in silico* search (Malinowska et al. 2013a). This domain is further predicted to be intrinsically disordered (Figure 1B), a prediction that we validated using circular dichroism spectroscopy. As shown in Figure 1C, indeed, spectra obtained from recombinant Imp PLD revealed that the majority of the domain does not fold into detectable α -helices or β -sheets secondary structures.

Imp RNA binding capacity, but not Imp PLD, is required for Imp granule assembly.

PLDs were shown in different contexts to drive the coalescence of RNP granule components into phase-separated higher order structures (Kato et al. 2012; Lin et al. 2015; Molliex et al. 2015; Patel et al. 2015). Thus, we investigated the importance of Imp PLD in the assembly of Imp RNP granules. In S2R+ cells, both endogenous Imp and transfected GFP-Imp distribute diffusely throughout the cytoplasm and accumulate within granules of an apparent diameter of 200 to 300 nm (Figure 2A and B) (Hansen et al. 2015). As revealed by the absence of co-localization with Stress Granule (SG) markers, these granules are

distinct from SGs (Figure S1A-B). To test if binding of Imp to RNA is essential for granule assembly, we generated a mutant form of Imp in which two negatively charged aspartate residues were introduced in the characteristic GxxG loop of all four KH domains (GxxG to GDDG substitutions). Such point mutations were described to preserve KH domain structure while strongly impairing nucleic acid binding (Hollingworth et al. 2012). Indeed, Imp-KH1-4DD proteins did not show any significant binding to RNA *in vitro* (Figure 2I, compare with wild-type Imp). When transfected into S2R+ cells, GFP-Imp-KH1-4DD proteins did not assemble into granules (Figure 2C), suggesting that the binding of Imp to target RNAs is essential for the formation of Imp RNP granules. To then test whether Imp PLD plays a role in this process, we generated a mutant form of Imp lacking this domain (Imp- Δ PLD) and analyzed its subcellular distribution. As shown in Figure 2D, GFP-Imp- Δ PLD fusions assembled into distinct cytoplasmic particles, indicating that the PLD of Imp is not required for the assembly of Imp RNP granules in S2R+ cells.

In vivo, both endogenous Imp (Figure 2E,F) and UAS-driven GFP-Imp fusions (Figure 2G) accumulate into cytoplasmic granules in Mushroom Body (MB) γ neurons. These granules contain *profilin* mRNA, a direct target of Imp (Figure S1C,D) (Medioni et al. 2014). As was observed *ex vivo*, GFP-Imp-KH1-4DD mutants did not assemble into visible granules when expressed in MB γ neurons (Figure 2H), whereas GFP-Imp- Δ PLD proteins accumulated into distinct punctate structures in the cytoplasm (Figure 2J). In these experiments, the presence of endogenous wild-type Imp proteins may influence the distribution of exogenous GFP-Imp- Δ PLD constructs. To generate flies that exclusively express GFP-Imp- Δ PLD proteins, we took advantage of an available knock-in line (Go80 protein-trap line) in which a GFP exon is inserted in frame in all *imp* transcripts, generating functional N-terminally tagged proteins (Figure 2F and S2A,B) (Medioni et al. 2014). Using the CRISPR/Cas9 technology, we introduced into this line two premature STOP codons in the *imp* locus, upstream of the PLD-coding sequence (Figure S2A). Remarkably, GFP-Imp- Δ PLD proteins produced by homozygous Go80-GFP-Imp-CRISPR- Δ PLD flies assembled

into cytoplasmic granules containing *profilin* mRNA (Figure 2K and S1D,E), confirming that the PLD of Imp is not required for the assembly of Imp RNP granules *in vivo*.

Imp PLD modulates granule size and number

As described, Imp PLD is not strictly required for granule assembly. Rather, careful examination and quantification of the cytoplasmic granules formed upon GFP-Imp- Δ PLD expression revealed that Imp PLD restricts granule coalescence. Indeed, a significantly higher number of granules was observed in GFP-Imp- Δ PLD-expressing cells compared to GFP-Imp-expressing cells (Figure 3A). Furthermore, GFP-Imp- Δ PLD granules were on average larger (9.3 +/-0.13 pixels *vs* 8.2 +/-0.17 for GFP-Imp granules; $P < 0.001$ in a Mann-Whitney test), as illustrated by the significant increase in the number of cells with very large (>25 pixels) granules (Figure 3B). Notably, such differences did not result from a differential expression of the two proteins, as both were expressed at similar levels (Figure S3B). Thus, these results suggest that Imp PLD normally restricts the number and size of Imp granules.

Next, we wondered whether Imp PLD is sufficient to limit the assembly of RNP granules. We found that, on its own, Imp PLD does not trigger particle assembly and cannot be recruited to Imp containing granules (Figure S3A-A' and data not shown). Thus, we next generated a chimeric construct in which we grafted the PLD of *Drosophila* Imp at the C-terminus of the human IMP1 protein, which naturally lacks such a domain (Figure 3C). Strikingly, addition of *Drosophila* Imp PLD significantly decreased both the number and the size of cytoplasmic granules formed by hIMP1 in S2R+ cells (Figures 3D-G), without affecting hIMP1 levels (Figure S3C). Together, these results thus indicate that Imp PLD is not only required, but also sufficient, to modulate Imp granule size and number.

Imp PLD position, but not primary sequence, is important for the regulation of granule size and number

To better understand the molecular determinants underlying Imp PLD function, we analyzed the function of variants in which Imp PLD sequence or position was altered. First,

we tested whether Imp PLD might encode interaction sites with specific sequence by generating two scrambled PLD variants with altered primary sequence but preserved overall amino acid composition (Imp-scr2 and Imp-scr4; Figures 4A-D). In these two PLD variants, the degree of disorder is predicted to be preserved (Figure S3D). Remarkably, expression of GFP-Imp-scr2 or GFP-Imp-scr4 proteins in S2R+ cells did not result in any changes in granule size or number (Figure 4A,D,E and Figure S3E,F). This result indicates that primary sequence is not important for Imp PLD function in granule assembly, and thus that Imp PLD does not regulate granule assembly through stereospecific interactions. To next test if the position of Imp PLD is important for its function, we generated a form of Imp in which we moved the PLD from the C-terminus of the protein to its N-terminus (Figure 4B). GFP-Imp-Nter-PLD proteins, while expressed at levels similar to GFP-Imp proteins (Figure S3G), accumulated in granules with altered properties (Figure 4F). In this context, indeed, increased granule number (Figures 4G) and size (Figure 4H) were observed, similarly to the GFP-Imp- Δ PLD condition. Thus, Imp PLD appears to be non-functional when located N-terminally, suggesting that domain arrangement is a key requirement for the functional modulation of granule assembly by Imp PLD.

Imp PLD renders Imp RNP granules more dynamic

RNP granules are dynamic assemblies whose components constantly exchange with the cytoplasm. To test if Imp PLD regulates the exchange of granule-associated Imp, we measured fluorescence recovery after photobleaching (FRAP) in GFP-Imp-expressing S2R+ cells. As shown in Figures 5A-B, a partial recovery was observed after photobleaching of the granule-associated pool of wild-type GFP-Imp proteins, suggesting that Imp may be a core particle component that moderately exchanges with the cytoplasmic fraction. Interestingly, a significantly lower recovery was observed when expressing GFP-Imp- Δ PLD fusions (Figure 5B), indicating that the PLD of Imp promotes the exchange of Imp in and out granules. Such a reduction in fluorescence recovery was observed when expressing GFP-Imp constructs in HeLa cells, a heterologous system where the identity of Imp partners and targets is likely

partially different (Figure S4). Furthermore, it was also visible in whole adult brains, after bleaching of endogenous GFP-Imp and GFP-Imp- Δ PLD neuronal granules (Figure 5C,D).

To investigate the behavior of Imp variants, we then performed FRAP experiments on GFP-Imp-scr2, GFP-Imp-scr4 and GFP-Imp-Nter-PLD granules in S2R+ cells. While the fluorescence recovery of GFP-Imp-scr2 and GFP-Imp-scr4 variants was similar to that of wild-type GFP-Imp proteins, the recovery of GFP-Imp-Nter-PLD was significantly lower (Figure 5E), consistent with a model in which granule dynamics is regulated by PLD position, but not through PLD-mediated stereospecific interactions.

Altogether, these results suggest that Imp PLD is a key contributor to RNP granule homeostasis. Instead of promoting granule assembly, it plays an important role in modulating RNP granule assembly and dynamics.

Imp PLD promotes the transport of Imp to Mushroom Body (MB) axons

We have previously shown that the distribution of Imp is precisely controlled *in vivo* during nervous system maturation: while Imp is restricted to the cell bodies of MB γ neurons during larval stages, it localizes to axons from metamorphosis onwards (Medioni et al. 2014). To investigate the role of Imp PLD in the developmentally-controlled recruitment of Imp to axons, we analyzed at larval and adult stages the localization of GFP-Imp fusions expressed in MB γ neurons under the control of 201Y-Gal4. Similar to wild-type GFP-Imp, GFP-Imp- Δ PLD proteins were restricted to γ neuron cell bodies at larval stages (data not shown). In contrast to GFP-Imp, however, GFP-Imp- Δ PLD proteins did not efficiently localize to the axons of adult MB γ axons (Figure 6A-C and Figure S6A), suggesting that Imp PLD is required *in vivo* to promote the localization of Imp to axons. To assess the distribution of endogenously-expressed Imp proteins, we then compared the localization of GFP-Imp proteins produced from the GFP protein-trap line with that of GFP-Imp- Δ PLD proteins produced from the Go80-GFP-Imp-CRISPR- Δ PLD line. As shown in Figure 6D-F, a strong reduction in the localization of GFP-Imp proteins to MB γ axons was observed in the absence

of Imp PLD. Such a difference in axonal signal intensity was not explained by differences in expression levels, as protein levels were similar in Go80-GFP-Imp and Go80-GFP-Imp-CRISPR- Δ PLD lines (Figures S2B and S6B).

To test whether Imp PLD is sufficient to promote the axonal recruitment of heterologous proteins, we then compared the distributions of GFP-tagged hIMP1 and hIMP1-drosPLD proteins expressed in MB γ neurons. Remarkably, a significant increase in axonal localization was observed upon addition of *Drosophila* Imp PLD to hIMP1 (Figure 6G-I), indicating that Imp PLD is both necessary and sufficient for axonal localization.

In vivo recruitment of Imp granules to axons is mediated by bi-directional, microtubule-dependent transport, a process triggered during early metamorphosis by a yet unknown instructive signal (Medioni et al. 2014). To investigate whether Imp PLD regulates the motility of Imp granules *in vivo*, we performed real-time imaging of endogenous axonal Imp granules in Go80-GFP-Imp and Go80-GFP-Imp-CRISPR- Δ PLD intact pupal brains (Medioni et al. 2015). As previously reported (Medioni et al. 2014), wild-type GFP-Imp granules exhibited a biased bi-directional motion (Figure 7A,B and Video1) characterized by a higher number of granules moving anterogradely (Figure 7C and S5A) and a higher anterograde mean velocity (Figure 7D). Remarkably, a decreased number of both unidirectional and bidirectional motile particles was observed in Go80-GFP-Imp-CRISPR- Δ PLD axons compared to wild-type Go80-GFP-Imp axons (Figure 7C; $P < 0.01$ in a Kruskal-Wallis test). Furthermore, although the proportion of anterograde particles was still higher than that of retrograde ones in Go80-GFP-Imp-CRISPR- Δ PLD brains (Figure S5A), an increased retrograde mean velocity was observed (Figure 7D and Figure S5B,C). Together, these results thus suggest that the PLD of Imp promotes the motility of axonal Imp granules *in vivo* and modulates the properties of their retrograde transport.

The function of Imp PLD is important for *imp*-dependent axonal remodeling.

As described previously (Medioni et al. 2014), *imp* function is required for the developmentally-controlled remodeling of MB γ axons that occurs during metamorphosis, in particular for the growth and branching of adult mature branches. Notably, Go80-GFP-Imp-CRISPR- Δ PLD flies did not exhibit major alterations in the global projection pattern of the adult γ axon population (Figure 6D',E'). To visualize the detailed morphology of individual neurons, we induced stochastic sparse labeling of γ neurons using the MultiColor FlpOut (MCFO) approach (Nern et al. 2015). While the majority of single labeled adult γ axons had a normal morphology, about 10% of them exhibited polarized growth defects (6/62 *vs* 0/21 in control flies). In this context, all γ neurons express truncated Imp- Δ PLD proteins. To then test the function of Imp- Δ PLD proteins in a condition where single mutant neurons are challenged by surrounding wild-type neurons growing simultaneously and competing for space, we performed rescue experiments using the MARCM technique (Wu and Luo 2006). About half of individual *imp⁷* mutant neurons grown in an otherwise wild-type environment failed to properly elongate, a phenotype significantly suppressed by expression of wild-type GFP-Imp (Figures 8A-C). Remarkably, expression of GFP-Imp- Δ PLD did not suppress the axon growth defects observed in adult *imp* mutant γ neurons in this assay (Figures 8C), indicating that the PLD of Imp is important for efficient growth, a process better highlighted in a competitive context.

The functions of Imp PLD in granule homeostasis and *in vivo* transport are uncoupled.

As described previously, changing the position of Imp PLD from the C-terminus to the N-terminus of the protein compromises its function in the regulation of Imp granule assembly. Surprisingly, expression of GFP-Imp-Nter-PLD in MB γ neurons revealed that this variant is able to localize to axons as efficiently as wild-type GFP-Imp fusions (Figure 8J-L). Furthermore, expressing the N-ter-PLD construct in an *imp* mutant background suppressed the axonal regrowth phenotypes observed upon *imp* inactivation (Figures 8C), suggesting

that the presence of Imp PLD, but not its position, is important for axonal transport and control of axonal regrowth. Together, these results thus indicate that Imp PLD has two independent functions in regulating Imp RNP granule assembly and axonal transport. Furthermore, they indicate that changes in RNP granule homeostasis do not directly impact on the *in vivo* function and regulation of Imp during developmental neuronal remodeling.

5.2.4 Discussion

Imp PLD modulates, rather than promotes RNP granule assembly.

Establishment of multivalent interactions is driving the self-assembly of components into phase-separated high-order structures (Li et al. 2012; Courchaine et al. 2016). In the context of RNP granules, multivalency was proposed to originate from repeats of RNA binding domains (Li et al. 2012), as well as from disordered low-complexity domains, which are prone to establish interaction networks and are found at high frequency in RNA binding proteins (Kato et al. 2012; Weber and Brangwynne 2012; Malinowska et al. 2013a; Courchaine et al. 2016). Here, we showed that preventing Imp binding to RNA by mutating all four KH domains interferes with Imp granule formation, consistent with the idea that RNA binding is a key driver of phase separation (Lin et al. 2015; Zhang et al. 2015), and that multivalent protein-RNA interactions may underly granule formation (Li et al. 2012). Imp PLD, however, is neither sufficient nor necessary for such a process. This finding contrasts with the capacity of described PLDs to trigger demixing into phase-separated structures (Kato et al. 2012; Lin et al. 2015; Molliex et al. 2015; Patel et al. 2015; Bakthavachalu et al. 2018), but is consistent with recent work showing that low-complexity sequences may not necessarily act as seeds for granule coalescence and rather modulate such a process (Riback et al. 2017; Franzmann and Alberti 2018; Franzmann et al. 2018). Indeed, our results show that Imp PLD restricts the capacity of Imp granule components to self-assemble into granules and reduces the exchange of Imp molecules with the cytoplasm. To our knowledge, Imp PLD is the first PLD that negatively regulates demixing. How this domain is acting at the molecular level still has to be resolved, but one possibility is that it dynamically regulates

access to binding sites and interferes with intra- and/or inter-molecular interactions, thus decreasing valency of binding or strengths of interactions within the complex. Strikingly, Imp PLD still modulates RNP assembly when ectopically grafted onto a heterologous protein, indicating that its modulatory function is transferable to a functionally related protein. Imp PLD functionality, however, depends on its position within the protein because a N-terminally-located PLD cannot restrict granule assembly. This suggests conformational constraints within the interaction network that is established during RNP granule assembly.

What is the *in vivo* impact of changes in granule homeostasis? Imp PLD-mediated changes in granule assembly appears to not have a major impact on Imp function during *Drosophila* development, as GFP-Imp-CRISPR- Δ PLD individuals, in contrast to *imp* mutants, are homozygous viable and fertile. Furthermore, these changes do not interfere with *imp*-dependent remodeling of MB γ axons, as revealed by the capacity of Imp-NterPLD proteins to efficiently rescue the *imp* re-growth and branching phenotypes. The capacity of Imp PLD to regulate Imp granule coalescence and dynamics might however be physiologically important in other contexts, to regulate synaptic plasticity in the adult nervous system, or in response to stress.

Molecular requirements for PLD functions

PLDs belong to a class of low-complexity domains defined by their biased amino acid composition, and in particular by their enrichment in uncharged polar amino acids such as glutamine, asparagine, serine or proline, a characteristic signature of prion domains (Alberti et al. 2009; Malinowska et al. 2013a). A key feature of PLDs is also their predicted lack of defined structure, a property we have experimentally confirmed for Imp PLD using circular dichroism spectroscopy. Because of their intrinsic disorder, PLDs have been proposed to bring “fuzziness” to macromolecular RNP complexes, and to provide both adaptability and reversibility to the metastable protein interaction networks characteristic of such assemblies (Fuxreiter 2012; Malinowska et al. 2013a; Wu and Fuxreiter 2016). To date, however, the precise molecular requirements underlying PLD functions are still unclear. Recent work

performed on the PLD of the yeast Nab3 protein has uncovered that some heterologous PLDs, but not all, can compensate for the lack of Nab3 PLD, suggesting the existence of distinct functional classes of PLDs (Loya et al. 2017). No correlation could however be established between PLD amino acid composition and/or length and functionality, leaving open the question of the molecular signature required for PLD function.

Aligning Imp PLD sequences from different *Drosophila* species reveals some variations in primary sequences, in particular an increased length of glutamine repeats in distantly-related species such as *D. grimshawi* or *D. mojavensis* (Figure S6C). To test if providing disorder was the main function of Imp PLD, or rather if PLD sequence was encoding some information, we generated scrambled versions of Imp PLD that preserved overall amino acid composition but not primary sequence. Interestingly, scrambled PLDs could restrict granule assembly and regulate interaction dynamics as efficiently as wild-type domains, suggesting that primary sequence is not a determinant of Imp PLD function in granule regulation.

How such disordered domains are regulated still has to be clarified, but both *in vitro* and *in vivo* work has shown that post-translational modifications of low-complexity domains (LCD), in particular phosphorylation of LCDs residues, can dramatically change phase separation behavior (Li et al. 2012; Kwon et al. 2013; Wang et al. 2014; Monahan et al. 2017). Imp PLD contain numerous serines, yet mutating all serines into non-phosphorylatable glycines did not impact on granule assembly and dynamics in S2R+ cells, nor on MB □ axon remodeling in developing brains (data not shown). Whether other post-translational modifications contribute to the regulation of Imp PLD, and to changes in granule properties, remains to be determined.

Imp PLD promotes the formation of transport-competent RNP granules

Our work has revealed that Imp PLD is both necessary and sufficient to promote Imp axonal localization *in vivo*, and uncovered a role for Imp PLD in the microtubule-dependent transport of axonal RNP granules. While previous work has shown that ALS-disease causing

point mutations in the low complexity domain of the TDP-43 RNA binding protein alter the transport of TDP-43 granules along the axons of cultured neurons (Alami et al. 2014), whether such changes resulted from observed alterations of granule dynamics and physical properties remained unclear. The capacity of Imp-Nter-PLD constructs to localize to axons demonstrates that the function of Imp PLD in axonal transport is uncoupled from that in the modulation of granule dynamics. As further revealed by our quantitative real-time *in vivo* imaging, Imp PLD appears to promote the motility of axonal granules, and to modulate the velocity of retrograde granules. Although we have not been able to detect physical interactions between Imp and microtubule-dependent motor components such as Kinesin-heavy chain or Dynein (data not shown), these results suggest that Imp PLD may be important for efficient activation or recruitment of such molecular motors. Intrinsically disordered regions were shown in different contexts to promote the establishment of multiple transient protein-protein interactions, and to employ short linear motifs for specific interactions (Miskei et al. 2017). Such motifs are however not likely to mediate interaction with motor molecules in the case of Imp PLD, as Imp proteins with scrambled domains can localize to axons *in vivo* (data not shown). Remarkably, localization of Imp neuronal granules to axons is under the control of a precise developmental program, as Imp granules, restricted to cell bodies during larval stages, start translocating to axons specifically during metamorphosis (Medioni et al. 2014). An interesting possibility is thus that the flexible nature of Imp PLD mediates a switch triggering maturation into transport-competent granules in response to developmental signals. This is particularly interesting in a context where the molecular principles underlying the physiological regulation and remodeling of neuronal RNP granules are still largely unclear.

5.2.5 Materials and Methods

Subcloning of Imp coding sequences

Imp- Δ PLD coding sequence was amplified by PCR from EST SD07045, using the impCS_sense/ KH34-Gtwy-RP couple of primers. To generate the pENTR_ImpKH1-4DD

variant, site directed mutagenesis was performed on previously described pENTR_Imp (Medioni et al. 2014) using primers listed in Table S1. Scrambled v2 and v4 PLDs were produced by gene synthesis, PCR-amplified, and added in frame to the Δ PLD sequence by SOE PCR using the primers listed in Table S1. PLD-Nter was generated by SOE PCR using the primers listed in Table S1. hIMP1 was amplified from cDNA (gift from J. Chao) using the hIMP1-Gtwy-FP/RP primers, and hIMP1-drosPLD was generated by SOE PCR. The exact sequence of all above-mentioned primers is detailed in Supplemental Table 1. All sequence variants were subcloned into pENTR-D/TOPO vector (Life Technologies), fully sequenced, and recombined into Gateway destination vectors to express N-terminally-tagged proteins. pAGW (Murphy lab) and pUAS-attB-GFP (Sanial et al. 2017) destination vectors were used for expression in S2R+ cells and *Drosophila* respectively. All constructs were inserted into the same genomic location (attP40), by PhiC31-mediated site-directed transgenesis.

Expression of GFP-Imp variants in S2R+ cells and particle quantification

S2R+ cells were plated in 6-well plates at a density of $5 \cdot 10^6$ cells/well, and incubated for 1 day at 25°C. Cells were then transfected with 600 ng plasmids using Effectene (Qiagen). After 12h, cells were resuspended in 1mL of Schneider's medium supplemented with 10% Fetal Bovine Serum and Penicillin/streptomycin (1%), and transferred 24h later to chambered Lab-Tek slides (4 chambers; 250 μ L/chamber). Cells were then fixed in 4% paraformaldehyde for 10 min, washed and permeabilized in PBS/0.1% Triton (PBT), and stained with DAPI. For detection of endogenous proteins, S2R+ cells were blocked in PBT supplemented with 1% BSA and then incubated overnight with rabbit anti-Imp antibodies (1:500) in PBT supplemented with 0.1% BSA. Cells were then washed with PBT, incubated with Alexa488 conjugated anti-rabbit antibody (1:500) in PBT/0.1% BSA for 1–2 h, and washed once before DAPI labeling (5 minutes, 5 μ g/mL). After two washes in PBT, cells were mounted in Vectashield for imaging. Images were acquired on a Spinning Disc confocal microscope equipped with a Yokogawa CSU-X1 confocal head, and a iXON DU-897-BV EMCCD camera (Andor technology), using a UPLSAPO 100X oil 1.4 NA objective. Cells with

low expression levels were selected for imaging and images were acquired using identical settings.

Granule size and number analysis were done on Maximum Intensity projections, and analysis performed using the SPADE algorithm (<https://raweb.inria.fr/rapportsactivite/RA2016/morpheme/uid13.html>), with manual edition for particles larger than 25 pixels. Minimal granule size was set to 4 pixels.

Immunostainings and imaging of adult brains

Dissection and immunostainings of fly brains were performed as described in (Medioni et al. 2014) using rat anti-Imp (1:1000), rabbit anti-GFP (Molecular Probes, 1:1000), mouse anti-FasciclinII (DSHB, 1D4 clone; 1:15). Images of immunostained brains were acquired on a LSM710, using a APO 40x NA 1.1 water objective for axon imaging, and a Plan Apo 63X NA 1.4 oil objective for cell body imaging. To assess the localisation of UAS-GFP-Imp variants in γ axons, GFP intensity was measured from a $41\mu\text{m}^2$ region of interest located in the distal part of the γ lobe (selected using FasciclinII staining as a template), subtracted from the intensity of a neighbouring background region, and normalised.

For detection of endogenous GFP fluorescence, 1-3 day old female flies (Go80-GFP-Imp; 201Y-Gal4,UAS-mCD8-RFP and Go80-GFP-Imp-CRISPR- Δ PLD; 201Y-Gal4,UAS-mCD8-RFP) were dissected in Schneider's medium, fixed with 4% formaldehyde, and washed three times with 0.1% PBs-Triton (PBT). Images were acquired on freshly mounted samples, with a Zeiss LSM780 NLO inverted confocal microscope equipped with a GaAsP *spectral detector* and a Plan Apo 40X 1.2 NA water objective for axons, and a 63x 1.4 NA oil objective for cell bodies. Measurement of endogenous GFP-Imp axonal signal was performed as explained above (using the 201Y>CD8-RFP marker as a template). To assess the fluorescence intensity of Imp in the cell body of MB γ neurons, GFP-Imp endogenous fluorescence was measured in a $332\mu\text{m}^2$ region of a single confocal section and background intensity subtracted. Average intensities were normalised to 1 for controls, and measured for the different variants.

FRAP experiments and analysis

FRAP experiments were performed on a Zeiss LSM780 NLO inverted confocal microscope, using the GaAsP *spectral detector*. Samples were imaged for five consecutive time frames and then bleached with 5 scan iterations (100% of a 35mV 488nm laser line). Fluorescence recovery was measured every 400 ms (for cells) and 1s (for brains) for 115 time points.

For FRAP on transfected S2R+ cells, cells were resuspended in 1 mL complete Schneider's medium after 24h of expression, and plated in Nunc Lab-Tek II chambered Coverglass (two wells). Imaging was performed using a Plan Apo 63X oil 1.4 NA objective, and a circular region of interest of 9 pixel diameter was bleached (pixel size: 0.15 μm). A maximum of 2 granules was recorded per cell. For FRAP on brains, 12-14 day old female flies were dissected (Go80-GFP-Imp; 201Y-Gal4,UAS-mCD8-RFP and Go80-GFP-Imp-CRISPR- Δ PLD; 201Y-Gal4,UAS-mCD8-RFP), their brains were mounted as described in (Medioni et al. 2015), and left at room temperature for 1 hour before imaging. Imaging was performed using a Plan Apo 40X water 1.2 NA objective, and a circular region of interest of 6 pixel diameter was bleached (pixel size: 0.083 μm). A maximum of 4 granules was recorded per hemisphere.

To quantify granule intensity over time, we manually tracked granules using the Fiji "Manual Tracking" plugin and used the xy coordinates of tracked particles to define ROI centers for each time points. Fluorescence intensities of the defined ROIs (3 pixel diameter) were measured using the Fiji "Measure Track" plugin (Chris Nicolai; <http://rsb.info.nih.gov/ij/plugins/measure-track/index.html>). Average intensities were normalized to pre-bleach intensities and corrected for acquisition bleaching (double normalization).

For experiments in HeLa cells, culture and FRAP assays were performed as described in (Mateju et al. 2017).

Particle imaging and tracking

For particle imaging on brains, 24h APF pupae were dissected (Go80-GFP-Imp; 201Y-Gal4, UAS-mCD8-RFP and Go80-GFP-Imp-CRISPR- Δ PLD; 201Y-Gal4,UAS-mCD8-RFP). Their brains were mounted as described in (Medioni et al. 2015), and left at room temperature for 1 hour before imaging. Experiment was performed on a Zeiss LSM880 Fast Airy Scan inverted confocal microscope, using the Fast Airy scan super resolution mode and a 40X water NA 1.1 objective. Stacks of 3 images (z step: 0.5 μ m) were acquired every 1.2 second and image analysis done on maximum intensity projections. The images were corrected for bleaching using the Fiji “Bleach correction > Histogram Matching method” plugin.

All moving particles detected in MB peduncles were manually tracked using the Fiji “Manual Tracking” plugin, and automatically analyzed as described in (Gaspar et al. 2014). Bidirectional granules were defined as granules undergoing at least one reversal that lasts for at least three consecutive steps. For analysis of run properties, runs were extracted from anterograde and retrograde granules, as well as from bidirectional granules for which both anterograde and retrograde components could be clearly assigned. Mean velocities were calculated using the following formula: $\text{Sqrt}((x_f-x_i)^2-(y_f-y_i)^2)/t_f-t_i$, where $(x,y)_f$ and $(x,y)_i$ refers to respectively the final and initial positions of individual tracked granules.

Fly genetics and generation of fly lines

Flies were raised on standard food at 25°C. All UAS-GFP-Imp constructs were inserted into the attP40 landing site *via* PhiC31-mediated integration and crossed with the 201Y-Gal4 line (gift of K. Ito) for analysis of subcellular distribution. To generate the GFP-Imp-CRISPR- Δ PLD line, gRNAs were cloned into the pDCC6 plasmid using the CTTCGCAACAGCAACAGAGCCTAGC and AAACGCTAGGCTCTGTTGCTGTTGC sense and antisense primers, and injected into Go80/+; attP40-nos-Cas9 embryos together with a donor construct containing a 3XP3-RFP selection cassette flanked by LoxP sites and 5' and 3'

homology arms. The 5' homology arm was amplified using the ATTGAGAACATGTCGCGTGC and ttactaCTGTTGCTGTTGTTGCAATTGTT primers, and the 3' homology arm using the AACAGCCACAGTCGCCATCT and ACGCTTTGCTCACTTCTCTTCT primers. RFP+ individuals were screened by PCR, and the Go80-GFP-Imp-CRISPR-□PLD line validated by sequencing. MCFO experiments were performed using the HA_V5_FLAG cassette and a hsp-flp inserted on the second chromosome (Nern et al. 2015); flies were raised at 18°C. MARCM experiments were performed as previously described (Wu and Luo 2006).

Western-Blots

For western-blots, protein extracts were subjected to electrophoresis, blotted to PVDF membranes, and probed with the following primary antibodies: rabbit anti-GFP (1:2500; Torey Pines); mouse anti-Tubulin (1:5000 ; Sigma).

Circular dichroism

The PLD of Imp was expressed in *E. coli* Rosetta2 bacterial cells transformed with pETM40-PLD containing a cleavable MBP N-ter tag and a His C-ter tag. The cells were sonicated in sonication buffer (20mM Tris Hcl pH 7.6, 200mM NaCl, protease inhibitors (Roche, 11836170001) and 1mg/ml lysozyme (Sigma L6876)) and the lysate treated with turbo DNase (Ambion™). Soluble MBP-tagged proteins were captured using amylose resin (NEB), and eluted with elution buffer A (20 mM Tris HCL pH 7.6, 15mM Maltose (Sigma M9171)). Recombinant proteins were then incubated with TEV, applied to a HI-TRAP TALON crude column (GE healthcare 10431065), eluted with elution buffer B (20 mM Tris HCL pH 7.6, 150mM Imidazole (sigma I2399)), and dialyzed into dialysis buffer (20mM Tris Hcl pH 7.6, 50mM NaCl and 20% glycerol).

Far ultraviolet circular dichroism spectra were recorded at 20°C using a JASCO J810 dichrograph equipped with a thermostatted cell holder and 0.1mm path-length quartz cuvettes (Hellma, Müllheim, Germany). Each spectrum was the average of 5 acquisitions recorded at a speed of 50nm min⁻¹, in 1nm increments from 260 to 190nm, and a bandwidth

of 1nm. All spectra were buffer-corrected and normalized to the mean residue weight ellipticity (θ MRW; degrees \times cm²/dmole) using the equation $\theta(\lambda)MRW = \theta(\lambda)mdeg/10cnd$, where $\theta(\lambda)mdeg$ is the recorded spectra in millidegrees, c is the sample concentration in moles per liter, n is the number of amino acid residues, and d is the path length of the cuvette in centimeters.

EMSA

EMSA experiments were performed as described in (Medioni et al. 2014), with recombinant GFP Imp and GFP Imp KH1234DD proteins expressed using the baculovirus expression system and purified as described in (Patel et al. 2015). Briefly, Imp sequences were cloned into pocc29 plasmids containing a Nter GFP tag and a cleavable MBP C-ter tag. After expression, cells were lysed in resuspension buffer (50 mM Tris-HCl pH 8, 1 M KCl, 5% glycerol, 0.1% CHAPS, 1 mM DTT), recombinant proteins were captured using amylose resin (NEB), and eluted with elution buffer (resuspension buffer complemented with 10mM maltose).

5.2.6 Figures

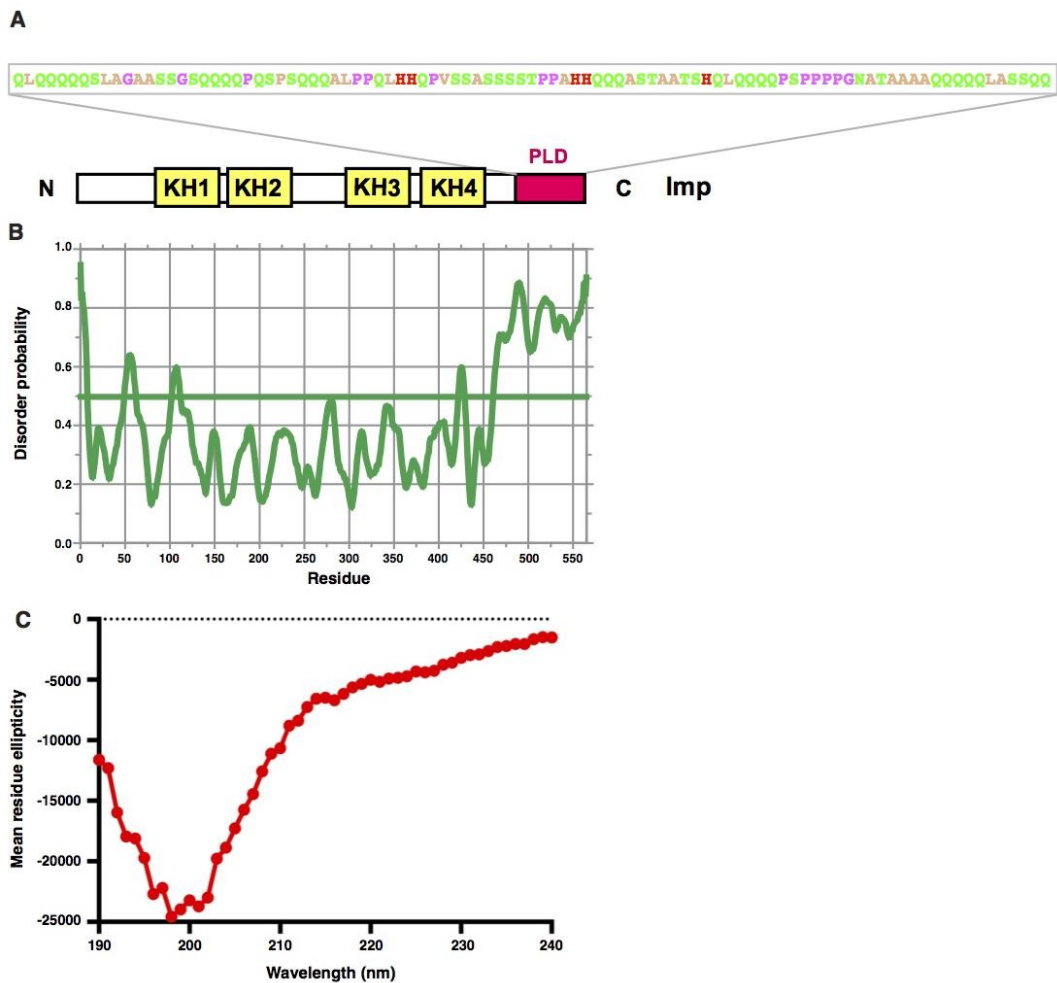


Figure 1. *Drosophila* Imp contains a C-terminal prion-like domain (PLD).

(A) Schematic representation of *Drosophila* Imp (PB isoform). The four KH RNA binding domains are shown in yellow, and the prion-like domain (PLD) in pink. Residues composing the prion-like domain are colored according to their physicochemical properties (Zappo color code). (B) Plot of the degree of disorder along the Imp protein, as predicted by the DisEMBL Intrinsic Protein Disorder Prediction 1.5 algorithm (Linding et al. 2003). (C) Far ultraviolet circular dichroism spectrum of the PLD of Imp.

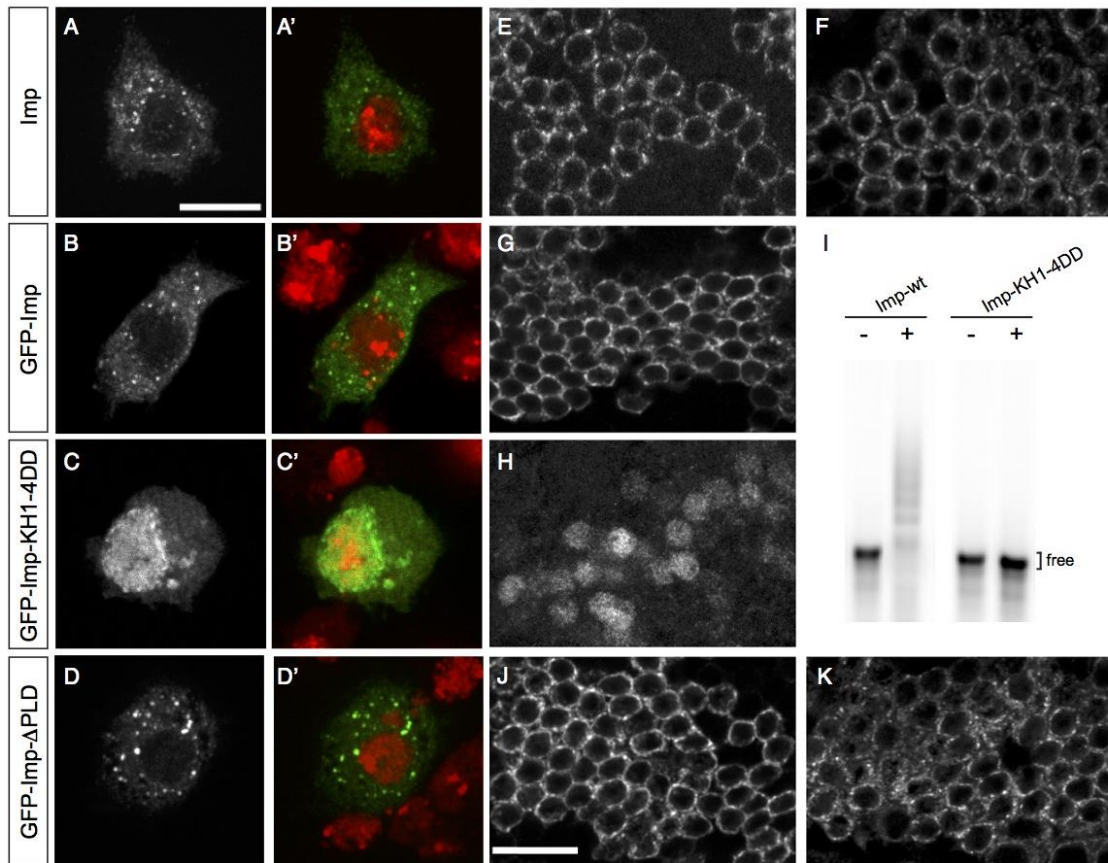


Figure 2. Imp PLD is dispensable for RNP granule assembly.

(A) S2R+ cell stained with anti-Imp antibodies (A, green in A'), and DAPI (red in A'). (B-D) S2R+ cells transfected with GFP-Imp (B), GFP-Imp-KH1-4DD (C) or GFP-Imp- Δ PLD (D) constructs, and stained with DAPI (red in B',C',D'). GFP signals are shown in white in B-D, and green in B'-D'. Scale bar in A-D: 10 μ m. Note that the KH1-4DD mutations induce a retention of Imp proteins in the nucleus, as described for the vertebrate protein (Wachter et al. 2013). (E) Cell bodies of wild-type adult MB γ neurons stained with anti-Imp antibodies. (F) Cell bodies of adult MB γ neurons homozygous for the Go80-GFP-Imp protein-trap insertion. GFP fluorescence is shown in white. (G-J) Cell bodies of adult MB γ neurons expressing wild-type GFP-Imp (G), GFP-Imp-KH1-4DD (H), or GFP-Imp- Δ PLD (J) under the control of the 201Y-Gal4 driver. GFP signals are shown in white. Complete genotypes: 201Y-Gal4/UAS-GFP-Imp, 201Y-Gal4/UAS-GFP-Imp-KH1-4DD, and 201Y-Gal4/UAS-GFP-Imp- Δ PLD. (I) EMSA analysis using fluorescently-labeled *profilin* 3'UTR in the absence (-) or presence (+) of 800 nM recombinant GFP-Imp (left) or GFP-Imp-KH1-4DD (right). (K) Cell bodies of adult MB γ neurons homozygous for the Go80-GFP-Imp-CRISPR- Δ PLD chromosome. GFP fluorescence is shown in white. Scale bar in E-K: 10 μ m.

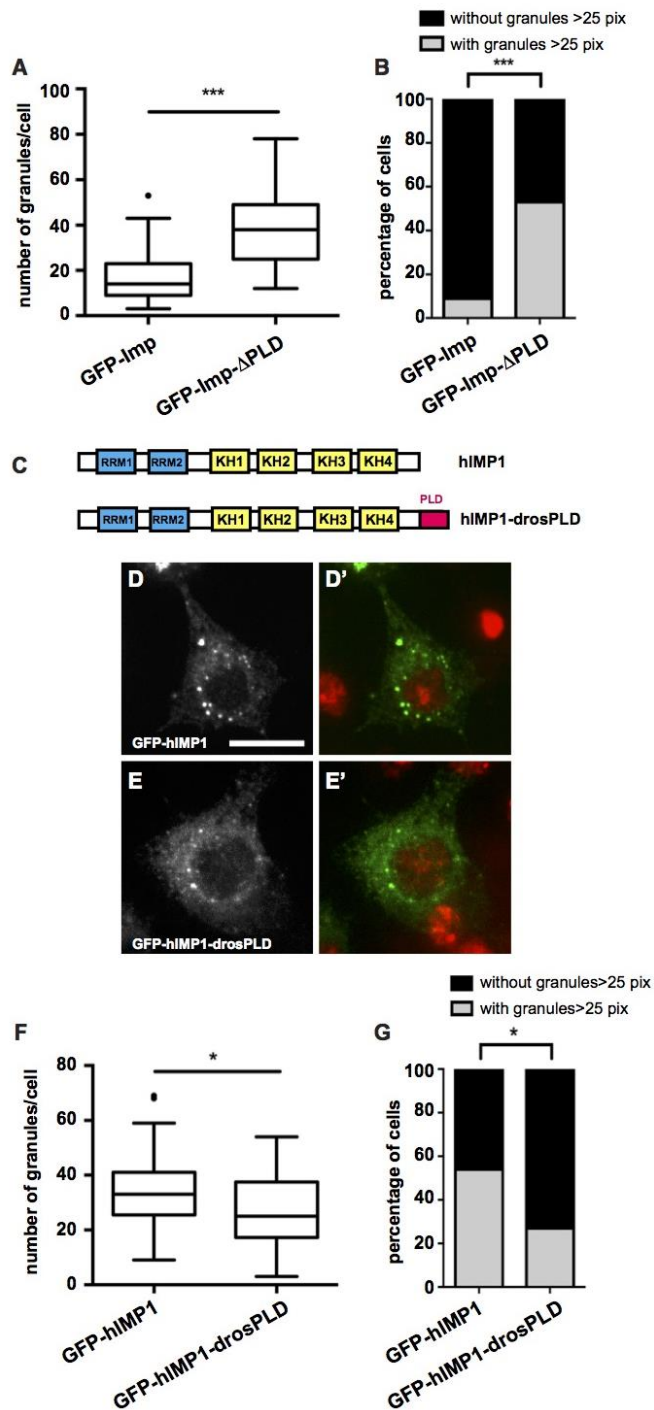


Figure 3. Imp PLD is both necessary and sufficient to restrict Imp granule size and number.

(A) Distribution of cells in function of their number of GFP-Imp (left) or GFP-Imp- Δ PLD (right) granules (Tukey box plots). ***, $P < 0.001$ (Mann-Whitney test). (B) Percentage of cells exhibiting granules larger than 25 pixels. ***, $P < 0.001$ (Fisher's exact test). 47 and 55 cells were analyzed for GFP-Imp and GFP-Imp- Δ PLD constructs respectively. (C) Schematic representation of hIMP1 (top)

and the chimeric construct hIMP1-drosPLD (bottom). (D,E) S2R+ cells transfected with GFP-hIMP1 (D) or GFP-hIMP1-drosPLD (E) constructs, and stained with DAPI (red in D', E'). GFP signals are shown in white in D,E, and green in D',E'. Scale bar: 10µm. (F) Distribution of cells in function of their number of granules (Tukey box plots). *, $P < 0.05$ (Mann-Whitney test). (G) Percentage of cells exhibiting granules larger than 25 pixels. *, $P < 0.05$ (Fisher's exact test). 37 and 49 cells were analyzed for GFP-hIMP1 and GFP-hIMP1-drosPLD respectively.

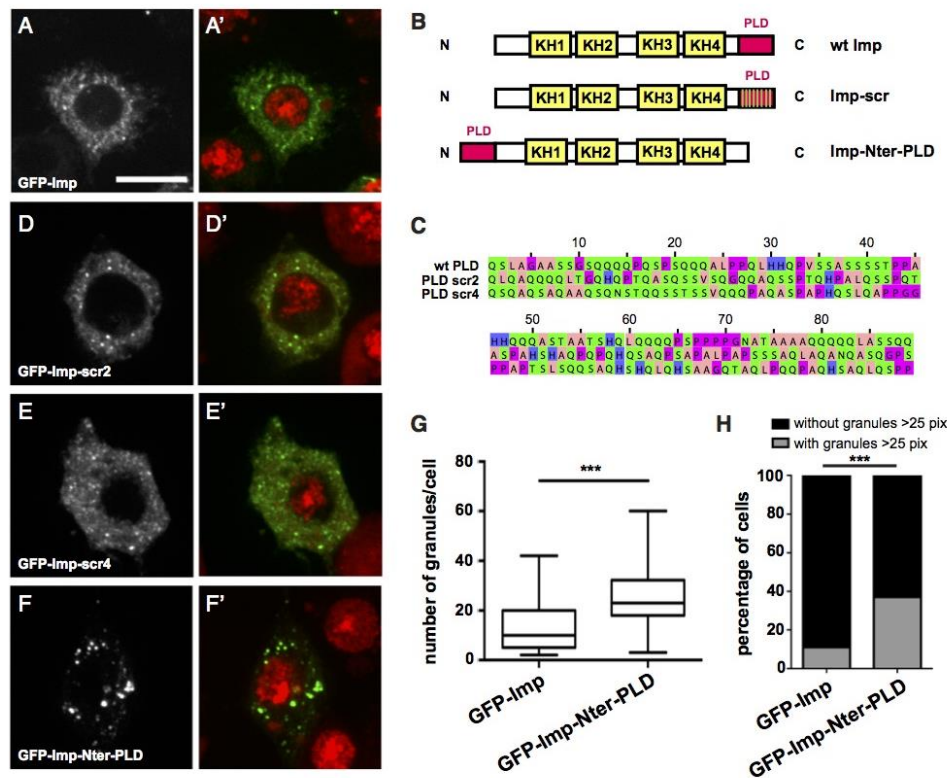


Figure 4. Molecular determinants underlying Imp PLD function in the regulation of Imp granule assembly.

(A,D,E,F) S2R+ cells transfected with GFP-Imp (A), GFP-Imp-scr2 (D), GFP-Imp-scr4 (E) or GFP-Imp-Nter-PLD (F) constructs, and stained with DAPI (red in A',D',E' and F'). GFP signals are shown in white in A,D,E,F and green in A',D',E',F'. Scale bar: 10µm. (B) Schematic representation of the generated Imp variants. (C) Primary sequences of the wild-type (top) and scrambled (bottom) PLDs. Scramble variants were generated randomly and exhibit different degree of Glutamine dispersion. (G) Distribution of cells in function of their number of GFP-Imp or GFP-Imp-Nter-PLD granules (Tukey box plots). ***, $P < 0.001$ (Mann-Whitney test). (H) Percentage of cells exhibiting granules larger than 25 pixels. ***, $P < 0.001$ (Fisher's exact test). 72 and 71 cells were analyzed for the GFP-Imp and GFP-Imp-Nter-PLD constructs respectively.

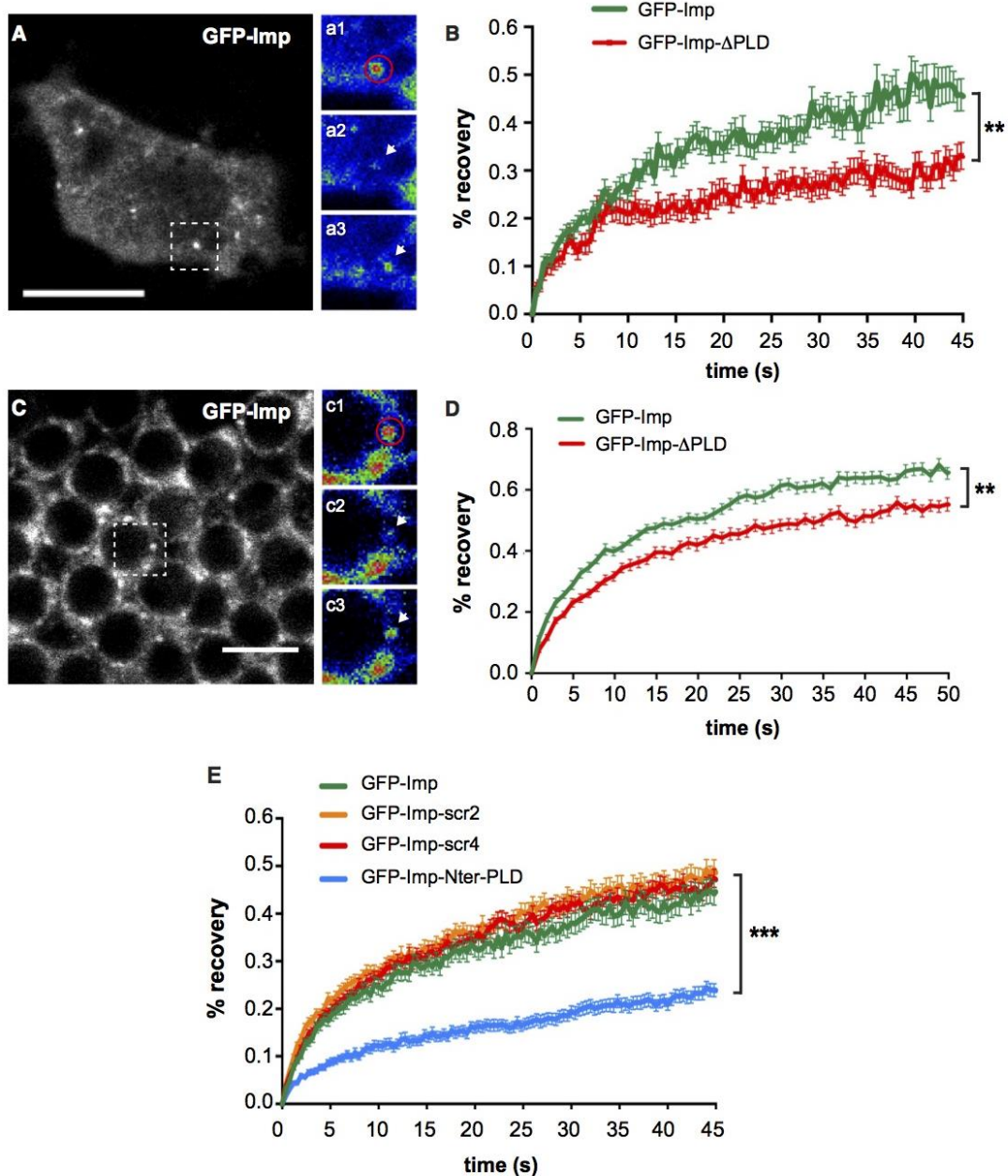


Figure 5. Imp PLD promotes the exchange of Imp in and out granules

S2R+ cell expressing GFP-Imp. The dashed box indicates the region shown in a1-a3. The red circle delimits the photobleached region, and the white arrows the position of the bleached granule over time. a1 and a2 correspond respectively to pre- and post-bleaching time points. a3 corresponds to the last recorded time point (t= 45s). Images in a1-a3 were color-coded using the Rainbow RGB function of ImageJ. Scale bar in A: 10 μ m. (B) Average FRAP curves obtained after photobleaching of GFP-positive particles from S2R+ cells. The following numbers of particles were analyzed: GFP-Imp: 44; GFP-Imp- Δ PLD: 41. (C) Cell bodies of adult MB γ neurons homozygous for the Go80-GFP-Imp protein-trap insertion (brain explant). The dashed box indicates the region shown in c1-c3. The red circle delimits the photobleached region, and the white arrows the position of the bleached granule

over time. c1 and c2 correspond respectively to pre- and post-bleaching time points. c3 corresponds to the last recorded time point ($t = 50s$). Images in c1-c3 were color-coded using the Rainbow RGB function of ImageJ. Scale bar in C: $5\mu m$. (D) Average FRAP curves obtained after photobleaching of GFP-positive particles from brain explants. The following numbers of particles were analyzed: Go80-GFP-Imp: 44; Go80-GFP-Imp-CRISPR- Δ PLD: 46. (E) Average FRAP curves obtained after photobleaching of GFP-positive particles from S2R+ cells. The following numbers of particles were analyzed: GFP-Imp: 55; GFP-Impscr2: 57; GFP-Imp-scr4: 51; GFP-Imp-Nter-PLD: 56. Error bars in B,D,E indicate s.e.m. **, $P < 0.01$; ***, $P < 0.001$ (Mann-Whitney test on the distributions of normalized intensity values at $t = 45s$ (B,E) or $50s$ (D)).

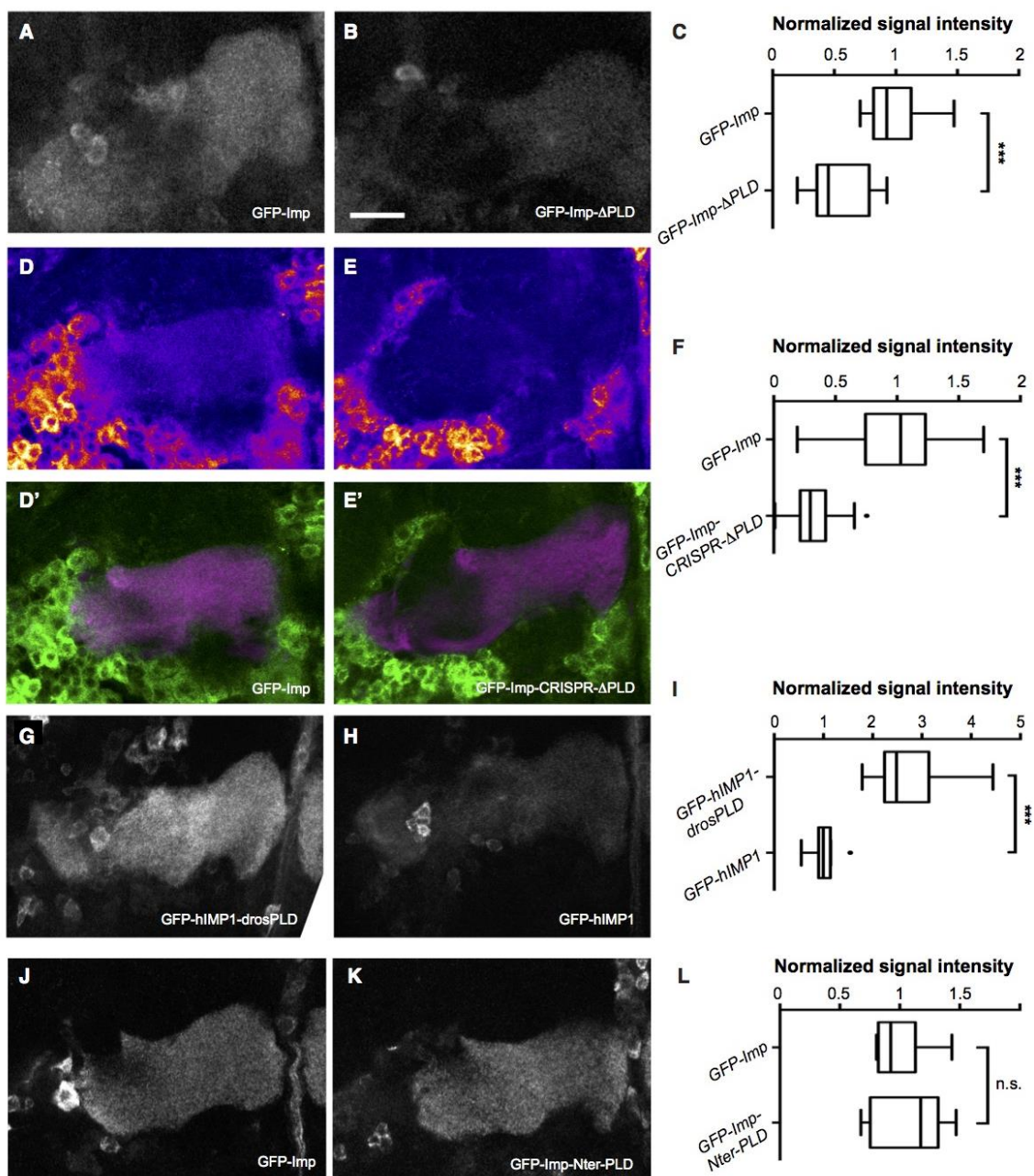


Figure 6. Imp PLD is essential for efficient localization of Imp to axons *in vivo*.

(A,B) Medial lobes of adult brains expressing GFP-Imp (A) or GFP-Imp- Δ PLD (B) under the control of the 201Y-Gal4 driver. The signal seen in medial lobes corresponds to the distal part of MB γ axon bundles (see Figure S6A). Genotypes: 201Y-Gal4/UAS-GFP-Imp and 201Y-Gal4/UAS-GFP-Imp- Δ PLD. (C) Distributions of normalized GFP signal intensities in distal axons (Tukey box plots). (D,E) Medial lobes of adult brains homozygous for the Go80-GFP-Imp (D,D') or Go80-GFP-Imp-CRISPR- Δ PLD (E,E') chromosomes. GFP signals are shown with the "Fire" look-up table of ImageJ in D,E, and in green in D',E'. 201Y-Gal4, UAS-mCD8-RFP signals are shown in magenta in D',E'. (F) Distributions of normalized GFP signal intensities in distal axons (Tukey box plots). (G,H) Medial lobes of adult brains expressing GFP-IMP1-drosPLD (G) or GFP-hIMP1 (H) under the control of the 201Y-Gal4 driver. Genotypes: 201Y-Gal4/UAS-GFP-hIMP1-drosPLD and 201Y-Gal4/UAS-GFP-hIMP1. (I) Distributions of normalized GFP signal intensities in distal axons (Tukey box plots). (J,K) Medial lobes of adult brains expressing GFP-Imp (J) or GFP-Imp-Nter-PLD (K) under the control of 201Y-Gal4 driver. (L) Distribution of normalized GFP signal intensities in distal axons (Tukey box plots). Numbers of MB analyzed: UAS-GFP-Imp: 25; UAS-GFP-Imp- Δ PLD: 24; Go80-GFP-Imp protein-trap: 33; Go80-GFP-Imp- CRISPR- Δ PLD: 32; UAS-GFP-hIMP1: 11; UAS-GFP-hIMP1-drosPLD: 12; UAS-GFP-Imp: 25; UAS-GFP-Imp-Nter-PLD: 24. ***, $P < 0.001$ (Mann-Whitney test). ns stands for not significant. Scale bar in A-K: 15 μ m.

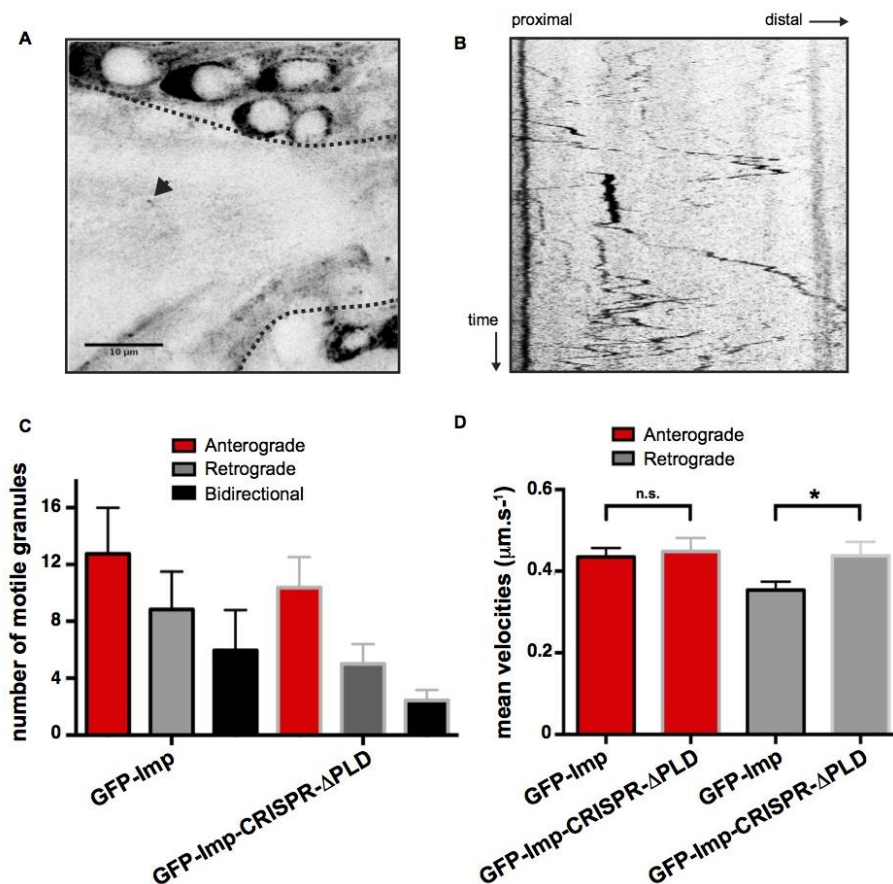


Figure 7. Imp PLD promotes Imp granule motility.

(A,B) Single image (A) and kymograph (B) extracted from a video generated from a Go80-GFP-Imp hemizygous pupal brain (24h APF; see also Video 1). The bundle of MB γ axons is delimited by dotted black lines. The arrowhead points to a GFP-Imp granule. (C) Average number of motile anterograde, retrograde and bidirectional GFP-Imp granules per 12min-long movie. Numbers of movies analyzed: $n=17$ for Go80-GFP-Imp and 16 for GFP-Imp-CRISPR- Δ PLD). Total numbers of granules analyzed: 468 for Go80-GFP-Imp and 284 for Go80-GFP-Imp-CRISPR- Δ PLD. (D) Mean anterograde and retrograde velocities. Numbers of anterograde granules analyzed: 271 (Go80-GFP-Imp) and 178 (Go80-GFP-Imp-CRISPR- Δ PLD); numbers of retrograde granules analyzed: 192 (Go80-GFP-Imp) and 91 (Go80-GFP-Imp-CRISPR- Δ PLD). Error bars in C,D represent sem. *, $P < 0.05$ (Unpaired t-test). ns stands for not significant.

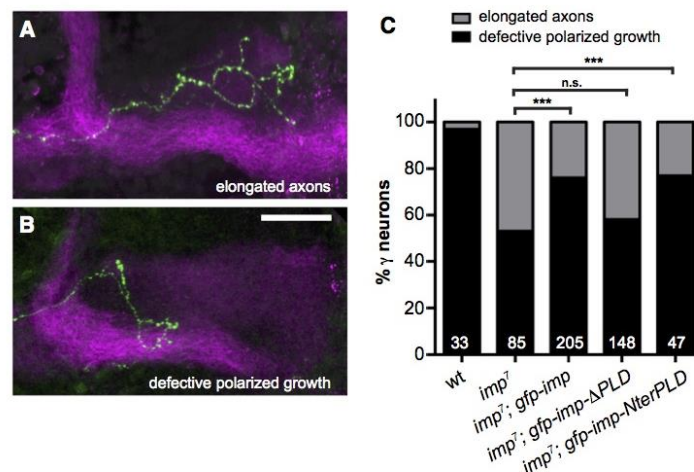


Figure 8. Imp PLD has independent functions in axonal remodeling and granule homeostasis.

(A,B) Representative images of adult MB γ neurons with properly “elongated axons” (A), or showing “defective polarized growth” (B). Single mutant axons were generated and labeled by GFP (green) using the MARCM technique. The shape of medial lobes is highlighted by Fasciclin II staining (magenta). Scale bar: 20 μ m. (C) Percentages of adult γ

axons that succeeded (elongated axon) or failed (defective axonal growth) to reach the extremity of the medial lobe. ***, $p < 0.001$ (Fisher’s exact test). n.s. stands for not significant. Numbers correspond to the total numbers of scored axons. Complete genotypes: FRT19A, tub-Gal80, hsp-flp/FRT19A; 201Y-Gal4, UAS-GFP/+ (wt); FRT19A, tub-Gal80, hsp-flp/FRT19A *imp*⁷; 201Y-Gal4, UAS-GFP/+ (*imp* mutant) and FRT19A, tub-Gal80, hsp-flp/FRT19A *imp*⁷; 201Y-Gal4, UAS-GFP/UAS-*gfp-imp*, UAS-*gfp-imp- Δ PLD* or UAS-*gfp-imp-Nter-PLD* (rescue conditions).

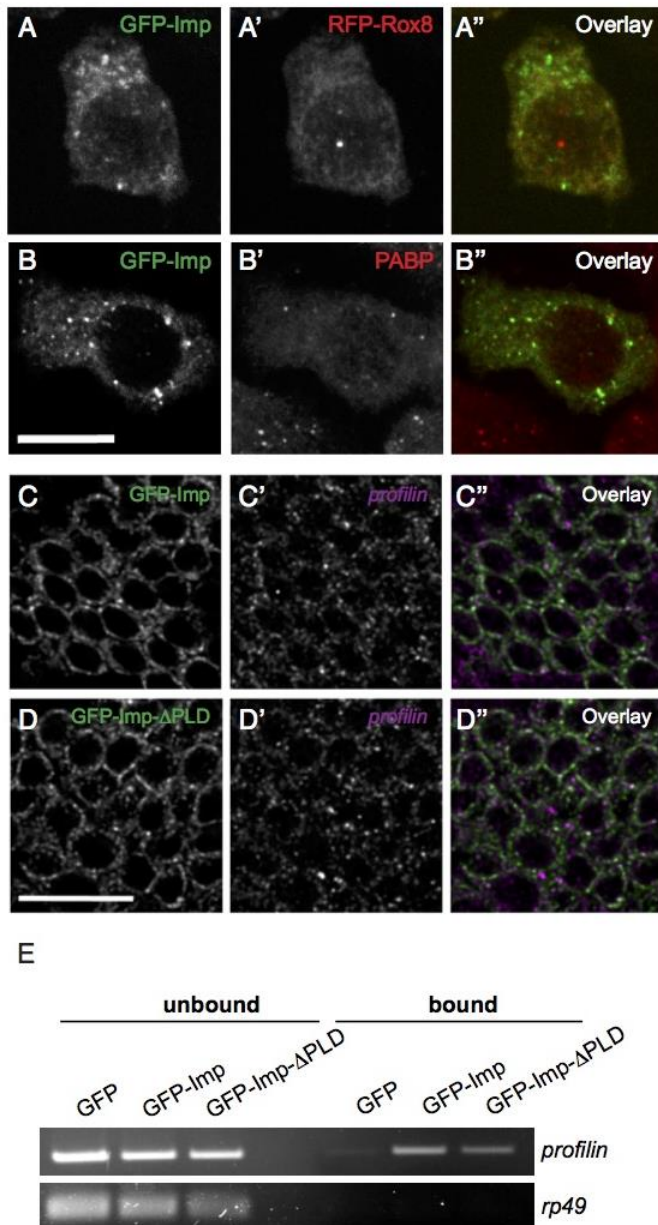


Figure S1. Characterization of Imp granules.

(A) S2R+ cells co-transfected with GFP-Imp (A, green in the overlay), and RFP-Rox8 (A', red in the overlay). Rox8 is the fly orthologue of Tia-1. (B) S2R+ cells transfected with GFP-Imp (B, green in the overlay) and stained with anti-PABP antibodies (B', red in the overlay). Scale bar: 10 μ m. (C,D) Cell bodies of adult MB γ neurons hemizygous for the Go80-GFP-Imp protein-trap insertion (C) or the Go80-GFP-Imp-CRISPR- Δ PLD chromosome (D). Brains were stained with anti-GFP antibodies (C,D; green in the overlay), and hybridized with fluorescently labeled *profilin* oligonucleotide probes (C',D'; magenta signal in the overlay). Scale bar: 10 μ m. (E) Semi-quantitative RT-PCR amplifications of mRNAs recovered in fractions immunoprecipitated from 201Y-Gal4/UAS-GFP (GFP), 201Y-

Gal4/UAS-GFP-Imp (GFP-Imp) or 201Y-Gal4/UAS-GFP-Imp- Δ PLD (GFP-Imp- Δ PLD) head extracts. *rp49* is used as a negative control.

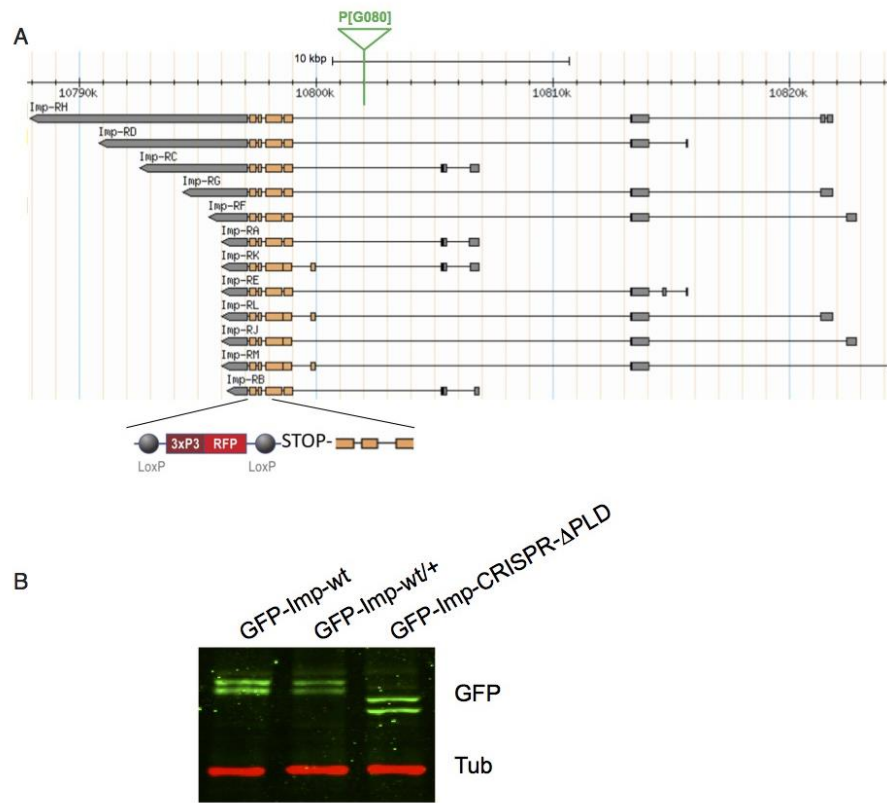


Figure S2. Description of the GFP-Imp-CRISPR- Δ PLD line

(A) Map of the *imp* genomic locus showing the Go80 protein-trap insertion together with the position of the CRISPR STOP cassette at the bottom (adapted from FlyBase). (B) Western-Blot of protein fractions recovered from heads homozygous (left) or heterozygous (middle) for the Go80-GFP-Imp protein-trap insertion, and heads homozygous for the Go80-GFP-Imp-CRISPR- Δ PLD chromosome (right). Proteins were stained with both anti-GFP (green) and anti-Tubulin (red) antibodies.

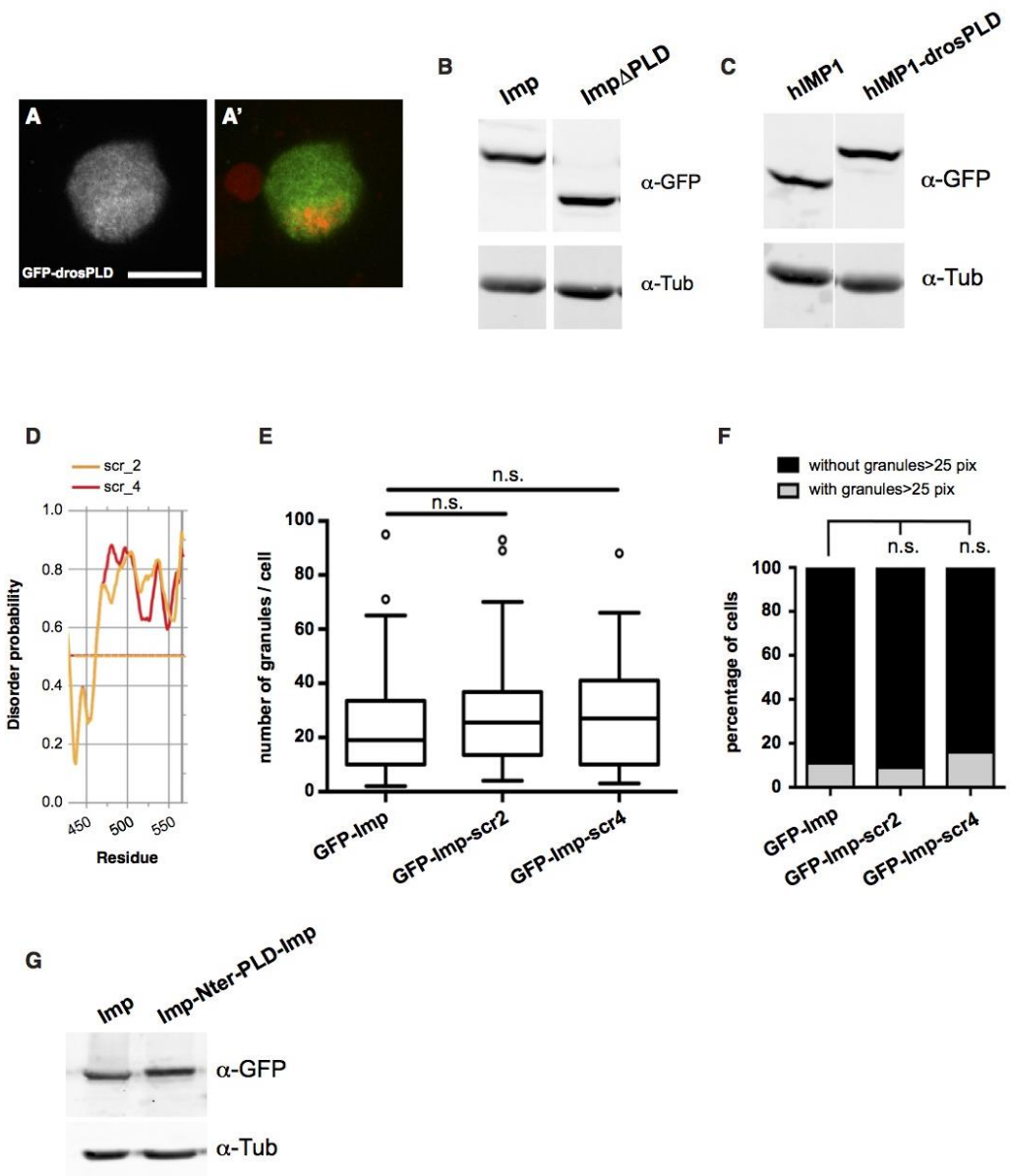


Figure S3. Imp PLD is sufficient to modulate granule size, and its function does not rely on a specific primary sequence.

(A) S2R+ cell transfected with GFP-drosPLD only (A, green A'), and stained with DAPI (red in A'). Scale bar: 10 μ m. (B) Western-Blot performed on extracts from S2R+ cells transfected with GFP-Imp (left) or GFP-Imp- Δ PLD (right) constructs, using anti-GFP and anti-Tubulin antibodies. (C) Western-Blot performed on extracts from S2R+ cells transfected with GFP-hIMP1 (left) and GFP-hIMP1-drosPLD (right) constructs, using anti-GFP and anti-Tubulin antibodies. (D) Plot of the degree of disorder along the Imp C-terminal region of Imp-scr2 and Imp-scr4 as predicted by the DisEMBL Intrinsic Protein Disorder Prediction 1.5 algorithm. Both variants have a predicted disordered C-terminal region. (E) Distribution of cells in function of their number of granules (Tukey box plots). (F) Percentage of cells exhibiting granules larger than 25 pixels. ns stands for not significant. 65, 80 and

62 cells were analyzed for GFP-Imp, GFP-Imp-scr2 and GFP-Imp-scr4 respectively. ns stands for not significant. (G) Western-Blot performed on extracts from S2R+ cells transfected with GFP-Imp (left), and GFP-Imp-Nter-PLD (right) constructs, using anti-GFP and anti-Tubulin antibodies.

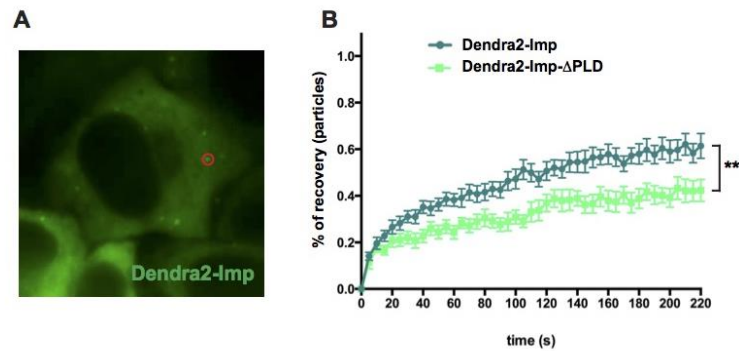


Figure S4. Imp PLD regulates the exchange of Imp in and out granules in HeLa cells.

(A) HeLa cell transfected with Dendra2-Imp (in green). The red circle delimits the photobleached region. (B) Average FRAP curves obtained after photobleaching of Dendra2-positive particles. The following numbers of particles were analyzed: Dendra2-Imp: 22; Dendra2-Imp-ΔPLD: 20. Error bars in B indicate s.e.m. **, $P < 0.01$ (Mann-Whitney test on the distributions of normalized intensity values at $t = 220$ s).

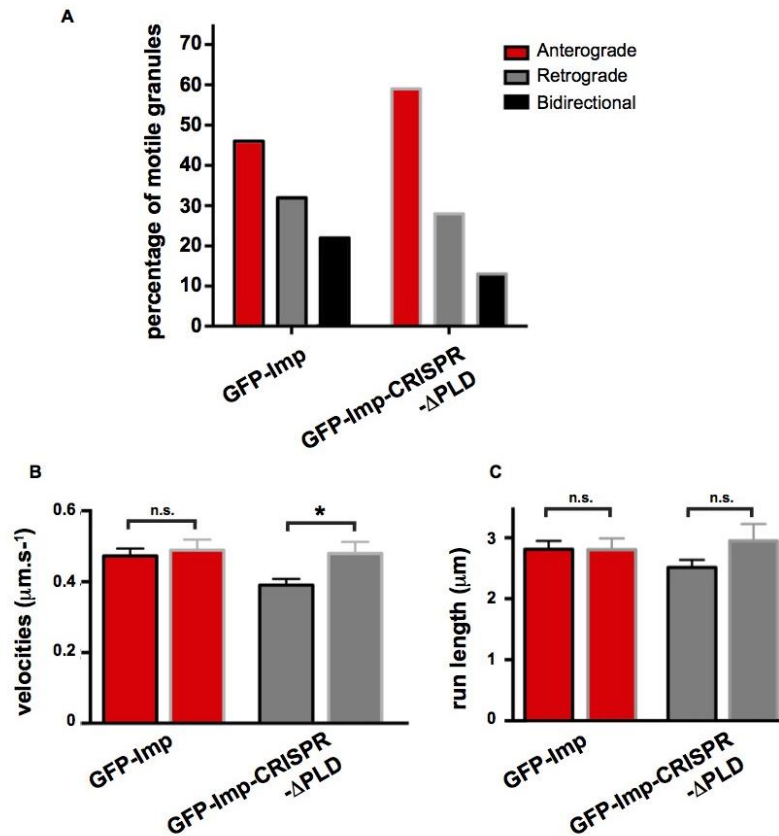


Figure S5. Characteristics of GFP-Imp granule motility.

(A) Percentage of anterograde, retrograde and bidirectional granules. Total numbers of granules analyzed: 468 for Go80-GFP-Imp and 284 for Go80-GFP-Imp-CRISPR-ΔPLD. (B,C) Average velocities (B) and length (C) of anterograde and retrograde runs. Numbers of anterograde runs analyzed: 286 (Go80-GFP-Imp) and 189 (Go80-GFP-Imp-CRISPR-ΔPLD); numbers of retrograde runs analyzed: 208 (Go80-GFP-Imp) and 93 (Go80-GFP-Imp-CRISPR-ΔPLD). Error bars represent sem. *, $P < 0.01$ (Unpaired t-test). ns stands for not significant.

5.3 Summary of my thesis work II

Experiments described above indicate that the PLD of Imp is not required for the assembly of the granules. Rather, cell culture and *in vivo* data indicates that the Imp PLD promotes the turnover of the Imp constituents within the RNP granules. Moreover, the PLD of Imp is important for the sub-cellular localization of Imp to MB γ axons, thereby supporting axon growth and branching.

In the following sections, I describe how I further probed the assembly and disassembly properties of Imp granules. First, as a preliminary experiment, I questioned the possibility of phosphorylation within the PLD domain (section 5.3.1). Specifically, I assessed the ability of a phospho-deficient Imp variant to modulate granule homeostasis and axon transport. Additionally, I assessed the ability of KH12 or KH34 di-domain point mutant constructs to assemble into granules. In the second part (section 5.3.2), I described the work I performed in the lab of Simon Alberti (MPI-CBG, Dresden) to establish *in vitro* phase-transition assays. There, I produced and purified both wild-type and mutant Imp proteins, and used them in phase-separation assays to understand the physico-chemical properties of the Imp RNP granules.

5.3.1 Imp PLD is not modulated through serine phosphorylation

Several studies have now shown that PLDs can be post-translationally modified, a process that affects the properties of RNP granules (Han et al. 2012; Monahan et al. 2017; Boeynaems et al. 2018; Carpenter et al. 2018). To test for a role of phosphorylation(s) in the PLD of Imp, I constructed a variant of Imp where all 17 serines were converted to non-phosphorylatable glycines. This variant of Imp, GFP-Imp-mut-ser, showed normal granule homeostasis i.e., granule size, number and turnover were similar to those of wildtype Imp granules (Table 1). Furthermore, GFP-Imp-mut-ser proteins localized normally to the axons of adult MB γ neurons, and rescued the *imp* axon growth defect phenotype (Table 1). Thus,

these experiments suggest that phosphorylation of PLD serines does not play a role in the regulation functions of Imp PLD.

Studies with the mammalian Imp indicated that the KH34 domain were essential for the interaction with RNA and assembly into granules. Initial experiment with the point mutation in the four KH domain indicated that interaction with RNA was essential for granule assembly. To better understand if the four KH domains were essential for granule assembly, KH12 or KH34 didomain mutants were constructed and transfected into S2R+ cells. I quantified the granules using the SPADE algorithm and observed that both the didomain mutant constructs had significantly less granules (Table. 1). Intriguingly, the KH 12 didomain mutant construct had significantly less granules than the KH34 construct suggesting that the interaction of the KH12 domains with transcripts was pivotal for granule assembly.

Table 1: Summary of Imp variants and their respective phenotypes in S2R+ cells and brain.

	Granule Appearance	Dynamics of the granules	Transport to γ axon	Rescue of axon remodeling defect
Imp wt	Normal	Normal	Transported	Rescued
Imp ΔPLD	Large and more granules	Less dynamic than Imp wt	Transported less efficiently	Does not rescue
Imp ScrPLD	Normal	Normal	Transported	Does not rescue
Nter Imp	Large and more granules	Less dynamic than Imp wt	Transported	Rescued
Imp mut ser	Normal	Normal	Transported	Rescued
Imp KH12DD	Normal but less granules	Not tested	Not tested	Not tested

Imp	Normal but less	Not tested	Not tested	Not tested
KH34DD	granules			

5.3.2 Imp PLD restricts the transition into aggregate state

Liquid-liquid phase separation has now been understood as the organizing principle for the assembly of RNP granules. As explained in the introduction, controlled *in vitro* assays can be used to assess the ability of *in vitro* purified proteins to self-assemble into semi-liquid droplets recapitulating the properties of RNP granules in conditions mimicking the cytosolic environment (Patel et al. 2015). In these assays, the influence of protein and salt concentrations, pH or RNA can be tested. To minimize protein aggregation, recombinant proteins were produced from SF9 insect cells infected with GFP-Imp or GFP Imp Δ PLD baculoviruses. Proteins were then purified in high salt buffer (1M KCl) and pH 8 using size exclusion chromatography to obtain pure, active and monomeric protein fractions (Fig. 17 A, B).

For phase separation assays, proteins were diluted into a buffer mimicking physiological salt concentrations and the solution spotted onto a plate. At 0.5 μ M, both wild-type and mutant proteins appeared diffuse in a non-crowded environment. However, addition of 10% dextran, a molecular crowding agent, to a protein concentration of 0.5 μ M resulted in the assembly of small (about 500 nm) macromolecular assemblies that separated from solution with both purified proteins (Fig. 17 C,C',D). These results are consistent with *in vivo* data indicating that the PLD domain is not required for assembly. Interestingly, this assay indicated that the GFP-Imp Δ PLD formed irregular assemblies that matured into large aggregates at a faster rate in comparison to GFP-Imp proteins (Fig. 17 D,D'). However, testing the *in vitro* macromolecular assemblies with a wide range of salt conditions did not modulate the phase diagram or the ageing of the granules (Fig. 17 E,F,G).

Nevertheless, these experiments performed in a simplified system suggested that the PLD of Imp might restrict the propensity of Imp proteins to self-assemble into high-order aggregates, possibly by interacting with Imp KH domains in *cis* or in *trans*.

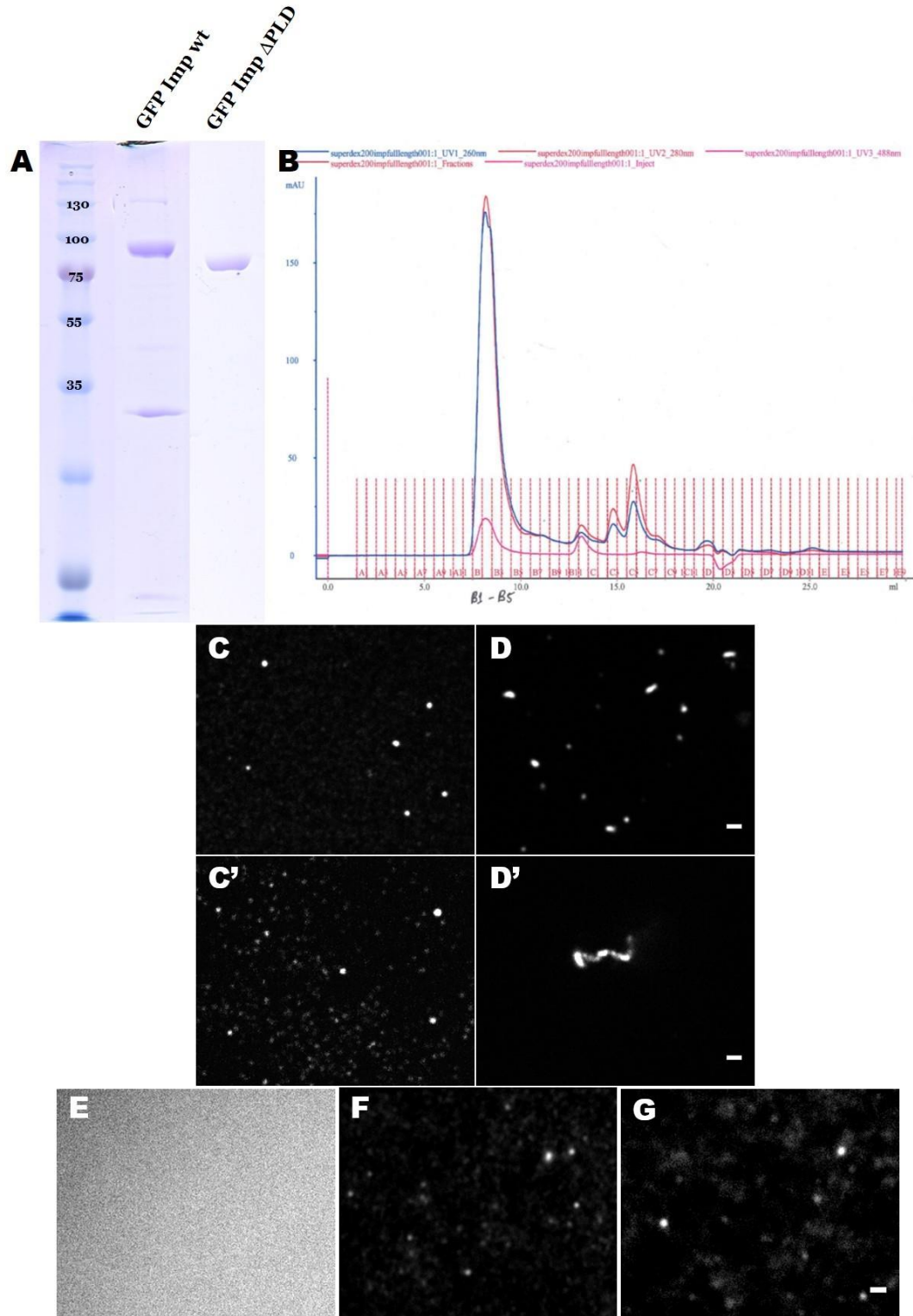


Figure 17. In Vitro Phase separation assay with GFP Imp and GFP Imp Δ PLD proteins.

A) Coomassie stained SDS PAGE gel of GFP Imp wt and GFP Imp Δ PLD proteins purified from SF9 insect cells. B) The cleaved and eluted proteins were passed through size exclusion chamber, Superdex 200 Increase 10/300 GL column, and the elution profile were recorded by following absorbance at 280 nm (protein: red peak) and 488 nm (GFP: pink peak). At 0 hour, both GFP Imp (C) and GFP Imp Δ PLD (D) formed condensates in the crowded environment. 4 hours later, GFP Imp (C') still remained as small condensates in the solution while GFP Imp Δ PLD (D') transitioned into aggregates, suggesting that the PLD behaves as a solubilizer and restricts the transition into aggregates. At 0.5 μ m protein concentration GFP Imp (E) remained diffuse, addition of 10% dextran led to the assembly of condensates at 300mM KCl which remained unaltered even at 500mM KCl (F) or 900 mM KCl (G) (Scale bar: 1 μ m).

6 Discussion and Perspectives

Together, my PhD work has unraveled a novel role for PLDs. First, in contrast to predominant model in the field, I observed that Imp PLD restricts the clustering of Imp molecules into cytoplasmic granules and promotes their dynamic exchange in and out granules (Fig. 18 A). Second, I have shown that Imp PLD promotes axonal localization, and is involved in the active transport of Imp RNP granules to MB γ axon, thus supporting the growth of adult axonal branches (Fig. 18 B). Notably, this study also unveiled that these two functions of Imp PLD are uncoupled.

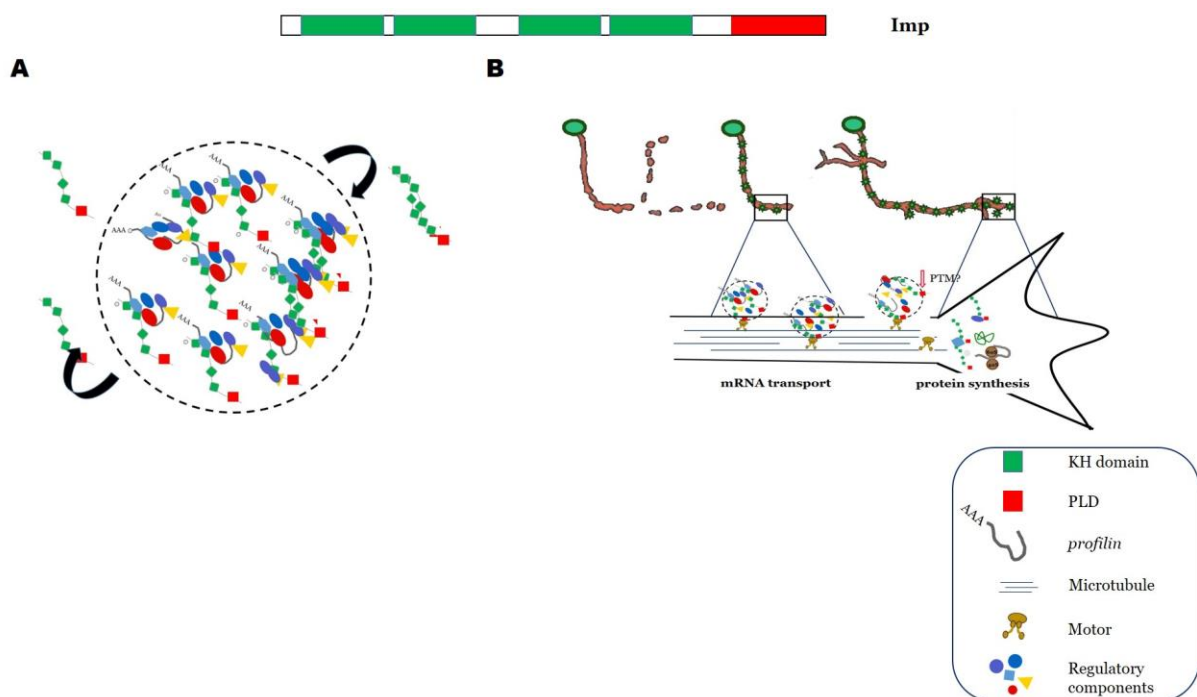


Figure 18: Model Illustrating the role of Imp PLD in granule homeostasis and Imp RNP granule transport.

(A) The PLD domain of Imp regulate granule homeostasis by restricting granule size and promoting the turnover of the Imp components with the RNP granules. (B) During γ neuron development, the PLD could undergo a stage-specific modification that results in interaction with motor proteins. This interaction leads to the transport of the Imp RNP granules along axonal MTs. The PLD-mediated transport of the RNP granules supports axon growth and branching, probably through the targeted release and local translation of the target transcript.

6.1 Modulators of Granule Assembly

With the advent of RNA CLIP and RNA capture analyses, it became evident that RNAs are often bound by a multitude RBPs regulating different aspects of their lifecycle. Furthermore, RBP/RNA interactions were shown to lead to the assembly of multimolecular complexes, and in some instances high-order assemblages called RNP granules. Eukaryotic cells contain a diverse range of membraneless RNP granules that behave as subcellular microcompartments concentrating macromolecules, controlling interactions with other components and exerting specific biological activity. Until recently, the factors driving assembly of RNP granules in space and time and the further recruitment of components to the granules had remained largely obscure. However, recent studies have unraveled the process of LLPS as an organizing principle promoting the assembly of RNP granules (Li et al. 2012; Lin et al. 2015; Molliex et al. 2015; Patel et al. 2015; Zhang et al. 2015; Smith et al. 2016; Zeng et al. 2016; Riback et al. 2017; Dao et al. 2018; Kroschwald et al. 2018; Protter et al. 2018). These studies indicated that multivalent interactions between proteins and nucleic acids either through multiple copies of interacting domains or PLDs in RBPs are a fundamental mechanism underlying the assembly of higher order structures. Consistent with this, studies have also reported that granules are enriched with proteins containing multiple modular domains or disordered PLD domain (Kato et al. 2012).

My work, using cell culture and *in vivo* MB γ neurons, revealed that the PLD of Imp is not essential for assembly into granules. On the other hand, introducing point mutations that abolish RNA binding in Imp four KH domains interfered with the assembly of Imp RNP granules. This suggests that the multivalent interaction between the modular KH domains of Imp and target mRNAs is a prerequisite for RNP granule assembly. Consistent with this hypothesis, I observed that the valency of interaction of the Imp KH domains with the transcript is essential for assembly, since the number of RNP granules formed by variants with point mutations in KH12 or KH34 didomains was significantly lower than in the wild-

type condition (see 5.3.1). Interestingly, I also noticed that KH12 didomain has a predominant role in granule assembly, as point mutations in both KH1 and KH2 reduced the number of granules observed more dramatically than point mutations in KH3 and KH4. This is in stark contrast to the human orthologue of Imp, where the KH34 didomain has been documented to be essential for RNA binding and granule assembly (Farina et al. 2003; Chao et al. 2010)

My work also showed that the removal of Imp PLD did not abolish granule assembly, but rather lead to the assembly of granules of increased size and number. This suggests that the PLD is not obligatory for assembly, but acts as modifiers of the RNP granule properties. Interestingly, this modulatory role was also observed in context where the PLD was ectopically grafted onto the human orthologue of Imp, indicating that the property of the PLD can be transferred to a functionally related protein. These results are consistent with the emerging view that PLDs act as solubilizers, and have a regulatory role in inhibiting the transition into aberrant aggregates (Franzmann and Alberti 2018; Franzmann et al. 2018; Kroschwald et al. 2018).

The FRAP data from cell culture as well as *ex vivo* brain explants revealed that Imp proteins have a short residence time within the granules, probably arising from transient interactions with other granule components. This demonstrates that Imp granules are dynamic structures constantly exchanging components with the cytoplasmic environment. Furthermore, my data indicated that, upon deletion of the PLD of Imp, the Imp protein had a low turnover rate. Surprisingly, the Imp-Nter PLD showed less dynamic granule property, suggesting that the position of the PLD could regulate the specificity of interactions either to the other domains of the Imp protein or with the components of the granules. Thus, this suggests that PLD promotes the turnover of the Imp proteins, and that the position of the PLD has an important role in this process.

How could the PLD act as solubilizer, and regulate the assembly and turnover of the complexes? One possible explanation would be that removal of the PLD affects the range of

specificity and affinity of interactions with the other components of the granules, resulting in a shift in the equilibrium from small to large and more static RNP granules. It is conceivable that the structured domains (e.g., the KH domains) are involved in specific interactions that promote assembly of the granules, while the PLD mediates promiscuous and transient interactions with other structured domains or PLDs present within the granule. Alternatively, the PLD could act *in cis* by binding to RBDs within the protein, as shown in other contexts (Wang et al. 2018). Removal of the PLD would unmask binding sites that may perturb interactions essential for regulating the property of the granule. Finally, the dynamic interaction of PLD with RBDs or other components of the granules can also be envisioned as a way to regulate the size of the granules.

Whether the activity of Imp PLD is regulated *in vivo* remains to be demonstrated, but studies have shown in neurons that RNP granules with diverse material properties exist (Cougot et al. 2008; Gopal et al. 2017). For example, the material properties of RNP granules have been shown to change in response to activity, and as the granules get transported along the axon. Such changes likely reflect changes in the interaction, subcellular contents, and/or maturation of the RNP granules (Cougot et al. 2008; Gopal et al. 2017), and may differentially control the transport, storage, local translation and degradation of the transcripts. While dynamic granules could be seen as compartments which recruit specific cellular components and perform biochemical reactions, solid-like static granules are likely involved in the storage of mRNA (Alberti and Hyman 2016).

Taken together, this work showed that Imp RNP granules are nanometer sized RNP granules that assemble through the interaction of Imp with target transcripts, and provides substantial evidence for the role of PLDs in modulating the physico-chemical properties of Imp granules. Both *in vitro* reconstitution experiments and *in vivo* assays uncovered that Imp PLD has solubilizing properties and restricts the condensation of Imp molecules into large higher order assemblies. Further experiments need to be performed to understand in depth the organizing principles, and the regulatory role of PLDs for the assembly and

transition of dynamic granules into aggregates. It is conceivable that Imp requires a specific type of posttranslational modification or other macromolecules like RNA or other RBPs, kinases that could modulate the granule properties.

6.2 Sequence features of the PLD

The unusual sequence of yeast and mammalian prion proteins, in particular their enrichment in Q/N amino acids allowed for broader search of similar domains in different species. Targeted *in silico* searches unveiled a large group of proteins showing prion-like domains characterized by an underrepresentation of charged and highly hydrophobic residues (March et al. 2016). Comparative proteomic studies led to the identification of short linear interaction motifs (SLiMs) of 3-10 residues observed within disordered regions. SLiMs are structured regions within the predominantly disordered IDRs and could be involved in stereospecific transient interactions with components of the granules (Babu 2016; Miskei et al. 2017). Recent computational analysis attributed the ability of higher order assembly to such specific sequence motifs found within the PLD (Sabate et al. 2015). However, considering the low primary sequence conservation of PLDs, it remains unclear whether the function of PLDs depends on their overall amino acid composition or specific sequence motifs. To test this in the context of Imp PLD, I generated scrambled variants whose overall amino acid composition, but not primary sequence, were preserved. The scrambled variants behaved similar to the wildtype Imp granules, restricting granule size and number and also regulating Imp granule dynamics. Thus, my data indicate that the overall amino acid composition and disorder in the PLD, not the primary sequence, is essential for granule homeostasis. This work is in agreement with previous work with yeast prion proteins that showed scrambled sequences were able to support prion formation (Ross et al. 2004; Ross et al. 2005a). However, in order to understand if disorder in the PLD or the composition of glutamine and serine are necessary for granule homeostasis, it would be important to assess these parameters in a chimeric protein with PLD from a different prion-like proteins and neutral sequences that don't have disorder propensity. Here, it would be essential to assess

PLDs with compositional enrichment for glutamines and serines, similar to Imp, but also different types of PLDs containing amino acids bias to arginine, glycine such as RGG repeats, [G/S]Y[G/S] etc.

6.3 A specific function of Imp PLD in the axonal transport of Imp granules to axons

RNP granules are very finely tuned microcompartments that control their composition to perform specific biochemical reaction, or adapt to the specific demands of the cell. Based on the observed difference in granule properties between wildtype and mutant Imp granules, we sought to characterize and compare the composition of complexes formed by wild-type and Imp- Δ PLD proteins. Surprisingly, immunoprecipitation-mass-spectrometry experiments performed from adult brains expressing GFP-tagged proteins in MB γ neurons revealed that the composition of complexes formed by Imp and Imp Δ PLD proteins is largely similar (Marjorie Heim and Florence Besse, unpublished).

Nevertheless, I questioned if the changes in Imp granule size and kinetics induced by Imp PLD deletion could have a functional impact. Previous work from the lab had demonstrated that the localization of Imp granules to MB γ axons is developmentally-regulated and driven by active, microtubule-dependent transport (Medioni et al. 2014). Thus, I examined the subcellular localization of wild-type and Δ PLD proteins and found that only the full-length protein efficiently translocated to MB γ axons during pupal and adult stages. Furthermore, real-time *in vivo* imaging shows that the Imp PLD appears to promote the motility of both anterograde and retrograde axonal RNP granules, and to modulate the velocity of retrograde directed granules. Thus, it suggests that Imp PLD is an essential regulator of the axonal transport of Imp granules induced during metamorphosis. Furthermore, I could show using the MARCM single neuron labelling technique that these defects in axonal transport are linked to defects in axon growth and branching,

demonstrating that the correct assembly and transport of Imp granules have important functional consequence for axon morphology.

Why Imp granules start being transported to axons specifically during early metamorphosis is unclear, but it is possible that the Imp PLD undergoes functional modifications during that stage, in response to developmental cues. Such changes may lead to the specific recruitment of motor proteins facilitating the transport of the Imp granules. The orthologues of Imp have been shown to differentially interact with actin and microtubule networks for docking and transport respectively (Nalavadi et al. 2012; Urbanska et al. 2017). Furthermore, vertebrate Imp have been demonstrated to be a part of motile RNP granules that interact with myosin and kinesin motor proteins, and have important function for cell motility and/or neurite growth and branching (Oleynikov and Singer 2003; Tiruchinapalli et al. 2003; Perycz et al. 2011; Welshhans and Bassell 2011; Kalous et al. 2014; Gaynes et al. 2015). However, not much is known about the interaction of *Drosophila* Imp with motor proteins. Our mass spectrometry data did not reveal any motor proteins among Imp interactors. One possible reason for this could be that the analysis was performed at the adult stage, a stage where interaction with motor proteins may not be as robust as during earlier developmental stage. Thus, it would be interesting to elucidate the interaction of Imp with motor proteins during late larval and pupal stages. This could be done by genetically manipulating the function of motor proteins and live imaging to assess the differences in the length and velocity of transport of the Imp RNP granules. Furthermore, co-immunoprecipitation experiments from wild-type and Imp Δ PLD head extracts from the three distinct stages of the *Drosophila* life cycle would help elucidate the differential recruitment and direct interaction of motor proteins to Imp granules.

As Imp proteins with scrambled domains localized to axons *in vivo*, SLiMs do not mediate interaction with motor molecules. Furthermore, the Imp-Nter PLD was transported to the γ axons, indicating that although during assembly the position of the PLD modifies the intermolecular contacts and affects granule dynamics, it does not affect the axonal transport

of Imp granules. Thus, the position of the PLD did not perturb its interaction with motor proteins. Remarkably, although Imp proteins with scrambled domains localized normally to axons *in vivo*, both variants were unable to rescue the *imp* dependent growth and branching defects (Table 1). A possible explanation could be that granule assembly, transport and disassembly are regulated by discrete sets of events with different molecular requirements. In this scenario, information contained in PLD primary sequence (SLiMs potentially) could be necessary to regulate the release and subsequent translation of transcripts supporting axon growth and branching. This might involve PTMs that could either result in the local remodeling of RNP granules in axons, or in a charge-dependent disassembly of the complex (Kim and Richter 2006; Monahan et al. 2017; Boeynaems et al. 2018; Carpenter et al. 2018).

The activity of the human Imp has been shown to be regulated through posttranslational modifications, which can modulate the release of transcripts from Imp in designated locations (Huttelmaier et al. 2005; Git et al. 2009; Huang et al. 2018). In particular, the affinity of binding and controlled release of the transcripts at specific destination have been shown to be regulated through a Src kinase-dependent phosphorylation of the linker between ZBP1 KH2 and KH3 (Huttelmaier et al. 2005; Git et al. 2009; Sasaki et al. 2010; Dai et al. 2015; Urbanska et al. 2017). However, this sequence is not conserved in the *Drosophila* Imp. Recent reports have indicated that sites that could undergo PTMs, particularly phosphorylation, are located within SLiMs found in PLDs (van der Lee et al. 2014; Latysheva et al. 2015; Boeynaems et al. 2018; Itakura et al. 2018). Therefore, it is possible that phosphorylation of a specific sequence within the *Drosophila* Imp PLD could modulate granule assembly and disassembly in space and time. In a preliminary experiment, I observed that mutating all 17 serines of the Imp PLD to non-phosphorylatable glycines neither modified the granule properties nor MB γ axon remodeling in developing brains, suggesting that the function of Imp PLD is not modulated by serine phosphorylation. However, more experiments need to be performed to find out whether Imp granules might be regulated through different PTMs. Mass spectrometry has been utilized predominantly to study PTMs. However, the biased amino acid sequence of the Imp PLD limits the use of classical site-

specific proteases to analyse the relative degree of PTMs within the PLD. Immunoprecipitation based techniques can be employed to detect PTMs. Antibodies that bind to target PTMs are bound to a column and lysates are passed through this column. Following elution, the eluted sample could be separated by SDS-PAGE and analysed using the specific Imp antibody via Western Blot. Recently, proximity ligation assay been gaining interest (Elfineh et al. 2014). This technique allows for the detection of PTM for a given protein by employing two antibodies: one against a specific PTM and another against the protein of interest. Fluorescence emission that occurs only as a result of the close proximity of the two antibodies thus could be employed to detect for PTM in Imp. Alternatively, biochemical and molecular approaches can be used to mutate single or multiple amino acids within the PLD to generate PTM mimics or deficient mutants of phosphorylation, s-nitrosylation, ubiquitination, acetylation etc. These variants could then be employed to assess the granule homeostasis and transport ability.

Altogether, this study has successfully unravelled that the localization of the mRNA transport machinery assembled by the conserved Imp protein occurs specifically through the unstructured PLD found in *Drosophila* Imp protein. Despite the conserved role in mRNA localisation, the vertebrate orthologues of Imp lack a PLD. Why this domain with a beneficial role in granule transport has not been conserved during evolution remains to be understood. The structural plasticity of PLDs enables them to interact with a wide range of proteins. It is possible that in some species this abundance of interactions could be undesirable and disrupt the balance of components that are bound specifically by other domains. Additionally, RNP granules have been shown to be enriched with several RBPs containing PLD. It is possible that the PLD of Imp was lost due to the abundance of different RBPs containing PLD with a redundant role in transport. Furthermore, growing lines of evidence indicate that PLD-containing proteins are prone to pathological aggregation, which can be exacerbated by random mutations or environmental factors (Alberti and Hyman, 2016). In this scenario, such high-risk mutations could require specific costly efforts from the cell to maintain homeostasis and prevent the transition to aggregate and disease-causing state.

Therefore, intolerance to undesirable interactions and the propensity for hyper-aggregation can be envisioned as a possible reason why Imp lost the PLD during evolution. It would thus be interesting to study if the Imp PLD are prone to such pathological aggregation and what leads to such aggregation that are seen as deleterious to the cell's physiological function.

6.4 Conclusion

In conclusion, my work has successfully unraveled a physiological function for a PLD in the maturing nervous system, and showed that these domains may play an important function in the spatio-temporal regulation mRNA transport machineries. This discovery is of interest in a context where such domains have been shown to be prevalent within RBPs, while prone to generate pathological aggregates upon aging or in neurodegenerative diseases.

It will now be interesting to get a broader view on the role of such domains beyond liquid-liquid phase separation, in the regulation of the physiological properties of RBPs. RBPs are involved in the orchestrating the life cycle of RNA right from splicing, efficient and rapid transport of RNA in a translationally repressed state to subcellular domains and finally up until degradation. However, several questions need to be addressed. How do RBPs recognize mRNAs and sort mRNAs into specific RNP granules? How do they control the components that are recruited to the granules? How do they restrict gene expression and prevent mRNA from recognition by translational machinery during transport? Is the loss of the dynamic state and aggregate formation intricately connected to neurodegenerative diseases? It is likely that PLDs will impact on these different processes, so understanding their role will help address these important questions as well as the functions that are regulated through the assembly of RNP granules, and how they transition into pathological aggregate state.

7 References

- Aakalu G, Smith WB, Nguyen N, Jiang C, Schuman EM. 2001. Dynamic visualization of local protein synthesis in hippocampal neurons. *Neuron* **30**: 489-502.
- Aguzzi A, Altmeyer M. 2016. Phase Separation: Linking Cellular Compartmentalization to Disease. *Trends Cell Biol* **26**: 547-558.
- Aizer A, Brody Y, Ler LW, Sonenberg N, Singer RH, Shav-Tal Y. 2008. The dynamics of mammalian P body transport, assembly, and disassembly in vivo. *Molecular biology of the cell* **19**: 4154-4166.
- Alami NH, Smith RB, Carrasco MA, Williams LA, Winborn CS, Han SSW, Kiskinis E, Winborn B, Freibaum BD, Kanagaraj A et al. 2014. Axonal transport of TDP-43 mRNA granules is impaired by ALS-causing mutations. *Neuron* **81**: 536-543.
- Alberti S. 2017. The wisdom of crowds: regulating cell function through condensed states of living matter. *J Cell Sci* **130**: 2789-2796.
- Alberti S, Halfmann R, King O, Kapila A, Lindquist S. 2009. A systematic survey identifies prions and illuminates sequence features of prionogenic proteins. *Cell* **137**: 146-158.
- Alberti S, Hyman AA. 2016. Are aberrant phase transitions a driver of cellular aging? *Bioessays* **38**: 959-968.
- Alvarez J, Giuditta A, Koenig E. 2000. Protein synthesis in axons and terminals: significance for maintenance, plasticity and regulation of phenotype. With a critique of slow transport theory. *Prog Neurobiol* **62**: 1-62.
- Anderson P, Kedersha N. 2009. RNA granules: post-transcriptional and epigenetic modulators of gene expression. *Nat Rev Mol Cell Biol* **10**: 430-436.
- Armijo-Weingart L, Gallo G. 2017. It takes a village to raise a branch: Cellular mechanisms of the initiation of axon collateral branches. *Mol Cell Neurosci* **84**: 36-47.
- Aronov S, Aranda G, Behar L, Ginzburg I. 2002. Visualization of translated tau protein in the axons of neuronal P19 cells and characterization of tau RNP granules. *J Cell Sci* **115**: 3817-3827.
- Babu MM. 2016. The contribution of intrinsically disordered regions to protein function, cellular complexity, and human disease. *Biochem Soc Trans* **44**: 1185-1200.
- Bah A, Forman-Kay JD. 2016. Modulation of Intrinsically Disordered Protein Function by Post-translational Modifications. *J Biol Chem* **291**: 6696-6705.
- Baj G, Leone E, Chao MV, Tongiorgi E. 2011. Spatial segregation of BDNF transcripts enables BDNF to differentially shape distinct dendritic compartments. *Proc Natl Acad Sci U S A* **108**: 16813-16818.
- Bakthavachalu B, Huelsmeier J, Sudhakaran IP, Hillebrand J, Singh A, Petrauskas A, Thiagarajan D, Sankaranarayanan M, Mizoue L, Anderson EN et al. 2018. RNP-Granule Assembly via Ataxin-2 Disordered Domains Is Required for Long-Term Memory and Neurodegeneration. *Neuron* **98**: 754-766 e754.
- Balasanyan V, Arnold DB. 2014. Actin and myosin-dependent localization of mRNA to dendrites. *PLoS One* **9**: e92349.
- Baleriola J, Hengst U. 2015. Targeting axonal protein synthesis in neuroregeneration and degeneration. *Neurotherapeutics* **12**: 57-65.
- Barbee SA, Estes PS, Cziko AM, Hillebrand J, Luedeman RA, Coller JM, Johnson N, Howlett IC, Geng C, Ueda R et al. 2006. Staufen- and FMRP-containing neuronal RNPs are structurally and functionally related to somatic P bodies. *Neuron* **52**: 997-1009.
- Bassell GJ, Zhang H, Byrd AL, Femino AM, Singer RH, Taneja KL, Lifshitz LM, Herman IM, Kosik KS. 1998. Sorting of beta-actin mRNA and protein to neurites and growth cones in culture. *J Neurosci* **18**: 251-265.
- Batish M, van den Bogaard P, Kramer FR, Tyagi S. 2012. Neuronal mRNAs travel singly into dendrites. *Proc Natl Acad Sci U S A* **109**: 4645-4650.

- Batista AF, Hengst U. 2016. Intra-axonal protein synthesis in development and beyond. *Int J Dev Neurosci* **55**: 140-149.
- Battich N, Stoeger T, Pelkmans L. 2013. Image-based transcriptomics in thousands of single human cells at single-molecule resolution. *Nat Methods* **10**: 1127-1133.
- Ben-Yaakov K, Dagan SY, Segal-Ruder Y, Shalem O, Vuppalachchi D, Willis DE, Yudin D, Rishal I, Rother F, Bader M et al. 2012. Axonal transcription factors signal retrogradely in lesioned peripheral nerve. *EMBO J* **31**: 1350-1363.
- Berry FB, Brown IR. 1996. CaM I mRNA is localized to apical dendrites during postnatal development of neurons in the rat brain. *J Neurosci Res* **43**: 565-575.
- Bertrand E, Chartrand P, Schaefer M, Shenoy SM, Singer RH, Long RM. 1998. Localization of ASH1 mRNA particles in living yeast. *Mol Cell* **2**: 437-445.
- Besse F, Ephrussi A. 2008. Translational control of localized mRNAs: restricting protein synthesis in space and time. *Nat Rev Mol Cell Biol* **9**: 971-980.
- Bianco A, Dienstbier M, Salter HK, Gatto G, Bullock SL. 2010. Bicaudal-D regulates fragile X mental retardation protein levels, motility, and function during neuronal morphogenesis. *Curr Biol* **20**: 1487-1492.
- Birnstiel ML, Flamm WG. 1964. Intranuclear Site of Histone Synthesis. *Science* **145**: 1435-1437.
- Blower MD, Feric E, Weis K, Heald R. 2007. Genome-wide analysis demonstrates conserved localization of messenger RNAs to mitotic microtubules. *J Cell Biol* **179**: 1365-1373.
- Bodian D. 1965. A Suggestive Relationship of Nerve Cell Rna with Specific Synaptic Sites. *Proc Natl Acad Sci U S A* **53**: 418-425.
- Boeynaems S, Alberti S, Fawzi NL, Mittag T, Polymenidou M, Rousseau F, Schymkowitz J, Shorter J, Wolozin B, Van Den Bosch L et al. 2018. Protein Phase Separation: A New Phase in Cell Biology. *Trends Cell Biol* **28**: 420-435.
- Bohnsack MT, Regener K, Schwappach B, Saffrich R, Paraskeva E, Hartmann E, Gorlich D. 2002. Exp5 exports eEF1A via tRNA from nuclei and synergizes with other transport pathways to confine translation to the cytoplasm. *EMBO J* **21**: 6205-6215.
- Boylan KL, Mische S, Li M, Marques G, Morin X, Chia W, Hays TS. 2008. Motility screen identifies Drosophila IGF-II mRNA-binding protein--zipcode-binding protein acting in oogenesis and synaptogenesis. *PLoS Genet* **4**: e36.
- Buchan JR. 2014. mRNP granules. Assembly, function, and connections with disease. *RNA Biol* **11**: 1019-1030.
- Burgin KE, Waxham MN, Rickling S, Westgate SA, Mobley WC, Kelly PT. 1990. In situ hybridization histochemistry of Ca²⁺/calmodulin-dependent protein kinase in developing rat brain. *J Neurosci* **10**: 1788-1798.
- Burke KA, Janke AM, Rhine CL, Fawzi NL. 2015. Residue-by-Residue View of In Vitro FUS Granules that Bind the C-Terminal Domain of RNA Polymerase II. *Mol Cell* **60**: 231-241.
- Buskila AA, Kannaiah S, Amster-Choder O. 2014. RNA localization in bacteria. *RNA Biol* **11**: 1051-1060.
- Buxbaum AR, Wu B, Singer RH. 2014. Single beta-actin mRNA detection in neurons reveals a mechanism for regulating its translatability. *Science* **343**: 419-422.
- Cagnetta R, Frese CK, Shigeoka T, Krijgsveld J, Holt CE. 2018. Rapid Cue-Specific Remodeling of the Nascent Axonal Proteome. *Neuron* **99**: 29-46 e24.
- Cajigas IJ, Tushev G, Will TJ, tom Dieck S, Fuerst N, Schuman EM. 2012. The local transcriptome in the synaptic neuropil revealed by deep sequencing and high-resolution imaging. *Neuron* **74**: 453-466.
- Calabretta S, Richard S. 2015. Emerging Roles of Disordered Sequences in RNA-Binding Proteins. *Trends Biochem Sci* **40**: 662-672.
- Cammarata GM, Bearce EA, Lowery LA. 2016. Cytoskeletal social networking in the growth cone: How +TIPs mediate microtubule-actin cross-linking to drive axon outgrowth and guidance. *Cytoskeleton (Hoboken)* **73**: 461-476.

- Campbell DS, Holt CE. 2001. Chemotropic responses of retinal growth cones mediated by rapid local protein synthesis and degradation. *Neuron* **32**: 1013-1026.
- Cao J, Mu Q, Huang H. 2018. The Roles of Insulin-Like Growth Factor 2 mRNA-Binding Protein 2 in Cancer and Cancer Stem Cells. *Stem Cells Int* **2018**: 4217259.
- Carpenter K, Bell RB, Yunus J, Amon A, Berchowitz LE. 2018. Phosphorylation-Mediated Clearance of Amyloid-like Assemblies in Meiosis. *Dev Cell* **45**: 392-405 e396.
- Carson JH, Cui H, Barbarese E. 2001. The balance of power in RNA trafficking. *Curr Opin Neurobiol* **11**: 558-563.
- Chao JA, Patskovsky Y, Patel V, Levy M, Almo SC, Singer RH. 2010. ZBP1 recognition of beta-actin zipcode induces RNA looping. *Genes Dev* **24**: 148-158.
- Chen Y, Sabatini BL. 2012. Signaling in dendritic spines and spine microdomains. *Curr Opin Neurobiol* **22**: 389-396.
- Cioni JM, Koppers M, Holt CE. 2018. Molecular control of local translation in axon development and maintenance. *Curr Opin Neurobiol* **51**: 86-94.
- Coles CH, Bradke F. 2015. Coordinating neuronal actin-microtubule dynamics. *Curr Biol* **25**: R677-691.
- Condeelis J, Singer RH. 2005. How and why does beta-actin mRNA target? *Biol Cell* **97**: 97-110.
- Conlon EG, Manley JL. 2017. RNA-binding proteins in neurodegeneration: mechanisms in aggregate. *Genes Dev* **31**: 1509-1528.
- Conway AE, Van Nostrand EL, Pratt GA, Aigner S, Wilbert ML, Sundararaman B, Freese P, Lambert NJ, Sathe S, Liang TY et al. 2016. Enhanced CLIP Uncovers IMP Protein-RNA Targets in Human Pluripotent Stem Cells Important for Cell Adhesion and Survival. *Cell Rep* **15**: 666-679.
- Costa CJ, Willis DE. 2018. To the end of the line: Axonal mRNA transport and local translation in health and neurodegenerative disease. *Dev Neurobiol* **78**: 209-220.
- Cougot N, Bhattacharyya SN, Tapia-Arancibia L, Bordonne R, Filipowicz W, Bertrand E, Rage F. 2008. Dendrites of mammalian neurons contain specialized P-body-like structures that respond to neuronal activation. *J Neurosci* **28**: 13793-13804.
- Courchaine EM, Lu A, Neugebauer KM. 2016. Droplet organelles? *EMBO J* **35**: 1603-1612.
- Court FA, Brophy PJ, Ribchester RR. 2008. Remodeling of motor nerve terminals in demyelinating axons of periaxin-null mice. *Glia* **56**: 471-479.
- Cox LJ, Hengst U, Gurskaya NG, Lukyanov KA, Jaffrey SR. 2008. Intra-axonal translation and retrograde trafficking of CREB promotes neuronal survival. *Nat Cell Biol* **10**: 149-159.
- Czapinski J, Kielbus M, Kalafut J, Kos M, Stepulak A, Rivero-Muller A. 2017. How to Train a Cell-Cutting-Edge Molecular Tools. *Front Chem* **5**: 12.
- Dahlberg JE, Lund E, Goodwin EB. 2003. Nuclear translation: what is the evidence? *RNA* **9**: 1-8.
- Dahm R, Kiebler M, Macchi P. 2007. RNA localisation in the nervous system. *Semin Cell Dev Biol* **18**: 216-223.
- Dai N, Zhao L, Wrighting D, Kramer D, Majithia A, Wang Y, Cracan V, Borges-Rivera D, Mootha VK, Nahrendorf M et al. 2015. IGF2BP2/IMP2-Deficient mice resist obesity through enhanced translation of Ucp1 mRNA and Other mRNAs encoding mitochondrial proteins. *Cell Metab* **21**: 609-621.
- Dao TP, Kolaitis RM, Kim HJ, O'Donovan K, Martyniak B, Colicino E, Hehnly H, Taylor JP, Castaneda CA. 2018. Ubiquitin Modulates Liquid-Liquid Phase Separation of UBQLN2 via Disruption of Multivalent Interactions. *Mol Cell* **69**: 965-978 e966.
- Darnell JC, Van Driesche SJ, Zhang C, Hung KY, Mele A, Fraser CE, Stone EF, Chen C, Fak JJ, Chi SW et al. 2011. FMRP stalls ribosomal translocation on mRNAs linked to synaptic function and autism. *Cell* **146**: 247-261.
- David A, Dolan BP, Hickman HD, Knowlton JJ, Clavarino G, Pierre P, Bennink JR, Yewdell JW. 2012. Nuclear translation visualized by ribosome-bound nascent chain puromycylation. *J Cell Biol* **197**: 45-57.

- Davidovic L, Jaglin XH, Lepagnol-Bestel AM, Tremblay S, Simonneau M, Bardoni B, Khandjian EW. 2007. The fragile X mental retardation protein is a molecular adaptor between the neurospecific KIF3C kinesin and dendritic RNA granules. *Hum Mol Genet* **16**: 3047-3058.
- De Graeve F, Besse F. 2018. Neuronal RNP granules: from physiological to pathological assemblies. *Biol Chem* **399**: 623-635.
- Degrauwe N, Schlumpf TB, Janiszewska M, Martin P, Cauderay A, Provero P, Riggi N, Suva ML, Paro R, Stamenkovic I. 2016a. The RNA Binding Protein IMP2 Preserves Glioblastoma Stem Cells by Preventing let-7 Target Gene Silencing. *Cell Rep* **15**: 1634-1647.
- Degrauwe N, Suva ML, Janiszewska M, Riggi N, Stamenkovic I. 2016b. IMPs: an RNA-binding protein family that provides a link between stem cell maintenance in normal development and cancer. *Genes Dev* **30**: 2459-2474.
- Deitch JS, Banker GA. 1993. An electron microscopic analysis of hippocampal neurons developing in culture: early stages in the emergence of polarity. *J Neurosci* **13**: 4301-4315.
- Deshler JO, Highett MI, Abramson T, Schnapp BJ. 1998. A highly conserved RNA-binding protein for cytoplasmic mRNA localization in vertebrates. *Curr Biol* **8**: 489-496.
- Deshler JO, Highett MI, Schnapp BJ. 1997. Localization of *Xenopus* Vg1 mRNA by Vera protein and the endoplasmic reticulum. *Science* **276**: 1128-1131.
- Di Liegro CM, Schiera G, Di Liegro I. 2014. Regulation of mRNA transport, localization and translation in the nervous system of mammals (Review). *Int J Mol Med* **33**: 747-762.
- Dictenberg JB, Swanger SA, Antar LN, Singer RH, Bassell GJ. 2008. A direct role for FMRP in activity-dependent dendritic mRNA transport links filopodial-spine morphogenesis to fragile X syndrome. *Dev Cell* **14**: 926-939.
- Doyle GA, Betz NA, Leeds PF, Fleisig AJ, Prokipcak RD, Ross J. 1998. The c-myc coding region determinant-binding protein: a member of a family of KH domain RNA-binding proteins. *Nucleic Acids Res* **26**: 5036-5044.
- Doyle M, Kiebler MA. 2011. Mechanisms of dendritic mRNA transport and its role in synaptic tagging. *EMBO J* **30**: 3540-3552.
- Dynes JL, Steward O. 2007. Dynamics of bidirectional transport of Arc mRNA in neuronal dendrites. *J Comp Neurol* **500**: 433-447.
- . 2012. Arc mRNA docks precisely at the base of individual dendritic spines indicating the existence of a specialized microdomain for synapse-specific mRNA translation. *J Comp Neurol* **520**: 3105-3119.
- El Fatimy R, Davidovic L, Tremblay S, Jaglin X, Dury A, Robert C, De Koninck P, Khandjian EW. 2016. Tracking the Fragile X Mental Retardation Protein in a Highly Ordered Neuronal RiboNucleoParticles Population: A Link between Stalled Polyribosomes and RNA Granules. *PLoS Genet* **12**: e1006192.
- Elfineh L, Classon C, Asplund A, Pettersson U, Kamali-Moghaddam M, Lind SB. 2014. Tyrosine phosphorylation profiling via in situ proximity ligation assay. *BMC Cancer* **14**: 435.
- Elisha Z, Havin L, Ringel I, Yisraeli JK. 1995. Vg1 RNA binding protein mediates the association of Vg1 RNA with microtubules in *Xenopus* oocytes. *EMBO J* **14**: 5109-5114.
- Elvira G, Wasiak S, Blandford V, Tong XK, Serrano A, Fan X, del Rayo Sanchez-Carbente M, Servant F, Bell AW, Boismenu D et al. 2006. Characterization of an RNA granule from developing brain. *Mol Cell Proteomics* **5**: 635-651.
- Eng H, Lund K, Campenot RB. 1999. Synthesis of beta-tubulin, actin, and other proteins in axons of sympathetic neurons in compartmented cultures. *J Neurosci* **19**: 1-9.
- Ephrussi A, Dickinson LK, Lehmann R. 1991. Oskar organizes the germ plasm and directs localization of the posterior determinant nanos. *Cell* **66**: 37-50.
- Farina KL, Huttelmaier S, Musunuru K, Darnell R, Singer RH. 2003. Two ZBP1 KH domains facilitate beta-actin mRNA localization, granule formation, and cytoskeletal attachment. *J Cell Biol* **160**: 77-87.

- Feig S, Lipton P. 1993. Pairing the cholinergic agonist carbachol with patterned Schaffer collateral stimulation initiates protein synthesis in hippocampal CA1 pyramidal cell dendrites via a muscarinic, NMDA-dependent mechanism. *J Neurosci* **13**: 1010-1021.
- Fiumara F, Fioriti L, Kandel ER, Hendrickson WA. 2010. Essential role of coiled coils for aggregation and activity of Q/N-rich prions and PolyQ proteins. *Cell* **143**: 1121-1135.
- Fonin AV, Darling AL, Kuznetsova IM, Turoverov KK, Uversky VN. 2018. Intrinsically disordered proteins in crowded milieu: when chaos prevails within the cellular gumbo. *Cell Mol Life Sci*.
- Franzmann T, Alberti S. 2018. Prion-like low-complexity sequences: Key regulators of protein solubility and phase behavior. *J Biol Chem*.
- Franzmann TM, Jahnel M, Pozniakovsky A, Mahamid J, Holehouse AS, Nuske E, Richter D, Baumeister W, Grill SW, Pappu RV et al. 2018. Phase separation of a yeast prion protein promotes cellular fitness. *Science* **359**.
- Frege T, Uversky VN. 2015. Intrinsically disordered proteins in the nucleus of human cells. *Biochem Biophys Rep* **1**: 33-51.
- Fritzsche R, Karra D, Bennett KL, Ang FY, Heraud-Farlow JE, Tolino M, Doyle M, Bauer KE, Thomas S, Planyavsky M et al. 2013. Interactome of two diverse RNA granules links mRNA localization to translational repression in neurons. *Cell Rep* **5**: 1749-1762.
- Fuxreiter M. 2012. Fuzziness: linking regulation to protein dynamics. *Molecular bioSystems* **8**: 168-177.
- Gao FB. 1998. Messenger RNAs in dendrites: localization, stability, and implications for neuronal function. *Bioessays* **20**: 70-78.
- Garner CC, Tucker RP, Matus A. 1988. Selective localization of messenger RNA for cytoskeletal protein MAP2 in dendrites. *Nature* **336**: 674-677.
- Gaspar I, Yu YV, Cotton SL, Kim DH, Ephrussi A, Welte MA. 2014. Klar ensures thermal robustness of oskar localization by restraining RNP motility. *J Cell Biol* **206**: 199-215.
- Gaynes JA, Otsuna H, Campbell DS, Manfredi JP, Levine EM, Chien CB. 2015. The RNA Binding Protein Igf2bp1 Is Required for Zebrafish RGC Axon Outgrowth In Vivo. *PLoS One* **10**: e0134751.
- Geng C, Macdonald PM. 2006. Imp associates with squid and Hrp48 and contributes to localized expression of gurken in the oocyte. *Mol Cell Biol* **26**: 9508-9516.
- Git A, Allison R, Perdiguero E, Nebreda AR, Houlston E, Standart N. 2009. Vg1RBP phosphorylation by Erk2 MAP kinase correlates with the cortical release of Vg1 mRNA during meiotic maturation of Xenopus oocytes. *RNA* **15**: 1121-1133.
- Gitler AD, Shorter J. 2011. RNA-binding proteins with prion-like domains in ALS and FTLD-U. *Prion* **5**: 179-187.
- Giuditta A, Cupello A, Lazzarini G. 1980. Ribosomal RNA in the axoplasm of the squid giant axon. *J Neurochem* **34**: 1757-1760.
- Giuditta A, Hunt T, Santella L. 1986. Rapid important paper Messenger RNA in squid axoplasm. *Neurochem Int* **8**: 435-442.
- Glisovic T, Bachorik JL, Yong J, Dreyfuss G. 2008. RNA-binding proteins and post-transcriptional gene regulation. *FEBS Lett* **582**: 1977-1986.
- Glock C, Heumuller M, Schuman EM. 2017. mRNA transport & local translation in neurons. *Curr Opin Neurobiol* **45**: 169-177.
- Goidl JA, Canaani D, Boublik M, Weissbach H, Dickerman H. 1975. Polyanion-induced release of polyribosomes from HeLa cell nuclei. *J Biol Chem* **250**: 9198-9205.
- Gomes E, Shorter J. 2018. The molecular language of membraneless organelles. *J Biol Chem*.
- Gonsalvez GB, Urbinati CR, Long RM. 2005. RNA localization in yeast: moving towards a mechanism. *Biol Cell* **97**: 75-86.
- Gopal PP, Nirschl JJ, Klinman E, Holzbaur EL. 2017. Amyotrophic lateral sclerosis-linked mutations increase the viscosity of liquid-like TDP-43 RNP granules in neurons. *Proc Natl Acad Sci U S A* **114**: E2466-E2475.

- Goswami S, Tarapore RS, Poenitzsch Strong AM, TeSlaa JJ, Grinblat Y, Setaluri V, Spiegelman VS. 2015. MicroRNA-340-mediated degradation of microphthalmia-associated transcription factor (MITF) mRNA is inhibited by coding region determinant-binding protein (CRD-BP). *J Biol Chem* **290**: 384-395.
- Graber TE, Hebert-Seropian S, Khoutorsky A, David A, Yewdell JW, Lacaille JC, Sossin WS. 2013. Reactivation of stalled polyribosomes in synaptic plasticity. *Proc Natl Acad Sci U S A* **110**: 16205-16210.
- Gu W, Pan F, Zhang H, Bassell GJ, Singer RH. 2002. A predominantly nuclear protein affecting cytoplasmic localization of beta-actin mRNA in fibroblasts and neurons. *J Cell Biol* **156**: 41-51.
- Gulledge AT, Kampa BM, Stuart GJ. 2005. Synaptic integration in dendritic trees. *J Neurobiol* **64**: 75-90.
- Gumy LF, Yeo GS, Tung YC, Zivraj KH, Willis D, Coppola G, Lam BY, Twiss JL, Holt CE, Fawcett JW. 2011. Transcriptome analysis of embryonic and adult sensory axons reveals changes in mRNA repertoire localization. *RNA* **17**: 85-98.
- Guo L, Shorter J. 2015. It's Raining Liquids: RNA Tunes Viscoelasticity and Dynamics of Membraneless Organelles. *Mol Cell* **60**: 189-192.
- Hafner M, Landthaler M, Burger L, Khorshid M, Hausser J, Berninger P, Rothballer A, Ascano M, Jr., Jungkamp AC, Munschauer M et al. 2010. Transcriptome-wide identification of RNA-binding protein and microRNA target sites by PAR-CLIP. *Cell* **141**: 129-141.
- Han TW, Kato M, Xie S, Wu LC, Mirzaei H, Pei J, Chen M, Xie Y, Allen J, Xiao G et al. 2012. Cell-free formation of RNA granules: bound RNAs identify features and components of cellular assemblies. *Cell* **149**: 768-779.
- Hansen HT, Rasmussen SH, Adolph SK, Plass M, Krogh A, Sanford J, Nielsen FC, Christiansen J. 2015. Drosophila Imp iCLIP identifies an RNA assemblage coordinating F-actin formation. *Genome Biol* **16**: 123.
- Hansen TV, Hammer NA, Nielsen J, Madsen M, Dalbaeck C, Wewer UM, Christiansen J, Nielsen FC. 2004. Dwarfism and impaired gut development in insulin-like growth factor II mRNA-binding protein 1-deficient mice. *Mol Cell Biol* **24**: 4448-4464.
- Hanz S, Perlson E, Willis D, Zheng JQ, Massarwa R, Huerta JJ, Koltzenburg M, Kohler M, van-Minnen J, Twiss JL et al. 2003. Axoplasmic importins enable retrograde injury signaling in lesioned nerve. *Neuron* **40**: 1095-1104.
- Harrison AF, Shorter J. 2017. RNA-binding proteins with prion-like domains in health and disease. *Biochem J* **474**: 1417-1438.
- Heinrich SU, Lindquist S. 2011. Protein-only mechanism induces self-perpetuating changes in the activity of neuronal Aplysia cytoplasmic polyadenylation element binding protein (CPEB). *Proc Natl Acad Sci U S A* **108**: 2999-3004.
- Heisenberg M. 2003. Mushroom body memoir: from maps to models. *Nat Rev Neurosci* **4**: 266-275.
- Hengst U, Deglincerti A, Kim HJ, Jeon NL, Jaffrey SR. 2009. Axonal elongation triggered by stimulus-induced local translation of a polarity complex protein. *Nat Cell Biol* **11**: 1024-1030.
- Hentze MW, Castello A, Schwarzl T, Preiss T. 2018. A brave new world of RNA-binding proteins. *Nat Rev Mol Cell Biol* **19**: 327-341.
- Hollingsworth D, Candel AM, Nicastro G, Martin SR, Briata P, Gherzi R, Ramos A. 2012. KH domains with impaired nucleic acid binding as a tool for functional analysis. *Nucleic Acids Res* **40**: 6873-6886.
- Holt CE, Schuman EM. 2013. The central dogma decentralized: new perspectives on RNA function and local translation in neurons. *Neuron* **80**: 648-657.
- Howley C, Ho RK. 2000. mRNA localization patterns in zebrafish oocytes. *Mech Dev* **92**: 305-309.
- Hu JY, Meng X, Schacher S. 2003. Redistribution of syntaxin mRNA in neuronal cell bodies regulates protein expression and transport during synapse formation and long-term synaptic plasticity. *J Neurosci* **23**: 1804-1815.

- Huang X, Zhang H, Guo X, Zhu Z, Cai H, Kong X. 2018. Insulin-like growth factor 2 mRNA-binding protein 1 (IGF2BP1) in cancer. *J Hematol Oncol* **11**: 88.
- Huang YS, Carson JH, Barbarese E, Richter JD. 2003. Facilitation of dendritic mRNA transport by CPEB. *Genes Dev* **17**: 638-653.
- Hubstenberger A, Noble SL, Cameron C, Evans TC. 2013. Translation repressors, an RNA helicase, and developmental cues control RNP phase transitions during early development. *Developmental cell* **27**: 161-173.
- Huttelmaier S, Zenklusen D, Lederer M, Dichtenberg J, Lorenz M, Meng X, Bassell GJ, Condeelis J, Singer RH. 2005. Spatial regulation of beta-actin translation by Src-dependent phosphorylation of ZBP1. *Nature* **438**: 512-515.
- Hyman AA, Weber CA, Julicher F. 2014. Liquid-liquid phase separation in biology. *Annu Rev Cell Dev Biol* **30**: 39-58.
- Iborra FJ, Jackson DA, Cook PR. 2001. Coupled transcription and translation within nuclei of mammalian cells. *Science* **293**: 1139-1142.
- Itakura AK, Futia RA, Jarosz DF. 2018. It Pays To Be in Phase. *Biochemistry* **57**: 2520-2529.
- Ito K, Hotta Y. 1992. Proliferation pattern of postembryonic neuroblasts in the brain of *Drosophila melanogaster*. *Dev Biol* **149**: 134-148.
- Jambhekar A, Derisi JL. 2007. Cis-acting determinants of asymmetric, cytoplasmic RNA transport. *RNA* **13**: 625-642.
- Jambor H, Mejstrik P, Tomancak P. 2016. Rapid Ovary Mass-Isolation (ROMi) to Obtain Large Quantities of *Drosophila* Egg Chambers for Fluorescent In Situ Hybridization. *Methods Mol Biol* **1478**: 253-262.
- Jeffery WR, Tomlinson CR, Brodeur RD. 1983. Localization of actin messenger RNA during early ascidian development. *Dev Biol* **99**: 408-417.
- Job C, Eberwine J. 2001. Localization and translation of mRNA in dendrites and axons. *Nat Rev Neurosci* **2**: 889-898.
- Johnstone O, Lasko P. 2001. Translational regulation and RNA localization in *Drosophila* oocytes and embryos. *Annu Rev Genet* **35**: 365-406.
- Jonson L, Christiansen J, Hansen TV, Vikesa J, Yamamoto Y, Nielsen FC. 2014. IMP3 RNP safe houses prevent miRNA-directed HMGA2 mRNA decay in cancer and development. *Cell Rep* **7**: 539-551.
- Jonson L, Vikesaa J, Krogh A, Nielsen LK, Hansen T, Borup R, Johnsen AH, Christiansen J, Nielsen FC. 2007. Molecular composition of IMP1 ribonucleoprotein granules. *Mol Cell Proteomics* **6**: 798-811.
- Jung H, Yoon BC, Holt CE. 2012. Axonal mRNA localization and local protein synthesis in nervous system assembly, maintenance and repair. *Nat Rev Neurosci* **13**: 308-324.
- Kalil K, Dent EW. 2014. Branch management: mechanisms of axon branching in the developing vertebrate CNS. *Nat Rev Neurosci* **15**: 7-18.
- Kalous A, Stake JI, Yisraeli JK, Holt CE. 2014. RNA-binding protein Vg1RBP regulates terminal arbor formation but not long-range axon navigation in the developing visual system. *Dev Neurobiol* **74**: 303-318.
- Kanai Y, Dohmae N, Hirokawa N. 2004. Kinesin transports RNA: isolation and characterization of an RNA-transporting granule. *Neuron* **43**: 513-525.
- Kang H, Schuman EM. 1996. A requirement for local protein synthesis in neurotrophin-induced hippocampal synaptic plasticity. *Science* **273**: 1402-1406.
- Kato M, Han TW, Xie S, Shi K, Du X, Wu LC, Mirzaei H, Goldsmith EJ, Longgood J, Pei J et al. 2012. Cell-free formation of RNA granules: low complexity sequence domains form dynamic fibers within hydrogels. *Cell* **149**: 753-767.
- Kedersha N, Stoecklin G, Ayodele M, Yacono P, Lykke-Andersen J, Fritzler MJ, Scheuner D, Kaufman RJ, Golan DE, Anderson P. 2005. Stress granules and processing bodies are dynamically linked sites of mRNP remodeling. *The Journal of cell biology* **169**: 871-884.

- Keleman K, Kruttner S, Alenius M, Dickson BJ. 2007. Function of the Drosophila CPEB protein Orb2 in long-term courtship memory. *Nat Neurosci* **10**: 1587-1593.
- Khan MR, Li L, Perez-Sanchez C, Saraf A, Florens L, Slaughter BD, Unruh JR, Si K. 2015. Amyloidogenic Oligomerization Transforms Drosophila Orb2 from a Translation Repressor to an Activator. *Cell* **163**: 1468-1483.
- Khayachi A, Gwizdek C, Poupon G, Alcor D, Chafai M, Casse F, Maurin T, Prieto M, Folci A, De Graeve F et al. 2018. Sumoylation regulates FMRP-mediated dendritic spine elimination and maturation. *Nat Commun* **9**: 757.
- Kiebler MA, Bassell GJ. 2006. Neuronal RNA granules: movers and makers. *Neuron* **51**: 685-690.
- Kim HJ, Kim NC, Wang YD, Scarborough EA, Moore J, Diaz Z, MacLea KS, Freibaum B, Li S, Molliex A et al. 2013. Mutations in prion-like domains in hnRNPA2B1 and hnRNPA1 cause multisystem proteinopathy and ALS. *Nature* **495**: 467-473.
- Kim JH, Richter JD. 2006. Opposing polymerase-deadenylase activities regulate cytoplasmic polyadenylation. *Mol Cell* **24**: 173-183.
- Kim S, Martin KC. 2015. Neuron-wide RNA transport combines with netrin-mediated local translation to spatially regulate the synaptic proteome. *Elife* **4**.
- King OD, Gitler AD, Shorter J. 2012. The tip of the iceberg: RNA-binding proteins with prion-like domains in neurodegenerative disease. *Brain Res* **1462**: 61-80.
- Kishore S, Lubner S, Zavolan M. 2010. Deciphering the role of RNA-binding proteins in the post-transcriptional control of gene expression. *Brief Funct Genomics* **9**: 391-404.
- Kislauskis EH, Zhu X, Singer RH. 1994. Sequences responsible for intracellular localization of beta-actin messenger RNA also affect cell phenotype. *J Cell Biol* **127**: 441-451.
- Kleiman R, Banker G, Steward O. 1990. Differential subcellular localization of particular mRNAs in hippocampal neurons in culture. *Neuron* **5**: 821-830.
- Kloc M, Dougherty MT, Bilinski S, Chan AP, Brey E, King ML, Patrick CW, Jr., Etkin LD. 2002a. Three-dimensional ultrastructural analysis of RNA distribution within germinal granules of *Xenopus*. *Dev Biol* **241**: 79-93.
- Kloc M, Zearfoss NR, Etkin LD. 2002b. Mechanisms of subcellular mRNA localization. *Cell* **108**: 533-544.
- Knowles RB, Sabry JH, Martone ME, Deerinck TJ, Ellisman MH, Bassell GJ, Kosik KS. 1996. Translocation of RNA granules in living neurons. *J Neurosci* **16**: 7812-7820.
- Koenig E, Martin R, Titmus M, Sotelo-Silveira JR. 2000. Cryptic peripheral ribosomal domains distributed intermittently along mammalian myelinated axons. *J Neurosci* **20**: 8390-8400.
- Kress TL, Yoon YJ, Mowry KL. 2004. Nuclear RNP complex assembly initiates cytoplasmic RNA localization. *J Cell Biol* **165**: 203-211.
- Krichevsky AM, Kosik KS. 2001. Neuronal RNA granules: a link between RNA localization and stimulation-dependent translation. *Neuron* **32**: 683-696.
- Kroschwald S, Munder MC, Maharana S, Franzmann TM, Richter D, Ruer M, Hyman AA, Alberti S. 2018. Different Material States of Pub1 Condensates Define Distinct Modes of Stress Adaptation and Recovery. *Cell Rep* **23**: 3327-3339.
- Kruttner S, Stepien B, Noordermeer JN, Mommaas MA, Mechtler K, Dickson BJ, Keleman K. 2012. Drosophila CPEB Orb2A mediates memory independent of its RNA-binding domain. *Neuron* **76**: 383-395.
- Kukurba KR, Montgomery SB. 2015. RNA Sequencing and Analysis. *Cold Spring Harb Protoc* **2015**: 951-969.
- Kwon I, Kato M, Xiang S, Wu L, Theodoropoulos P, Mirzaei H, Han T, Xie S, Corden JL, McKnight SL. 2013. Phosphorylation-regulated binding of RNA polymerase II to fibrous polymers of low-complexity domains. *Cell* **155**: 1049-1060.
- Latysheva NS, Flock T, Weatheritt RJ, Chavali S, Babu MM. 2015. How do disordered regions achieve comparable functions to structured domains? *Protein Sci* **24**: 909-922.

- Lawrence JB, Singer RH. 1986. Intracellular localization of messenger RNAs for cytoskeletal proteins. *Cell* **45**: 407-415.
- Lecuyer E, Yoshida H, Krause HM. 2009. Global implications of mRNA localization pathways in cellular organization. *Curr Opin Cell Biol* **21**: 409-415.
- Lecuyer E, Yoshida H, Parthasarathy N, Alm C, Babak T, Cerovina T, Hughes TR, Tomancak P, Krause HM. 2007. Global analysis of mRNA localization reveals a prominent role in organizing cellular architecture and function. *Cell* **131**: 174-187.
- Lee T, Lee A, Luo L. 1999. Development of the Drosophila mushroom bodies: sequential generation of three distinct types of neurons from a neuroblast. *Development* **126**: 4065-4076.
- Lepelletier L, Langlois SD, Kent CB, Welshhans K, Morin S, Bassell GJ, Yam PT, Charron F. 2017. Sonic Hedgehog Guides Axons via Zipcode Binding Protein 1-Mediated Local Translation. *J Neurosci* **37**: 1685-1695.
- Leung KM, van Horck FP, Lin AC, Allison R, Standart N, Holt CE. 2006. Asymmetrical beta-actin mRNA translation in growth cones mediates attractive turning to netrin-1. *Nat Neurosci* **9**: 1247-1256.
- Leung LC, Urbancic V, Baudet ML, Dwivedy A, Bayley TG, Lee AC, Harris WA, Holt CE. 2013. Coupling of NF-protocadherin signaling to axon guidance by cue-induced translation. *Nat Neurosci* **16**: 166-173.
- Li HR, Chiang WC, Chou PC, Wang WJ, Huang JR. 2018. TAR DNA-binding protein 43 (TDP-43) liquid-liquid phase separation is mediated by just a few aromatic residues. *J Biol Chem* **293**: 6090-6098.
- Li J, Feng Y, Wang X, Li J, Liu W, Rong L, Bao J. 2015. An Overview of Predictors for Intrinsically Disordered Proteins over 2010-2014. *Int J Mol Sci* **16**: 23446-23462.
- Li P, Banjade S, Cheng HC, Kim S, Chen B, Guo L, Llaguno M, Hollingsworth JV, King DS, Banani SF et al. 2012. Phase transitions in the assembly of multivalent signalling proteins. *Nature* **483**: 336-340.
- Liao G, Simone B, Liu G. 2011. Mis-localization of Arp2 mRNA impairs persistence of directional cell migration. *Exp Cell Res* **317**: 812-822.
- Lin AC, Holt CE. 2007. Local translation and directional steering in axons. *EMBO J* **26**: 3729-3736.
- Lin Y, Protter DS, Rosen MK, Parker R. 2015. Formation and Maturation of Phase-Separated Liquid Droplets by RNA-Binding Proteins. *Mol Cell* **60**: 208-219.
- Linding R, Jensen LJ, Diella F, Bork P, Gibson TJ, Russell RB. 2003. Protein disorder prediction: implications for structural proteomics. *Structure* **11**: 1453-1459.
- Litman P, Barg J, Rindzoonski L, Ginzburg I. 1993. Subcellular localization of tau mRNA in differentiating neuronal cell culture: implications for neuronal polarity. *Neuron* **10**: 627-638.
- Liu Z, Yang CP, Sugino K, Fu CC, Liu LY, Yao X, Lee LP, Lee T. 2015. Opposing intrinsic temporal gradients guide neural stem cell production of varied neuronal fates. *Science* **350**: 317-320.
- Loya TJ, O'Rourke TW, Reines D. 2017. The hnRNP-like Nab3 termination factor can employ heterologous prion-like domains in place of its own essential low complexity domain. *PLoS One* **12**: e0186187.
- Luo L, O'Leary DD. 2005. Axon retraction and degeneration in development and disease. *Annu Rev Neurosci* **28**: 127-156.
- Lyles V, Zhao Y, Martin KC. 2006. Synapse formation and mRNA localization in cultured Aplysia neurons. *Neuron* **49**: 349-356.
- Ma B, Savas JN, Yu MS, Culver BP, Chao MV, Tanese N. 2011. Huntingtin mediates dendritic transport of beta-actin mRNA in rat neurons. *Sci Rep* **1**: 140.
- Majumdar A, Cesario WC, White-Grindley E, Jiang H, Ren F, Khan MR, Li L, Choi EM, Kannan K, Guo F et al. 2012. Critical role of amyloid-like oligomers of Drosophila Orb2 in the persistence of memory. *Cell* **148**: 515-529.
- Malinovska L, Kroschwald S, Alberti S. 2013a. Protein disorder, prion propensities, and self-organizing macromolecular collectives. *Biochimica et biophysica acta* **1834**: 918-931.

- . 2013b. Protein disorder, prion propensities, and self-organizing macromolecular collectives. *Biochim Biophys Acta* **1834**: 918-931.
- Malinowska L, Kroschwald S, Munder MC, Richter D, Alberti S. 2012. Molecular chaperones and stress-inducible protein-sorting factors coordinate the spatiotemporal distribution of protein aggregates. *Mol Biol Cell* **23**: 3041-3056.
- March ZM, King OD, Shorter J. 2016. Prion-like domains as epigenetic regulators, scaffolds for subcellular organization, and drivers of neurodegenerative disease. *Brain Res* **1647**: 9-18.
- Martin KC, Casadio A, Zhu H, Yaping E, Rose JC, Chen M, Bailey CH, Kandel ER. 1997. Synapse-specific, long-term facilitation of aplysia sensory to motor synapses: a function for local protein synthesis in memory storage. *Cell* **91**: 927-938.
- Martin KC, Ephrussi A. 2009. mRNA localization: gene expression in the spatial dimension. *Cell* **136**: 719-730.
- Mastushita-Sakai T, White-Grindley E, Samuelson J, Seidel C, Si K. 2010. Drosophila Orb2 targets genes involved in neuronal growth, synapse formation, and protein turnover. *Proc Natl Acad Sci U S A* **107**: 11987-11992.
- Mateju D, Franzmann TM, Patel A, Kopach A, Boczek EE, Maharana S, Lee HO, Carra S, Hyman AA, Alberti S. 2017. An aberrant phase transition of stress granules triggered by misfolded protein and prevented by chaperone function. *EMBO J* **36**: 1669-1687.
- Mayford M, Baranes D, Podsypanina K, Kandel ER. 1996. The 3'-untranslated region of CaMKII alpha is a cis-acting signal for the localization and translation of mRNA in dendrites. *Proc Natl Acad Sci U S A* **93**: 13250-13255.
- Medioni C, Ephrussi A, Besse F. 2015. Live imaging of axonal transport in Drosophila pupal brain explants. *Nat Protoc* **10**: 574-584.
- Medioni C, Mowry K, Besse F. 2012. Principles and roles of mRNA localization in animal development. *Development* **139**: 3263-3276.
- Medioni C, Ramialison M, Ephrussi A, Besse F. 2014. Imp promotes axonal remodeling by regulating profilin mRNA during brain development. *Curr Biol* **24**: 793-800.
- Meer EJ, Wang DO, Kim S, Barr I, Guo F, Martin KC. 2012. Identification of a cis-acting element that localizes mRNA to synapses. *Proc Natl Acad Sci U S A* **109**: 4639-4644.
- Merianda TT, Lin AC, Lam JS, Vuppalachchi D, Willis DE, Karin N, Holt CE, Twiss JL. 2009. A functional equivalent of endoplasmic reticulum and Golgi in axons for secretion of locally synthesized proteins. *Mol Cell Neurosci* **40**: 128-142.
- Mikl M, Vendra G, Kiebler MA. 2011. Independent localization of MAP2, CaMKIIalpha and beta-actin RNAs in low copy numbers. *EMBO Rep* **12**: 1077-1084.
- Mili S, Moissoglu K, Macara IG. 2008. Genome-wide screen reveals APC-associated RNAs enriched in cell protrusions. *Nature* **453**: 115-119.
- Miller S, Yasuda M, Coats JK, Jones Y, Martone ME, Mayford M. 2002. Disruption of dendritic translation of CaMKIIalpha impairs stabilization of synaptic plasticity and memory consolidation. *Neuron* **36**: 507-519.
- Minis A, Dahary D, Manor O, Leshkowitz D, Pilpel Y, Yaron A. 2014. Subcellular transcriptomics-dissection of the mRNA composition in the axonal compartment of sensory neurons. *Dev Neurobiol* **74**: 365-381.
- Miskei M, Gregus A, Sharma R, Duro N, Zsolyomi F, Fuxreiter M. 2017. Fuzziness enables context dependence of protein interactions. *FEBS Lett* **591**: 2682-2695.
- Misra M, Edmund H, Ennis D, Schlueter MA, Marot JE, Tambasco J, Barlow I, Sigurbjornsdottir S, Mathew R, Valles AM et al. 2016. A Genome-Wide Screen for Dendritically Localized RNAs Identifies Genes Required for Dendrite Morphogenesis. *G3 (Bethesda)* **6**: 2397-2405.
- Mitchell SF, Parker R. 2014. Principles and properties of eukaryotic mRNPs. *Mol Cell* **54**: 547-558.
- Miyashiro K, Dichter M, Eberwine J. 1994. On the nature and differential distribution of mRNAs in hippocampal neurites: implications for neuronal functioning. *Proc Natl Acad Sci U S A* **91**: 10800-10804.

- Mohr E. 1999. Subcellular RNA compartmentalization. *Prog Neurobiol* **57**: 507-525.
- Molliex A, Temirov J, Lee J, Coughlin M, Kanagaraj AP, Kim HJ, Mittag T, Taylor JP. 2015. Phase separation by low complexity domains promotes stress granule assembly and drives pathological fibrillization. *Cell* **163**: 123-133.
- Monahan Z, Ryan VH, Janke AM, Burke KA, Rhoads SN, Zerze GH, O'Meally R, Dignon GL, Conicella AE, Zheng W et al. 2017. Phosphorylation of the FUS low-complexity domain disrupts phase separation, aggregation, and toxicity. *EMBO J* **36**: 2951-2967.
- Moon IS, Cho SJ, Seog DH, Walikonis R. 2009. Neuronal activation increases the density of eukaryotic translation initiation factor 4E mRNA clusters in dendrites of cultured hippocampal neurons. *Exp Mol Med* **41**: 601-610.
- Morisaki T, Lyon K, DeLuca KF, DeLuca JG, English BP, Zhang Z, Lavis LD, Grimm JB, Viswanathan S, Looger LL et al. 2016. Real-time quantification of single RNA translation dynamics in living cells. *Science* **352**: 1425-1429.
- Muller-McNicoll M, Neugebauer KM. 2013. How cells get the message: dynamic assembly and function of mRNA-protein complexes. *Nat Rev Genet* **14**: 275-287.
- Munro TP, Kwon S, Schnapp BJ, St Johnston D. 2006. A repeated IMP-binding motif controls oskar mRNA translation and anchoring independently of *Drosophila melanogaster* IMP. *J Cell Biol* **172**: 577-588.
- Murakami T, Qamar S, Lin JQ, Schierle GS, Rees E, Miyashita A, Costa AR, Dodd RB, Chan FT, Michel CH et al. 2015. ALS/FTD Mutation-Induced Phase Transition of FUS Liquid Droplets and Reversible Hydrogels into Irreversible Hydrogels Impairs RNP Granule Function. *Neuron* **88**: 678-690.
- Muslimov IA, Santi E, Homel P, Perini S, Higgins D, Tiedge H. 1997. RNA transport in dendrites: a cis-acting targeting element is contained within neuronal BC1 RNA. *J Neurosci* **17**: 4722-4733.
- Nalavadi VC, Griffin LE, Picard-Fraser P, Swanson AM, Takumi T, Bassell GJ. 2012. Regulation of zipcode binding protein 1 transport dynamics in axons by myosin Va. *J Neurosci* **32**: 15133-15141.
- Nern A, Pfeiffer BD, Rubin GM. 2015. Optimized tools for multicolor stochastic labeling reveal diverse stereotyped cell arrangements in the fly visual system. *Proc Natl Acad Sci U S A* **112**: E2967-2976.
- Nevo-Dinur K, Govindarajan S, Amster-Choder O. 2012. Subcellular localization of RNA and proteins in prokaryotes. *Trends Genet* **28**: 314-322.
- Nevo-Dinur K, Nussbaum-Shochat A, Ben-Yehuda S, Amster-Choder O. 2011. Translation-independent localization of mRNA in *E. coli*. *Science* **331**: 1081-1084.
- Nielsen J, Christiansen J, Lykke-Andersen J, Johnsen AH, Wewer UM, Nielsen FC. 1999. A family of insulin-like growth factor II mRNA-binding proteins represses translation in late development. *Mol Cell Biol* **19**: 1262-1270.
- Nielsen J, Cilius Nielsen F, Kragh Jakobsen R, Christiansen J. 2000. The biphasic expression of IMP/Vg1-RBP is conserved between vertebrates and *Drosophila*. *Mech Dev* **96**: 129-132.
- Nishino J, Kim S, Zhu Y, Zhu H, Morrison SJ. 2013. A network of heterochronic genes including *Imp1* regulates temporal changes in stem cell properties. *Elife* **2**: e00924.
- Nott TJ, Petsalaki E, Farber P, Jervis D, Fussner E, Plochowietz A, Craggs TD, Bazett-Jones DP, Pawson T, Forman-Kay JD et al. 2015. Phase transition of a disordered nuage protein generates environmentally responsive membraneless organelles. *Mol Cell* **57**: 936-947.
- Oleynikov Y, Singer RH. 2003. Real-time visualization of ZBP1 association with beta-actin mRNA during transcription and localization. *Curr Biol* **13**: 199-207.
- Ostroff LE, Fiala JC, Allwardt B, Harris KM. 2002. Polyribosomes redistribute from dendritic shafts into spines with enlarged synapses during LTP in developing rat hippocampal slices. *Neuron* **35**: 535-545.
- Ouwenga R, Lake AM, O'Brien D, Mogha A, Dani A, Dougherty JD. 2017. Transcriptomic Analysis of Ribosome-Bound mRNA in Cortical Neurites In Vivo. *J Neurosci* **37**: 8688-8705.

- Ouyang Y, Rosenstein A, Kreiman G, Schuman EM, Kennedy MB. 1999. Tetanic stimulation leads to increased accumulation of Ca(2+)/calmodulin-dependent protein kinase II via dendritic protein synthesis in hippocampal neurons. *J Neurosci* **19**: 7823-7833.
- Pacheco A, Gallo G. 2016. Actin filament-microtubule interactions in axon initiation and branching. *Brain Res Bull* **126**: 300-310.
- Pan F, Huttelmaier S, Singer RH, Gu W. 2007. ZBP2 facilitates binding of ZBP1 to beta-actin mRNA during transcription. *Mol Cell Biol* **27**: 8340-8351.
- Park HY, Buxbaum AR, Singer RH. 2010. Single mRNA tracking in live cells. *Methods Enzymol* **472**: 387-406.
- Park HY, Lim H, Yoon YJ, Follenzi A, Nwokafor C, Lopez-Jones M, Meng X, Singer RH. 2014. Visualization of dynamics of single endogenous mRNA labeled in live mouse. *Science* **343**: 422-424.
- Patel A, Lee HO, Jawerth L, Maharana S, Janel M, Hein MY, Stoyanov S, Mahamid J, Saha S, Franzmann TM et al. 2015. A Liquid-to-Solid Phase Transition of the ALS Protein FUS Accelerated by Disease Mutation. *Cell* **162**: 1066-1077.
- Patel VL, Mitra S, Harris R, Buxbaum AR, Lionnet T, Brenowitz M, Girvin M, Levy M, Almo SC, Singer RH et al. 2012. Spatial arrangement of an RNA zipcode identifies mRNAs under post-transcriptional control. *Genes Dev* **26**: 43-53.
- Perry RB, Doron-Mandel E, Iavnilovitch E, Rishal I, Dagan SY, Tsoory M, Coppola G, McDonald MK, Gomes C, Geschwind DH et al. 2012. Subcellular knockout of importin beta1 perturbs axonal retrograde signaling. *Neuron* **75**: 294-305.
- Perycz M, Urbanska AS, Krawczyk PS, Parobczak K, Jaworski J. 2011. Zipcode binding protein 1 regulates the development of dendritic arbors in hippocampal neurons. *J Neurosci* **31**: 5271-5285.
- Pimentel J, Boccaccio GL. 2014. Translation and silencing in RNA granules: a tale of sand grains. *Front Mol Neurosci* **7**: 68.
- Piper M, Anderson R, Dwivedy A, Weinl C, van Horck F, Leung KM, Cogill E, Holt C. 2006. Signaling mechanisms underlying Slit2-induced collapse of *Xenopus* retinal growth cones. *Neuron* **49**: 215-228.
- Piper M, Holt C. 2004. RNA translation in axons. *Annu Rev Cell Dev Biol* **20**: 505-523.
- Piper M, Lee AC, van Horck FP, McNeilly H, Lu TB, Harris WA, Holt CE. 2015. Differential requirement of F-actin and microtubule cytoskeleton in cue-induced local protein synthesis in axonal growth cones. *Neural Dev* **10**: 3.
- Poon MM, Choi SH, Jamieson CA, Geschwind DH, Martin KC. 2006. Identification of process-localized mRNAs from cultured rodent hippocampal neurons. *J Neurosci* **26**: 13390-13399.
- Pratt CA, Mowry KL. 2013. Taking a cellular road-trip: mRNA transport and anchoring. *Curr Opin Cell Biol* **25**: 99-106.
- Prokop A. 2013. The intricate relationship between microtubules and their associated motor proteins during axon growth and maintenance. *Neural Dev* **8**: 17.
- Protter DSW, Parker R. 2016. Principles and Properties of Stress Granules. *Trends Cell Biol* **26**: 668-679.
- Protter DSW, Rao BS, Van Treeck B, Lin Y, Mizoue L, Rosen MK, Parker R. 2018. Intrinsically Disordered Regions Can Contribute Promiscuous Interactions to RNP Granule Assembly. *Cell Rep* **22**: 1401-1412.
- Rangaraju V, Tom Dieck S, Schuman EM. 2017. Local translation in neuronal compartments: how local is local? *EMBO Rep* **18**: 693-711.
- Ravanidis S, Kattan FG, Doxakis E. 2018. Unraveling the Pathways to Neuronal Homeostasis and Disease: Mechanistic Insights into the Role of RNA-Binding Proteins and Associated Factors. *Int J Mol Sci* **19**.

- Riback JA, Katanski CD, Kear-Scott JL, Pilipenko EV, Rojek AE, Sosnick TR, Drummond DA. 2017. Stress-Triggered Phase Separation Is an Adaptive, Evolutionarily Tuned Response. *Cell* **168**: 1028-1040 e1019.
- Rook MS, Lu M, Kosik KS. 2000. CaMKIIalpha 3' untranslated region-directed mRNA translocation in living neurons: visualization by GFP linkage. *J Neurosci* **20**: 6385-6393.
- Ross AF, Oleynikov Y, Kislauskis EH, Taneja KL, Singer RH. 1997. Characterization of a beta-actin mRNA zipcode-binding protein. *Mol Cell Biol* **17**: 2158-2165.
- Ross ED, Baxa U, Wickner RB. 2004. Scrambled prion domains form prions and amyloid. *Mol Cell Biol* **24**: 7206-7213.
- Ross ED, Edskes HK, Terry MJ, Wickner RB. 2005a. Primary sequence independence for prion formation. *Proc Natl Acad Sci U S A* **102**: 12825-12830.
- Ross ED, Minton A, Wickner RB. 2005b. Prion domains: sequences, structures and interactions. *Nat Cell Biol* **7**: 1039-1044.
- Rozenbaum M, Rajman M, Rishal I, Koppel I, Koley S, Medzihradzky KF, Oses-Prieto JA, Kawaguchi R, Amieux PS, Burlingame AL et al. 2018. Translatome Regulation in Neuronal Injury and Axon Regrowth. *eNeuro* **5**.
- Sabate R, Rousseau F, Schymkowitz J, Ventura S. 2015. What makes a protein sequence a prion? *PLoS Comput Biol* **11**: e1004013.
- Sañal M, Becam I, Hofmann L, Behague J, Arguelles C, Gourhand V, Bruzzone L, Holmgren RA, Plessis A. 2017. Dose-dependent transduction of Hedgehog relies on phosphorylation-based feedback between the G-protein-coupled receptor Smoothed and the kinase Fused. *Development* **144**: 1841-1850.
- Sasaki Y, Welshhans K, Wen Z, Yao J, Xu M, Goshima Y, Zheng JQ, Bassell GJ. 2010. Phosphorylation of zipcode binding protein 1 is required for brain-derived neurotrophic factor signaling of local beta-actin synthesis and growth cone turning. *J Neurosci* **30**: 9349-9358.
- Schacher S, Wu F, Panyko JD, Sun ZY, Wang D. 1999. Expression and branch-specific export of mRNA are regulated by synapse formation and interaction with specific postsynaptic targets. *J Neurosci* **19**: 6338-6347.
- Scheetz AJ, Nairn AC, Constantine-Paton M. 2000. NMDA receptor-mediated control of protein synthesis at developing synapses. *Nat Neurosci* **3**: 211-216.
- Schisa JA. 2014. Effects of stress and aging on ribonucleoprotein assembly and function in the germ line. *Wiley interdisciplinary reviews RNA* **5**: 231-246.
- Shandilya J, Roberts SG. 2012. The transcription cycle in eukaryotes: from productive initiation to RNA polymerase II recycling. *Biochim Biophys Acta* **1819**: 391-400.
- Shestakova EA, Singer RH, Condeelis J. 2001. The physiological significance of beta -actin mRNA localization in determining cell polarity and directional motility. *Proc Natl Acad Sci U S A* **98**: 7045-7050.
- Shigeoka T, Jung H, Jung J, Turner-Bridger B, Ohk J, Lin JQ, Amieux PS, Holt CE. 2016. Dynamic Axonal Translation in Developing and Mature Visual Circuits. *Cell* **166**: 181-192.
- Shin Y, Brangwynne CP. 2017. Liquid phase condensation in cell physiology and disease. *Science* **357**.
- Shorter J, Lindquist S. 2005. Prions as adaptive conduits of memory and inheritance. *Nat Rev Genet* **6**: 435-450.
- Si K, Giustetto M, Etkin A, Hsu R, Janisiewicz AM, Miniaci MC, Kim JH, Zhu H, Kandel ER. 2003. A neuronal isoform of CPEB regulates local protein synthesis and stabilizes synapse-specific long-term facilitation in aplysia. *Cell* **115**: 893-904.
- Smith J, Calidas D, Schmidt H, Lu T, Rasoloson D, Seydoux G. 2016. Spatial patterning of P granules by RNA-induced phase separation of the intrinsically-disordered protein MEG-3. *Elife* **5**.
- Smith WB, Aakalu G, Schuman EM. 2001. Local protein synthesis in neurons. *Curr Biol* **11**: R901-903.
- Sossin WS, DesGroseillers L. 2006. Intracellular trafficking of RNA in neurons. *Traffic* **7**: 1581-1589.
- Steward O, Banker GA. 1992. Getting the message from the gene to the synapse: sorting and intracellular transport of RNA in neurons. *Trends Neurosci* **15**: 180-186.

- Steward O, Davis L, Dotti C, Phillips LL, Rao A, Banker G. 1988. Protein synthesis and processing in cytoplasmic microdomains beneath postsynaptic sites on CNS neurons. A mechanism for establishing and maintaining a mosaic postsynaptic receptive surface. *Mol Neurobiol* **2**: 227-261.
- Steward O, Falk PM. 1986. Protein-synthetic machinery at postsynaptic sites during synaptogenesis: a quantitative study of the association between polyribosomes and developing synapses. *J Neurosci* **6**: 412-423.
- Steward O, Levy WB. 1982. Preferential localization of polyribosomes under the base of dendritic spines in granule cells of the dentate gyrus. *J Neurosci* **2**: 284-291.
- Steward O, Ribak CE. 1986. Polyribosomes associated with synaptic specializations on axon initial segments: localization of protein-synthetic machinery at inhibitory synapses. *J Neurosci* **6**: 3079-3085.
- Steward O, Schuman EM. 2001. Protein synthesis at synaptic sites on dendrites. *Annu Rev Neurosci* **24**: 299-325.
- Steward O, Wallace CS, Lyford GL, Worley PF. 1998. Synaptic activation causes the mRNA for the IEG Arc to localize selectively near activated postsynaptic sites on dendrites. *Neuron* **21**: 741-751.
- Strohl F, Lin JQ, Laine RF, Wong HH, Urbancic V, Cagnetta R, Holt CE, Kaminski CF. 2017. Single Molecule Translation Imaging Visualizes the Dynamics of Local beta-Actin Synthesis in Retinal Axons. *Sci Rep* **7**: 709.
- Suprenant KA. 1993. Microtubules, ribosomes, and RNA: evidence for cytoplasmic localization and translational regulation. *Cell Motil Cytoskeleton* **25**: 1-9.
- Surmeier DJ, Eberwine J, Wilson CJ, Cao Y, Stefani A, Kitai ST. 1992. Dopamine receptor subtypes colocalize in rat striatonigral neurons. *Proc Natl Acad Sci U S A* **89**: 10178-10182.
- Takeuchi T, Duzskiewicz AJ, Morris RG. 2014. The synaptic plasticity and memory hypothesis: encoding, storage and persistence. *Philos Trans R Soc Lond B Biol Sci* **369**: 20130288.
- Taliaferro JM, Wang ET, Burge CB. 2014. Genomic analysis of RNA localization. *RNA Biol* **11**: 1040-1050.
- Tanenbaum ME, Gilbert LA, Qi LS, Weissman JS, Vale RD. 2014. A protein-tagging system for signal amplification in gene expression and fluorescence imaging. *Cell* **159**: 635-646.
- Tang SJ, Schuman EM. 2002. Protein synthesis in the dendrite. *Philos Trans R Soc Lond B Biol Sci* **357**: 521-529.
- Taylor AM, Berchtold NC, Perreau VM, Tu CH, Li Jeon N, Cotman CW. 2009. Axonal mRNA in uninjured and regenerating cortical mammalian axons. *J Neurosci* **29**: 4697-4707.
- Tessier CR, Doyle GA, Clark BA, Pitot HC, Ross J. 2004. Mammary tumor induction in transgenic mice expressing an RNA-binding protein. *Cancer Res* **64**: 209-214.
- Tiruchinapalli DM, Oleynikov Y, Kelic S, Shenoy SM, Hartley A, Stanton PK, Singer RH, Bassell GJ. 2003. Activity-dependent trafficking and dynamic localization of zipcode binding protein 1 and beta-actin mRNA in dendrites and spines of hippocampal neurons. *J Neurosci* **23**: 3251-3261.
- Toledano H, D'Alterio C, Czech B, Levine E, Jones DL. 2012. The let-7-Imp axis regulates ageing of the *Drosophila* testis stem-cell niche. *Nature* **485**: 605-610.
- Tomba P. 2005. The interplay between structure and function in intrinsically unstructured proteins. *FEBS Lett* **579**: 3346-3354.
- Toretsky JA, Wright PE. 2014. Assemblages: functional units formed by cellular phase separation. *J Cell Biol* **206**: 579-588.
- Torre ER, Steward O. 1992. Demonstration of local protein synthesis within dendrites using a new cell culture system that permits the isolation of living axons and dendrites from their cell bodies. *J Neurosci* **12**: 762-772.
- Tutucci E, Stutz F. 2011. Keeping mRNPs in check during assembly and nuclear export. *Nat Rev Mol Cell Biol* **12**: 377-384.

- Twiss JL, Fainzilber M. 2009. Ribosomes in axons--scrounging from the neighbors? *Trends Cell Biol* **19**: 236-243.
- Urbanska AS, Janusz-Kaminska A, Switon K, Hawthorne AL, Perycz M, Urbanska M, Bassell GJ, Jaworski J. 2017. ZBP1 phosphorylation at serine 181 regulates its dendritic transport and the development of dendritic trees of hippocampal neurons. *Sci Rep* **7**: 1876.
- Uversky VN. 2015. Functional roles of transiently and intrinsically disordered regions within proteins. *FEBS J* **282**: 1182-1189.
- . 2017. Intrinsically disordered proteins in overcrowded milieu: Membrane-less organelles, phase separation, and intrinsic disorder. *Curr Opin Struct Biol* **44**: 18-30.
- Valencia-Burton M, Shah A, Sutin J, Borogovac A, McCullough RM, Cantor CR, Meller A, Broude NE. 2009. Spatiotemporal patterns and transcription kinetics of induced RNA in single bacterial cells. *Proc Natl Acad Sci U S A* **106**: 16399-16404.
- van der Lee R, Buljan M, Lang B, Weatheritt RJ, Daughdrill GW, Dunker AK, Fuxreiter M, Gough J, Gsponer J, Jones DT et al. 2014. Classification of intrinsically disordered regions and proteins. *Chem Rev* **114**: 6589-6631.
- Verma P, Chierzi S, Codd AM, Campbell DS, Meyer RL, Holt CE, Fawcett JW. 2005. Axonal protein synthesis and degradation are necessary for efficient growth cone regeneration. *J Neurosci* **25**: 331-342.
- Vuppalanchi D, Coleman J, Yoo S, Merianda TT, Yadhati AG, Hossain J, Blesch A, Willis DE, Twiss JL. 2010. Conserved 3'-untranslated region sequences direct subcellular localization of chaperone protein mRNAs in neurons. *J Biol Chem* **285**: 18025-18038.
- Wachter K, Kohn M, Stohr N, Huttelmaier S. 2013. Subcellular localization and RNP formation of IGF2BPs (IGF2 mRNA-binding proteins) is modulated by distinct RNA-binding domains. *Biol Chem* **394**: 1077-1090.
- Wang C, Han B, Zhou R, Zhuang X. 2016. Real-Time Imaging of Translation on Single mRNA Transcripts in Live Cells. *Cell* **165**: 990-1001.
- Wang DO, Kim SM, Zhao Y, Hwang H, Miura SK, Sossin WS, Martin KC. 2009. Synapse- and stimulus-specific local translation during long-term neuronal plasticity. *Science* **324**: 1536-1540.
- Wang J, Choi JM, Holehouse AS, Lee HO, Zhang X, Jahnel M, Maharana S, Lemaitre R, Pozniakovsky A, Drechsel D et al. 2018. A Molecular Grammar Governing the Driving Forces for Phase Separation of Prion-like RNA Binding Proteins. *Cell* **174**: 688-699 e616.
- Wang JT, Smith J, Chen BC, Schmidt H, Rasoloson D, Paix A, Lambrus BG, Calidas D, Betzig E, Seydoux G. 2014. Regulation of RNA granule dynamics by phosphorylation of serine-rich, intrinsically disordered proteins in *C. elegans*. *Elife* **3**: e04591.
- Weber SC, Brangwynne CP. 2012. Getting RNA and protein in phase. *Cell* **149**: 1188-1191.
- Weidensdorfer D, Stohr N, Baude A, Lederer M, Kohn M, Schierhorn A, Buchmeier S, Wahle E, Huttelmaier S. 2009. Control of c-myc mRNA stability by IGF2BP1-associated cytoplasmic RNPs. *RNA* **15**: 104-115.
- Weil TT. 2014. mRNA localization in the *Drosophila* germline. *RNA Biol* **11**: 1010-1018.
- Welshhans K, Bassell GJ. 2011. Netrin-1-induced local beta-actin synthesis and growth cone guidance requires zipcode binding protein 1. *J Neurosci* **31**: 9800-9813.
- Wheeler RJ, Hyman AA. 2018. Controlling compartmentalization by non-membrane-bound organelles. *Philos Trans R Soc Lond B Biol Sci* **373**.
- Wilk R, Hu J, Blotsky D, Krause HM. 2016. Diverse and pervasive subcellular distributions for both coding and long noncoding RNAs. *Genes Dev* **30**: 594-609.
- Willis D, Li KW, Zheng JQ, Chang JH, Smit AB, Kelly T, Merianda TT, Sylvester J, van Minnen J, Twiss JL. 2005. Differential transport and local translation of cytoskeletal, injury-response, and neurodegeneration protein mRNAs in axons. *J Neurosci* **25**: 778-791.
- Wong HH, Lin JQ, Strohl F, Roque CG, Cioni JM, Cagnetta R, Turner-Bridger B, Laine RF, Harris WA, Kaminski CF et al. 2017. RNA Docking and Local Translation Regulate Site-Specific Axon Remodeling In Vivo. *Neuron* **95**: 852-868 e858.

- Wright PE, Dyson HJ. 2015. Intrinsically disordered proteins in cellular signalling and regulation. *Nat Rev Mol Cell Biol* **16**: 18-29.
- Wu B, Eliscovich C, Yoon YJ, Singer RH. 2016. Translation dynamics of single mRNAs in live cells and neurons. *Science* **352**: 1430-1435.
- Wu H, Fuxreiter M. 2016. The Structure and Dynamics of Higher-Order Assemblies: Amyloids, Signalosomes, and Granules. *Cell* **165**: 1055-1066.
- Wu JS, Luo L. 2006. A protocol for mosaic analysis with a repressible cell marker (MARCM) in *Drosophila*. *Nat Protoc* **1**: 2583-2589.
- Wu KY, Hengst U, Cox LJ, Macosko EZ, Jeromin A, Urquhart ER, Jaffrey SR. 2005. Local translation of RhoA regulates growth cone collapse. *Nature* **436**: 1020-1024.
- Xing L, Bassell GJ. 2013. mRNA localization: an orchestration of assembly, traffic and synthesis. *Traffic* **14**: 2-14.
- Yan X, Hoek TA, Vale RD, Tanenbaum ME. 2016. Dynamics of Translation of Single mRNA Molecules In Vivo. *Cell* **165**: 976-989.
- Yaniv K, Fainsod A, Kalcheim C, Yisraeli JK. 2003. The RNA-binding protein Vg1 RBP is required for cell migration during early neural development. *Development* **130**: 5649-5661.
- Yao J, Sasaki Y, Wen Z, Bassell GJ, Zheng JQ. 2006. An essential role for beta-actin mRNA localization and translation in Ca²⁺-dependent growth cone guidance. *Nat Neurosci* **9**: 1265-1273.
- Yisraeli JK, Sokol S, Melton DA. 1990. A two-step model for the localization of maternal mRNA in *Xenopus* oocytes: involvement of microtubules and microfilaments in the translocation and anchoring of Vg1 mRNA. *Development* **108**: 289-298.
- Yoon BC, Jung H, Dwivedy A, O'Hare CM, Zivraj KH, Holt CE. 2012. Local translation of extranuclear lamin B promotes axon maintenance. *Cell* **148**: 752-764.
- Yoon YJ, Wu B, Buxbaum AR, Das S, Tsai A, English BP, Grimm JB, Lavis LD, Singer RH. 2016. Glutamate-induced RNA localization and translation in neurons. *Proc Natl Acad Sci U S A* **113**: E6877-E6886.
- Yoshimura A, Fujii R, Watanabe Y, Okabe S, Fukui K, Takumi T. 2006. Myosin-Va facilitates the accumulation of mRNA/protein complex in dendritic spines. *Curr Biol* **16**: 2345-2351.
- Yu F, Schuldiner O. 2014. Axon and dendrite pruning in *Drosophila*. *Curr Opin Neurobiol* **27**: 192-198.
- Zappulo A, van den Bruck D, Ciolli Mattioli C, Franke V, Imami K, McShane E, Moreno-Estelles M, Calviello L, Filipchuk A, Peguero-Sanchez E et al. 2017. RNA localization is a key determinant of neurite-enriched proteome. *Nat Commun* **8**: 583.
- Zeng M, Shang Y, Araki Y, Guo T, Haganir RL, Zhang M. 2016. Phase Transition in Postsynaptic Densities Underlies Formation of Synaptic Complexes and Synaptic Plasticity. *Cell* **166**: 1163-1175 e1112.
- Zhang H, Elbaum-Garfinkle S, Langdon EM, Taylor N, Occhipinti P, Bridges AA, Brangwynne CP, Gladfelter AS. 2015. RNA Controls PolyQ Protein Phase Transitions. *Mol Cell* **60**: 220-230.
- Zhang HL, Eom T, Olynykov Y, Shenoy SM, Liebelt DA, Dichtenberg JB, Singer RH, Bassell GJ. 2001. Neurotrophin-induced transport of a beta-actin mRNP complex increases beta-actin levels and stimulates growth cone motility. *Neuron* **31**: 261-275.
- Zhang J, Okabe K, Tani T, Funatsu T. 2011. Dynamic association-dissociation and harboring of endogenous mRNAs in stress granules. *Journal of cell science* **124**: 4087-4095.
- Zhang JY, Chan EK, Peng XX, Tan EM. 1999. A novel cytoplasmic protein with RNA-binding motifs is an autoantigen in human hepatocellular carcinoma. *J Exp Med* **189**: 1101-1110.
- Zheng JQ, Kelly TK, Chang B, Ryazantsev S, Rajasekaran AK, Martin KC, Twiss JL. 2001. A functional role for intra-axonal protein synthesis during axonal regeneration from adult sensory neurons. *J Neurosci* **21**: 9291-9303.
- Zivraj KH, Tung YC, Piper M, Gumy L, Fawcett JW, Yeo GS, Holt CE. 2010. Subcellular profiling reveals distinct and developmentally regulated repertoire of growth cone mRNAs. *J Neurosci* **30**: 15464-15478.